



Western Michigan University
ScholarWorks at WMU

Dissertations

Graduate College

8-2008

Zeolite-Based Nanosized TiO₂ Photocatalytic Paper for Antimicrobial Barrier and Toxin Passivation in Packaging: Design, Synthesis and Characterization

Seonghyuk Ko
Western Michigan University

Follow this and additional works at: <https://scholarworks.wmich.edu/dissertations>



Part of the Engineering Commons

Recommended Citation

Ko, Seonghyuk, "Zeolite-Based Nanosized TiO₂ Photocatalytic Paper for Antimicrobial Barrier and Toxin Passivation in Packaging: Design, Synthesis and Characterization" (2008). *Dissertations*. 785.
<https://scholarworks.wmich.edu/dissertations/785>

This Dissertation-Open Access is brought to you for free and open access by the Graduate College at ScholarWorks at WMU. It has been accepted for inclusion in Dissertations by an authorized administrator of ScholarWorks at WMU. For more information, please contact wmu-scholarworks@wmich.edu.



ZEOLITE-BASED NANOSIZED TiO_2 PHOTOCATALYTIC PAPER FOR
ANTIMICROBIAL BARRIER AND TOXIN PASSIVATION IN
PACKAGING: DESIGN, SYNTHESIS AND
CHARACTERIZATION

by

Seonghyuk Ko

A Dissertation
Submitted to the
Faculty of The Graduate College
in partial fulfillment of the
requirements for the
Degree of Doctor of Philosophy
Department of Paper Engineering, Chemical Engineering and Imaging
Dr. Paul D. Fleming, Advisor

Western Michigan University
Kalamazoo, Michigan
August 2008

UMI Number: 3323526

INFORMATION TO USERS

The quality of this reproduction is dependent upon the quality of the copy submitted. Broken or indistinct print, colored or poor quality illustrations and photographs, print bleed-through, substandard margins, and improper alignment can adversely affect reproduction.

In the unlikely event that the author did not send a complete manuscript and there are missing pages, these will be noted. Also, if unauthorized copyright material had to be removed, a note will indicate the deletion.

UMI[®]

UMI Microform 3323526

Copyright 2008 by ProQuest LLC.

All rights reserved. This microform edition is protected against unauthorized copying under Title 17, United States Code.

ProQuest LLC
789 E. Eisenhower Parkway
PO Box 1346
Ann Arbor, MI 48106-1346

Copyright by
Seonghyuk Ko
2008

ACKNOWLEDGMENTS

I would like to express my deepest gratitude to academic advisor, Dr. Pual D. Fleming, for his worthy advice, assistance and guidance through my research years. I would also like to extend my sincere thanks to my committee members, Dr. Margaret K. Joyce and Dr. Pnina Ari-Gur, for their professional suggestions and review of my dissertation.

I especially wish to thank National Council for Air and Stream Improvement Inc. (NCASI) for their thoughtful consideration and financial support during the course of my doctoral program. Special thanks to Dr. John Cameron, Dr. Jan Pekarovic and Mr. Matt Stoops for helping me in use of instruments and laboratory set up. Many thanks to my family friends and colleagues in PCI department for making enjoyable time and all their help.

I cannot express the depth of my gratitude in words to my mother and my parents-in-law, for all the love and their affection and I cannot think of any way right now to return their great love and sacrifice for me. I also give thanks to my sister's and brothers-in-law for their persistent interest and support. Finally, I give heartfelt thanks to my lovely wife, Hyunjung, and my lovely sons, Yoonwoo and Geonwoo, for all their sacrifice, quite patience and constant encouragement.

Seonghyuk Ko

TABLE OF CONTENTS

ACKNOWLEDGMENTS	ii
LIST OF TABLES.....	viii
LIST OF FIGURES.....	ix
CHAPTER	
I. INTRODUCTION	1
References	7
II. LITERATURE REVIEW.....	12
Photocatalyst and Photocatalysis	12
What is the photocatalyst?.....	12
Crystalline structure of TiO ₂	13
Basic principles of photocatalysis.....	15
Environmental applications of TiO ₂ photocatalyst.....	18
Zeolite: Principles and Applications.....	20
Zeolite composition and structure	20
Industrial applications of zeolites	22
Natural zeolite and its use in papermaking and paper coating	25
Photocatalytic Paper.....	27

Table of Contents-Continued

CHAPTER		
	Definition and overview	27
	Preparation methods of photocatalytic paper	29
	Applications of photocatalytic paper	30
	References	31
III.	RESEARCH SCOPE AND OBJECTIVES	41
IV.	EXPERIMENTALS	43
	Materials	43
	Synthesis of Photocatalytic Materials	43
	TiO ₂ colloidal nanoparticles	43
	Zeolite-based photocatalyst	44
	Photocatalytic Papermaking	45
	Determination of TiO ₂ retention	45
	Preparation of photocatalytic paper	46
	Characterization of Photocatalyst-Based Materials	47
	Crystallographic examination	47
	Particle size measurement	48
	Optical properties of TiO ₂ nanoparticles	48
	Morphology of photocatalytic papers	48
	Evaluation of Photocatalytic Activity	49
	References	50

Table of Contents-Continued

CHAPTER

V. SYNTEHTIC BEHAVIOR AND PHOTOCATALYTIC ACTIVITY OF NANOCRYSTALLINE TiO ₂ FROM SOL-GEL DERIVED COLLOIDS	51
Introduction.....	51
Experimental	53
Results and Discussion	54
Conclusions	60
References	61
Appendix	64
DLS Distribution and TEM Image of Colloidal TiO ₂ Nanoparticles.....	64
VI. OPTIMIZATION OF OPTICAL PROPERTIES AND PHOTOCATALYTIC ACTIVITY OF POLYCRYSTALLINE TiO ₂ NANOPARTICLES TOWARD PHOTOCATALYTIC PAPER	66
Introduction.....	67
Experimental	69
Sample preparation	69
Characterization of TiO ₂	70
Evaluation of photocatalysis	71
Results and Discussion	71
XRD patterns and crystalline phase transition.....	71
Optical properties	73

Table of Contents-Continued

CHAPTER		
	Photocatalytic Activity	76
	Conclusion	77
	References	78
VII.	PREPARATION AND STUDY OF VOC REMOVAL OF NANO TITANIA PHOTOCATALYTIC PAPER USING A NATURAL ZEOLITE MICROPARTICULATE SYSTEM.....	81
	Introduction.....	82
	Experimental	84
	Materials.....	84
	Characterization of TiO ₂ nanoparticles.....	85
	Retention of TiO ₂	85
	Preparation of photocatalytic paper.....	86
	Evaluation of photocatalysis	86
	Results and Discussion	87
	TiO ₂ photocatalyst characterization.....	87
	TiO ₂ retention	88
	Photocatalytic activity	92
	Conclusion	93
	References	94
	Appendices	98
	A. The Effect of TiO ₂ and Natural Zeolite Contents on Retention Rate.....	98

Table of Contents-Continued

CHAPTER		
	B. The Effect of Cationic Starch Contents on TiO ₂ Retention Rate	99
	C. The Effect of Cationic Polymer (C-PAM) on TiO ₂ Retention Rate	100
VIII.	NATURAL ZEOLITE-BASED NANO TiO ₂ PHOTOCATALYTIC PAPER: PREPARATION, CHARACTERIZATION AND PHOTOCATALYSIS ASSESSMENT.....	101
	Introduction.....	102
	Experimental	105
	Materials.....	105
	Combination of TiO ₂ and natural zeolite	106
	Preparation of photocatalytic paper.....	106
	Characterization.....	107
	Evaluation of photocatalytic activity	108
	Results and Discussion	108
	Characterization of zeolite-based TiO ₂	108
	Morphology of photocatalytic paper	112
	Evaluation of photocatalytic activity	114
	Conclusion	117
	References	117
IX.	CONCLUSION	122

LIST OF TABLES

2.1	Comparison of Rutile and Anatase Crystalline Properties.....	14
2.2	Primary Process and Time Domains in Titania-Catalyzed Mineralization of Organic Pollutants.....	17
2.3	Selected Applications of Photocatalysis	19
2.4	Pore Types and Diameters in Zeolites	23
2.5	Major Commercial Process Based on Zeolite Catalysts.....	24
2.6	The Expanding Applications of Photocatalytic Paper	31
4.1	Experimental Factors for TiO ₂ Colloidal Nanoparticles.....	44
4.2	Factors and Levels for the 2 ³ Factorial Design in TiO ₂ Retention Test	46
5.1	Experimental Factors for TiO ₂ Colloidal Nanoparticles and Their Particle Size.....	55
7.1	Factors and Levels for the 2 ³ Factorial Experimental Design	89

LIST OF FIGURES

2.1	TiO ₂ crystal structures: Rutile (left) and Anatase (right).....	14
2.2	Schematic mechanism of photocatalytic process over TiO ₂	16
2.3	Illustration of three- and two-dimensional zeolite framework.....	21
2.4	Framework structures of selected zeolites.	23
2.5	Framework structure of Clinoptilolite.....	26
2.6	Photocatalysis process on photocatalytic paper.....	28
5.1	Representative TEM images of TiO ₂ colloidal nanoparticles and DLS particle diameter distribution (the upper insert); (A) DOE #2, scale bar=10nm, (B) DOE #5, scale bar=50nm.	56
5.2	XRD diffraction patterns of as-prepared TiO ₂ nanoparticles; (A) DOE #2, (B) DOE #5.....	58
5.3	The relationship of particle growth and rutile weight fraction as a function of annealing temperature.....	59
5.4	Photodegradation of gaseous toluene under UV irradiation.	60
6.1	XRD patterns of phase modulated P25 TiO ₂ nanoparticles.....	72
6.2	Crystallite fractions of TiO ₂ nanoparticles annealed at varied temperature.....	73
6.3	Opacity and brightness of TiO ₂ nanoparticles according to different rutile fractions.	74
6.4	Diagram of CIEL*a*b* values of TiO ₂ nanoparticles with different rutile weight fraction.....	75

List of Figures-Continued

6.5	Photodegradation of toluene with varied crystalline phase of TiO ₂ nanoparticles under UV irradiation.....	77
7.1	XRD pattern of Degussa P25 TiO ₂ powder.	87
7.2	Representative TEM images of P25 TiO ₂ nanoparticles; scale bar=50nm.	88
7.3	TiO ₂ retention values in bleached softwood pulp with varying retention aids; CSF=430 ml, 750rpm	90
7.4	Main effect and interaction plot for TiO ₂ retention (%) in natural zeolite microparticle system.....	91
7.5	Photodecomposition of gaseous toluene by nano TiO ₂ photocatalytic sheets.	93
8.1	XRD patterns of natural zeolite-based TiO ₂ with varying calcination temperature.	110
8.2	Representative TEM images of TiO ₂ nanoparticles on natural zeolite at different calcination temperature; (A) no calcination, (B) 600C and (C) 800C, scale bar = 50nm.....	111
8.3	SEM images of photocatalytic papers; (A) blank sheet, (B) P25 TiO ₂ /natural zeolite sheet, (C) natural zeolite-based nano TiO ₂ paper and (D) Ahlstrom sample.	113
8.4	Decomposition of gaseous toluene on photocatalytic papers under UV irradiation.....	115
8.5	Comparison of toluene photodegradation by different types of photocatalytic papers.	116

CHAPTER I

INTRODUCTION

Titanium dioxide (TiO_2) has been widely used for two major purposes, an opacifying pigment and photocatalytic agent [1]. Due to its unique optical properties of a high refractive index and whiteness, TiO_2 has long been used in applications requiring high opacity and brightness such as coatings, paints, plastics, inks, and paper [2]. However, because of its relatively high cost compared to other pigments, such as clay and calcium carbonate, its use in papermaking and coating has been limited to high valued products [3]. Of great interest to many R&D communities in academia and industry is to improve TiO_2 performance to meet the ideal requirements of high optical properties and lower cost.

By contrast, since the remarkable discovery of the Fujishima-Honda effect, that is the photoinduced splitting of water into hydrogen on titania electrodes using only light in 1972 [4], there have been huge breakthroughs achieved, both scientifically and practically, in various applications of semiconductor photocatalysis. In particular, nanocrystalline TiO_2 has recently drawn enormous attention among the possible photocatalytic semiconductor materials, because of their photosensitive, inexpensive, non-toxic and chemically stable characteristics [5-8]. Examples include solar cells [9-11], fuel cells [12-13], optical sensors [14-16], hygienic disinfection [17-20], self-cleaning [21] and extensive environmental cleanup for both air pollutants [22-24] and wastewater [25-27], which is often referred to as "Light Cleaning" [1].

TiO_2 is well known to have three main crystalline structures, which

have different optical and physical properties, namely anatase, brookite and rutile [1]. For the photocatalytic oxidation, anatase is superior to the others, because its conduction band is favorably located to support sufficient conjugation involving electrons and it also can generate very stable peroxide radicals on the surface during the oxidation reaction [28]. Anatase is typically transformed to rutile with an increase in temperature, because the surface free energy has to be minimized to become thermodynamically stable and rutile is the most stable at high temperature among the three main phases [29]. As noticed, different structures govern dissimilar optical and physical properties, which lead to different applications. Indeed, TiO_2 is a material that highly depends on its crystalline phase to determine its pigment and photocatalyst properties.

Photocatalysis occurs when a photocatalyst, such as titanium dioxide, is exposed to photons with at least as much energy as the band gap energy of the photocatalyst. When the band gap energy is exceeded, the material forms electron-hole pairs, which are sets of negatively charged electrons and positively charged vacancies, where the electrons used to be. In general, the holes react with H_2O to form hydroxyl ($\text{OH}\cdot$) radicals, which lead to an oxidation reaction of a variety of contaminants, such as environmental pollutants and microorganisms [1, 30]. In other words, the oxidizing power of these radicals is the means by which organic chemicals are degraded during photocatalysis, whether in aqueous and gaseous media.

Out of this variety of TiO_2 -based applications, there has been an emerging interest in attempting to create innovative applications to increase the value of functional paper, named photocatalytic paper, for deodorizing,

disinfection, disintegration of toxins. Photocatalytic paper has been defined as a smart paper that has a light-activated catalytic function to decompose organic pollutants and kill pathogens [31]. Of specific interests are two possible applications, antimicrobial active and VOCs removing paper. In recent years, food-borne microbial outbreaks have been an issue and it is important to promote developing the next generation of materials incorporating anti-bacterial properties in active food packaging [32-33]. This is an advanced packaging system functionalized by interacting package components with food products to satisfy demands for fresh-like foods safe from pathogens [34]. More recently, a new bioactive paper and its packaging has been designed and developed to detect and deactivate any pathogens, such as E-coli and salmonella, borne by food, air and water [35]. Therefore, it would not be an overstatement to say that photocatalytic paper can be used in such new applications as antimicrobial food packaging, bioactive conjugated catalytic paper, as well as toxin passivation and deodorizing paper.

As an effective means of decomposing organic compounds, it is of particular interest to immobilize nanosized TiO_2 particles on such supporting or anchoring materials as silica [36-37], glass beads [38,39], alumina [39], fiber glass [40], clay [41] and zeolite [42-43] with the ultimate aim of intact photoactivity and the enhancement of photocatalytic efficiency. Of various supports, zeolites have been found to be more favorable to be used for supporting TiO_2 , due to their unique crystal structure and uniform nanoscaled pores and channels, which lead to large surface area and induce synergetic adsorption effect of organic matters in turn. A great deal of

previous works has been performed on synthetic zeolites, for instance, HZSM-5 [44], Y zeolite [45] and MCM-41 zeolite [46], because of the relatively larger surface area and supercages in the infrastructure which enable the trapping of TiO₂ nanoparticles.

As distinct from synthetic zeolites, however, natural zeolite provides significant advantages of cost, it's naturally abundant and is more easily accessible. Surprisingly, though, relatively few studies have been devoted to the anchoring and incorporation of TiO₂ on natural zeolite. Moreover, attempts to use natural zeolite in paper making and coating has been performed recently and it was revealed that natural zeolite pigment makes it possible to significantly improve the print quality of ink jet and digital papers and it is also efficient for filler retention enhancement [47-51]. It is therefore expected that natural zeolite plays important roles between fibers and TiO₂ particles, not only as an effective microparticle retention aid, but as a photocatalytic activity enhancer as well in photocatalytic paper. It is worthwhile, thus, to investigate the integration of natural zeolite and nanosized TiO₂ and to evaluate the photocatalytic activity of photocatalytic paper containing as-prepared natural zeolite-based nano TiO₂. These studies have not, so far, been noticed, nor have they been researched in detail in the area of photocatalytic paper.

The present work aims to design, synthesize and characterize newly developed natural zeolite-nano titania composites and to develop novel photocatalytic papers having the functions of disinfection and decomposition of organic contaminants. In line with these purposes, this research generated the following journal articles referred to as Papers I-IV: (I) Synthetic behavior

and photocatalytic activity of nanocrystalline TiO₂ from sol-gel derived colloids, (II) Optimization of optical properties and photocatalytic activity of polycrystalline TiO₂ nanoparticles toward photocatalytic paper, (III) Preparation and study of VOC removal of nano titania photocatalytic paper using a natural zeolite microparticulate system, and (IV) Natural zeolite-based nanosized TiO₂ photocatalytic paper; preparation, characterization and photocatalysis assessment.

In paper I, colloidal titania nanoparticles were synthesized by the sol-gel process based on an experimental design and as-prepared TiO₂ nanoparticles were comprehensively characterized from primitive colloids to solid nanoparticles with regard to particle size and photocatalytic activity. Compared to well-known Degussa P25 TiO₂, which is the most widely used product in photocatalysis process, TiO₂ nanoparticles obtained from this work were determined to have an optimal synthetic passage that surpassed P25 TiO₂ in photocatalytic activity of toluene removal as one representative of VOCs.

The goal of the paper II was to optimize the ratio of crystalline phases of polycrystalline TiO₂ nanoparticles to satisfy required optical properties, such as opacity, brightness and L*a*b* values, while maintaining high photocatalytic activity. TiO₂ nanoparticles were treated by heat to vary the crystalline fraction of anatase and rutile, and subsequently, the crystalline phase of the as-modulated TiO₂ samples were used after deposition onto filter paper. Structural change and optical analyses of the TiO₂ particles were carried out with various characterization tools such as XRD, BNL Dyano 10 Opacimeter, Technidyne Brightimeter and X-rite 530 SpectroDensitometer,

while at the same time their photocatalytic activity was also evaluated with toluene decomposition. As a result, the optimal ranges of crystalline phase fraction for influencing both the optical properties and photocatalytic activity are suggested in detail.

Paper III deals with nanosized TiO₂ photocatalytic paper prepared by a natural zeolite microparticulate system and its photocatalytic performance in VOC decomposition. In order to confirm the importance of natural zeolite, the retention of TiO₂ nanoparticles was first tested with a dynamic drainage jar (Britt Jar™ [52]) according to the factorial experimental design and factors influencing retention of TiO₂ nanoparticles discussed by using statistical analysis tools. TiO₂ nanoparticles used in this study were characterized by TEM and XRD and the photocatalytic effect was evaluated by toluene removal with a gas chromatograph.

Paper IV describes how to synthesize and characterize nano TiO₂-supported natural zeolite from sol-gel derived nano titania colloids and to use as-fabricated zeolite-based TiO₂ nanoparticles in preparation of photocatalytic paper using a microparticle retention system. Photocatalytic performance on VOC decomposition was evaluated with gaseous toluene, and to compare photocatalytic activity, two different types of photocatalytic papers were also tested, Ahalstrom commercial photocatalytic non-woven paper and a lab-sample made using Degussa P25 TiO₂, which is the most referred to TiO₂ pigment for photocatalysis. In the end, the phenomenon of enhanced photocatalysis, as well as, the physical properties of both zeolite-TiO₂ hybrid material and its photocatalytic paper were shown and discussed. Indeed, the results in this paper bring us much closer to understanding the

potential of photocatalytic paper and to the day when photocatalytic paper might move beyond fantasy.

References

- [1] A. Fujishima, K. Hashimoto and H. Watanabe, "TiO₂ Photocatalysis: Fundamentals and Applications", BKC, Inc. Tokyo, Japan, 1997.
- [2] G. Buxbaum, G. Pfaff, "Industrial Inorganic Pigments", Wiley-VCH, Weinheim, Germany 3rd Ed. 2005.
- [3] C. J. Biermann, "Handbook of pulp and papermaking", Academic Press, 1996.
- [4] A. Fujishima, K. Honda, "Electrochemical Photolysis of Water at a Semiconductor Electrode", Nature 238 (1972) 37-38.
- [5] M. R. Hoffmann, S. T. Martin, W. Choi, D.W. Bahnemann, "Environmental applications of semiconductor photocatalysis", Chem. Rev. 95 (1995) 69-96.
- [6] A. L. Linsebigler, G. Lu, J.T. Yates Jr., "Photocatalysis on TiO₂ surfaces: Principles, Mechanisms, and Selected Results", Chem. Rev. 95 (1995) 735-758.
- [7] A. Fujishima, T.N. Rao, D.A. Tryk, "Titanium dioxide photocatalysis", J. Photoch. Photobio. C 1 (2000) 1-21.
- [8] T. L. Thompson, J. T. Yates Jr., "Surface science studies of the photoactivation of TiO₂-New photochemical processes", Chem. Rev. 106 (2006) 4428-4453.
- [9] M. Gratzel, "Photoelectrochemical cells ", Nature 414 (2001) 338-344.
- [10] M. Gratzel, "Dye-sensitized solar cells", J. Photoch. Photobio. C 4 (2003) 145-153.
- [11] L. Yang, Y. Lin, J. Jia, X. Li, X. Xiao, X. Zhou, "Cauliflower-like TiO₂ rough spheres: Synthesis and applications in dye sensitized solar cells",

Micropor. Mesopor. Mat. 112 (2008) 45-52.

[12] H. Ekström, B. Wickman, M. Gustavsson, P. Hanarp, L. Eurenus, E. Olsson, G. Lindbergh, "Nanometer-thick films of titanium oxide acting as electrolyte in the polymer electrolyte fuel cell", *Electrochim. Acta* 52 (2007) 4239-4235.

[13] M. Gustavson, H. Ekström, P. Hanarp et al., "Thin film Pt/TiO₂ catalysts for the polymer electrolyte fuel cell", *J. Power Sources* 163 (2007) 671-678.

[14] A. Curulli, F. Valentini, G. Padeletti et al., "Smart (Nano) materials: TiO₂ nanostructured films to modify electrodes for assembling of new electrochemical probes", *Sensor. Actuat. B-Chem.* 111-112 (2005) 441-449.

[15] L. Francioso, A.M. Taurino, A. Forleo, P. Siciliano, "TiO₂ nanowires array fabrication and gas sensing properties", *Sensor. Actuat. B-Chem.* 130 (2008) 70-76.

[16] M. G. Manera, J. Spadavecchia, D. Buso, C. de J. Fernández, G. Mattei, A. Martucci, P. Mulvaney, J. Pérez-Juste, R. Rella, L. Vasanelli, P. Mazzoldi, "Optical gas sensing of TiO₂ and TiO₂/Au nanocomposite thin films", *Sensor. Actuat. B-Chem.* 132 (2008) 107-115.

[17] K. Sunada, Y. Kikuchi, K. Hashimoto, A. Fujishima, "Bactericidal and Detoxification Effects of TiO₂ Thin Film Photocatalyst", *Environ. Sci. Technol.* 32 (1998) 726-728.

[18] G. Fu, P.S. Vary, C.-T. Lin, "Anatase TiO₂ Nanocomposites for Antimicrobial Coatings", *J. Phys. Chem. B* 109 (2005) 8889-8898.

[19] K.S. Yao, D.Y. Wang, W.Y. Ho, J.J. Yan, K.C. Tzeng, "Photocatalytic bactericidal effect of TiO₂ thin film on plant pathogens", *Surf. Coat. Tech.* 201 (2007) 6886-6888.

[20] C. Guillard, T.-H. Bui, C. Felix, V. Moules, B. Lina, P. Lejeune, "Microbiological disinfection of water and air by photocatalysis", *C. R. Chim.* 11 (2008) 107-113.

[21] C. Euvananont, C. Junin, K. Inpor, P. Limthongkul, C. Thanachayanont, "TiO₂ optical coating layers for self-cleaning applications", *Ceram. Int.* 34 (2008) 1067-1071.

- [22] C. H. Ao, S. C. Lee, Y. Z. Yu, J. H. Xu, "Photodegradation of formaldehyde by photocatalyst TiO₂: effects on the presences of NO, SO₂ and VOCs", *Appl. Catal. B- Environ.* 54 (2004) 41-50.
- [23] A. Strini, S. Cassese, L. Schiavi, "Measurement of benzene, toluene, ethylbenzene and O-xylene gas phase photodegradation by titanium dioxides dispersed in cementitious materials using a mixed flow reactor", *Appl. Catal. B- Environ.* 61 (2005) 90-97.
- [24] L. Reijnders, "Hazard reduction for the application of titania nanoparticles in environmental technology", *J. Hazard. Mater.* 152 (2008) 440-445.
- [25] A. C. Rodrigues, M. Boroski, N.S. Shimada, J.C. Garcia, J. Nozaki, N. Hioka, "Treatment of paper pulp and paper mill wastewater by coagulation-flocculation followed by heterogeneous photocatalysis" *J. Photoch. Photobio. A* 194 (2008) 1-10.
- [26] I. J. Ochuma, R.P. Fishwick, J. Wood, J.M. Winterbottom, "Photocatalytic oxidation of 2,4,6-trichlorophenol in water using a concurrent downflow contactor reactor", *J. Hazard. Mater.* 144 (2007) 627-633.
- [27] S. Doh, C. Kim, S. Lee, S. Lee, H. Kim, "Development of photocatalytic TiO₂ nanofibers by electrospinning and its application to degradation of dye pollutants", *J. Hazard. Mater.* 154 (2008) 118-127.
- [28] J. Zhao, X. Yang, "Photocatalytic oxidation for indoor air purification: a literature review", *Build. Environ.* 38 (2003) 645-654.
- [29] C.N.R Rao, K.J. Rao, "Phase transitions in solids", McGraw-Hill, New York, 1978.
- [30] K.-W. Kim, E.-H. Lee, Y.-J. Kim, M.-H. Lee, K.-H. Kim, D.-W. Shin, "A relation between the non-stoichiometry and hydroxyl radical generated at photocatalytic TiO₂ on 4CP decomposition", *J. Photoch. Photobio. A* 159 (2003) 301-310.
- [31] R. Pelton, X. Geng, M. Brook, "Photocatalytic paper from colloidal TiO₂-factor or fantasy", *Adv. Colloid. Interfac.* 127 (2006) 43-53.

- [32] P. Appendini, J. H. Hotchkiss, "Review of antimicrobial food packaging", *Innova. Food Sci. Emerg. Technol.* 3 (2002) 113-126.
- [33] C. Chawengkijwanich, Y. Hayata, "Development of TiO₂ powder-coated food packaging film and its ability to inactivate *Escherichia coli* in *vitro* and in actual tests", *Int. J. Food Microbiol.* 123 (2008) 288-292.
- [34] M. Ozdemir, J.D. Floros, "Active Food Packaging Technologies", *Crit. Rev. Food Sci. Nutri.* 44 (2004) 185-193.
- [35] SENTINEL Bioactive Paper Network, <http://www.bioactivepaper.ca>
- [36] H.-J. Kim, Y.-G. Shul, H. Han, "Photocatalytic properties of silica-supported TiO₂", *Top. Catal.* 35 (2005) 287-293.
- [37] L. Zou, Y. Luo, M. Hooper, E. Hu, "Removal of VOCs by photocatalysis process using adsorption enhanced TiO₂-SiO₂ catalyst", *Chem. Eng. Proc.* 45 (2006) 959-964.
- [38] C.-S. Chiou, J.-L. Shie, C.-Y. Chang, C.-C. Liu, C.-T. Chang, "Degradation of di-n-butyl phthalate using photoreactor packed with TiO₂ immobilized on glass beads", *J. Hazard. Mater.* 137 (2006) 1123-1129.
- [39] S. Sakthivel, M.V. Shankar, M. Palanichami, B. Arabindoo, V. Murugesan, "Photocatalytic decomposition of leather dye Comparative study of TiO₂ supported on alumina and glass beads", *J. Photoch. Photobio. A* 148 (2002) 153-159.
- [40] H. Yu, S.C. Lee, J. Yu, C.H. Ao, "Photocatalytic activity of dispersed TiO₂ particles deposited on glass fibers", *J. Mol. Catal. A-Chem.* 246 (2006) 206-211.
- [41] L.M. Daniel, R.L. Frost, H. Zhu, "Laponite-supported titania photocatalysts", *J. Colloid Interf. Sci.* 322 (2008) 190-195.
- [42] N. Dubey, S.S. Rayalu, N.K. Labhsetwar et al., "Photocatalytic properties of zeolite-based materials for the photoreduction of methyl orange", *Appl. Catal. A-Gen.* 303 (2006) 152-157.
- [43] W. Panpa, P. Sujaridworakun, S. Jinawath, "Photocatalytic activity of TiO₂/ZSM-5 composites in the presence of SO₄²⁻ ion", *Appl. Catal. B-Environ.* 80 (2008) 271-276.

- [44] M. Noorjahan, V. D. Kumari, M. Subrahmanyam, P. Boule, "A novel and efficient photocatalyst: TiO₂-HZSM-5 combine thin film", Appl. Catal. B-Environ. 47 (2004) 209-213.
- [45] S. Anandan, M. Yoon, "Review: Photocatalytic activities of the nano-sized TiO₂-supported Y-zeolites", J. Photoch. Photobio. C 4 (2003) 5-18.
- [46] X. Wang, W. Lian, X. Fu, J-M. Basset, F. Lefebvre, " Structure, preparation and photocatalytic activity of titanium oxides on MCM-41 surface", J. Catal. 238 (2006) 13-20.
- [47] L. Pal, "Ef fect of Modified Clay- ZEOLITE PIGMENT on the Viscoelastic, Optical, and Printing Properties of a LWC Gravure Coating", Masters Thesis, Western Michigan University, April 2003.
- [48] M. Padigala, "Ap plication of Porous Media for Inkjet Coatings", Masters Thesis, Western Michigan University, August 2002
- [49] C. P. Klass, "Ne w modified natural zeolite: An effective ink jet coating pigment, and an affordable microparticle retention aid", Paper 360°, August 2007.
- [50] C. P. Klass, M. K. Joyce, "High performance purified natural zeolite pigment for papermaking and paper coating", US 6616748, September 2003.
- [51] C. P. Klass, M. D. Sikora, "Hi gh performance natural zeolite microparticle retention aid for papermaking", US 7201826, April 2007
- [52] TAPPI test method T 261 cm-00, Fines fraction by weight of paper stock by wet screening

CHAPTER II

LITERATURE REVIEW

Photocatalyst and Photocatalysis

What is a photocatalyst?

A photocatalyst is generally defined as a material that has an ability to induce chemical reactions of substances of interest adsorbed on the surface by light-generated active radicals and photocatalysis primarily refers to the chemical transformations of reactive species occurring on the photocatalyst in the presence of the proper light energy [1].

Semiconductors, which have band gaps between conduction and valence bands, are the most common materials used in photocatalysis [1]. Due to such unique physical properties of semiconductor as light absorbers, charge excitation and transport and advantaged combination characteristic of electronic structure, metal oxide semiconductors are of great advantaged to photocatalysis agents [2-4]. Among various semiconductor materials, titanium dioxide (TiO_2) has been widely used as the most effective photocatalyst, which is well-defined photoinduced oxidative and reductive processes resulting from creating charge carriers on titania surface [5].

In particular, since an epoch-making discovery of TiO_2 photoelectrochemical water splitting and hydrogen production using light in 1972 [6], which also referred to as the Fujishima-Honda effect, there have been huge breakthroughs, both scientifically and practically, in various applications of semiconductor photocatalysis. Such research is of constant interest in the field of hydrogen generation by water splitting [7-8],

alternative energy [9-13], sensors [14-16], disinfection [17-20] and extensive environmental cleanup [21-29]. On these wide applications, nanocrystalline TiO₂ has been unchallenged among other semiconductor materials, largely because of their photosensitivity, low cost, easy availability, non-toxicity, chemical and biological stability, even in extreme chemical conditions [30-35].

Crystalline structures of TiO₂

Titanium dioxide is well known to have three main crystalline structures, which have different optical and physical properties, namely anatase, rutile and brookite. The brookite, which has a structure belonging to the orthorhombic crystal system, is usually not used because it is extremely difficult to synthesize pure brookite without coexistence of rutile or anatase phase on single particle. For this reason, although the brookite-type TiO₂ has proper band gap energy (3.14 eV) between anatase and rutile, application of brookite TiO₂ has been highly limited and only found in nature [4].

On the other hand, both anatase and rutile TiO₂ are more common to investigate in industrial and experimental applications and are also easier to make. Diebold [36] has recently reviewed the basic structural characteristics of both anatase and rutile TiO₂, which can be classified into distorted octahedron crystals. Two different crystal structures of anatase and rutile are shown in Figure 2.1 and their different physical properties are summarized in Table 2.1.

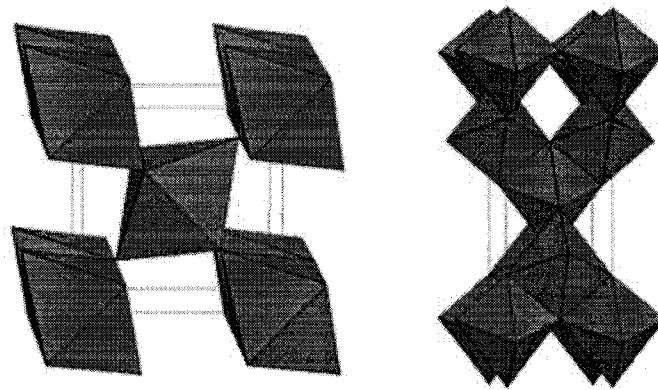


Figure 2.1. TiO₂ crystal structures: Rutile (left) and Anatase (right).
 Source: <http://ruby.colorado.edu/~smyth/min/tio2.html>

Table 2.1. Comparison of Rutile and Anatase Crystalline Properties
 Source: TiO₂ Photocatalysis: Fundamentals and Applications, pp 125

Properties	Rutile	Anatase
Crystalline form	Tetragonal system	Tetragonal system
Band Gap E	3.0 eV	3.2 eV
Corresponding Wavelength	413 nm	388 nm
Lattice constant a	4.58 Å	3.78 Å
Lattice constant c	2.95 Å	9.49 Å
Specific gravity	4.2	3.9
Refractive index	2.71	2.52
Hardness	6.0-7.0	5.5-6.0
Permittivity	114	31
Melting point	1858°C	Changes to Rutile at high temperature.

It is generally known that anatase is transformed to rutile with an

increase in temperature, because the surface free energy has to be minimized to become thermodynamically stable and rutile is the most stable at high temperature among the three main phases [37]. It is also of importance that anatase is more photoactive than the rutile phase, mostly due to the different characteristics of energy levels in the conduction band (CB), as will be more discussed in the mechanism study, the CB energy for rutile is lower in the energy diagram than that of anatase, indicating insufficient reducing potential to produce a superoxide ($O_2^{\cdot-}$) from molecular oxygen (O_2). The superoxide turned out to be one of the important reactant species with the holes and hydroxyl radicals in photooxidative degradation of organic contaminants.

As is well known, different structures govern dissimilar optical and physical properties, which lead to different applications by definition. Indeed, TiO_2 is a material that highly depends on its crystalline phase to determine its pigment and photocatalyst properties.

Basic principles of photocatalysis

Photocatalysis occurs when a photocatalyst such as titanium dioxide, also known as titania, is exposed to photons with at least as much energy as the band gap energy of the photocatalyst. Band gap energy between valence and conduction band means the minimum light energy required to excite the electrons from the valence band to the conduction band, which makes semiconductor materials electrically conductive [38]. Figure 2.2 gives a conceptual mechanism of titania-assisted photocatalytic process on TiO_2 . When the band gap energy is exceeded under 380 nm, the material forms

electron(e^-)-hole(h^+) pairs, which are sets of negatively charged electrons and positively charged vacancies where the electrons used to be. In general, the holes react with H_2O to form hydroxyl ($\cdot OH$) radicals on valence band, which lead to an oxidation reaction of a variety kind of contaminants, such as environmental pollutants and microorganisms [39]. In other words, the oxidizing power of these radicals is the means by which organic chemicals are degraded during photocatalysis, regardless of both aqueous and gaseous surroundings of TiO_2 . On the other hand, electrons (e^-) produced concurrently react with oxygen in the atmosphere to create activated oxygen, the superoxide radical anion ($O_2^{\cdot -}$), acting as a reductant.

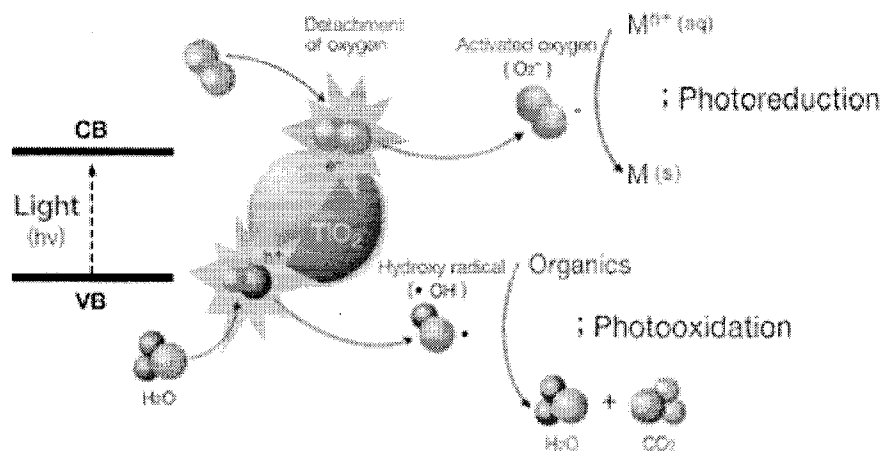


Figure 2.2. Schematic mechanism of photocatalytic process over TiO_2 .
Source: <http://www.nanoin.com>

A number of fundamental mechanistic studies have been conducted on photodecomposition of organic compounds over TiO_2 surfaces [40-42] and the featured time for each primary elementary process has been described as

shown in Table 2.2. The steps of photocatalytic reactions from activation by UV light to decompose organic compounds can be reasonably simplified as follows; [1, 43-44]

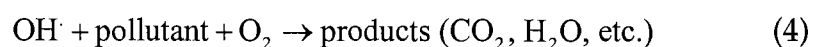
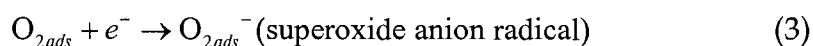


Table 2.2. Primary Process and Time Domains in Titania-Catalyzed Mineralization of Organic Pollutants
Source: J. Photoch. Photobio. C 9 (2008) pp3

Primary Process	Characteristic time
Charge carrier generation $\text{TiO}_2 + h\nu \rightarrow e^- + h^+$	Fs (very fast)
Charge carrier trapping $h^+ + >\text{Ti}^{\text{IV}}\text{OH} \rightarrow \{>\text{Ti}^{\text{IV}}\text{OH}^{++}\}$ $e^- + >\text{Ti}^{\text{IV}}\text{OH} \rightleftharpoons \{>\text{TiOH}^{\text{III}}\}$ $e^- + >\text{Ti}^{\text{IV}} \rightarrow \text{Ti}^{\text{III}}$	10 ns (fast) 100 ps (shallow trap; dynamic equilibrium) 10 ns (deep trap)
Charge carrier combination $e^- + \{>\text{Ti}^{\text{IV}}\text{OH}^{++}\} \rightarrow >\text{Ti}^{\text{IV}}\text{OH}$ $h^+ + >\text{Ti}^{\text{III}}\text{OH} \rightarrow \text{Ti}^{\text{IV}}\text{OH}$	100 ns (slow) 10 ns (fast)
Interfacial charge transfer $\{>\text{Ti}^{\text{IV}}\text{OH}^{++}\} + \text{organic molecule} \rightarrow >\text{Ti}^{\text{IV}}\text{OH} + \text{oxidized molecule}$ $\{>\text{Ti}^{\text{III}}\text{OH}\} + \text{O}_2 \rightarrow >\text{Ti}^{\text{IV}}\text{OH} + \text{O}_2^{\cdot-}$	100 ns (slow) mili second (very slow)

Environmental applications of TiO₂ photocatalyst

Titanium dioxide (TiO₂) is one of the basic materials that are found easily in our circumstance and daily life. Due to its superior optical properties of a high refractive index and whiteness, TiO₂ has long been engaged in such applications requiring high opacity and brightness as coatings, paints, plastics, ink, cosmetics and paper [45-46].

During the last two decades, especially as a photocatalytic semiconductor material, TiO₂ has become more attractive as a promising means of environmental purification attributing to exceptional characteristics, to be exact, it is photosensitive to promote photooxidation at room temperature, it is inexpensive, non-toxic and chemically stable, no chemicals needed in the photocatalytic system to complete photodegradation and wide range of pollutants of our choice can be decomposed by this system [28-33]. These benefits have led to its broad applications [5-27] and a diversity of TiO₂-based photocatalytic products has been commercialized since the mid-1990s. The volume of markets and industries has been growing in prominence both environmental and bactericidal applications, as listed in Table 2.3.

Table 2.3. Selected Applications of Photocatalysis
 Source: International J. Hydrogen Energy 32 (2007) pp 2670

Property	Category	Application
Self-Cleaning	Materials for residential and office buildings	Exterior tiles, kitchen and bathroom components, interior furnishings, plastic surfaces, aluminum siding
	Indoor and outdoor lamps and related systems	Translucent paper for indoor lamp covers, coatings on fluorescent lamps and highway tunnel lamp cover glass
	Materials for roads	Tunnel wall, soundproofed wall, traffic signs and reflectors
	Others	Tent material, cloth for hospital garments and uniforms and spray coating for cars
Air Cleaning	Indoor air cleaners	Room air cleaner, photocatalyst-equipped air conditioners and interior air cleaner for factories
	Outdoor air purifiers	Concrete for highways, roadways and footpaths
Water Purification	Drinking water	River water, ground water, lakes and water-storage tanks
	Others	Fish feeding tanks, drainage water and industrial wastewater
Antitumor	Cancer therapy	Endoscopic-like instruments
Self-sterilizing	Hospital	Tiles and coatings to cover the floor, walls and ceiling of operation rooms, hospital garments and uniforms
	Others	Public restroom, pet breeding rooms

Zeolite: Principles and Applications

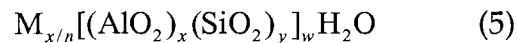
Zeolite composition and structure

The zeolite is named after the two Greek words, boils for 'Zeo' and stones for 'lithos' [47]. By Smith in 1971 [48], a zeolite has been conceptually defined as:

a crystalline aluminosilicate with a tetrahedral framework structure enclosing cavities occupied by cations and water molecules, both of which have enough freedom of movement to permit cation exchange and reversible dehydration.

According to the above definition, zeolites are highly crystalline aluminosilicate materials with well-defined pore structure originating from a three dimensional framework of SiO_4 and AlO_4 tetrahedra [49-50]. Figure 2.3 depicts the framework structure of zeolite. Either a Si^{4+} or an Al^{3+} can be located within the tetrahedral sites, which are formed by sharing the oxygen atoms between interconnected tetrahedra, and thus it sometimes called TO_4^- tetrahedral, where T is silicon or aluminum. Due to the unbalance charge between $(\text{AlO}_4)^{5-}$ and $(\text{SiO}_4)^{4-}$, zeolite is structurally negative charged and thus extra counterions are required to the AlO_4^- to produce electrical neutrality that make zeolite ion-exchangeable [51].

Zeolites are exemplified by structure formula consisting of the crystallographic unit cell as follows;



where n is the cation (M) balance, w is the number of water molecules per unit cell, x and y are total number of tetrahedral per unit cell and x/y is a ratio of Si/Al in framework referring to as zeolite composition [52]. The cations are feasible to exchange with either proton or transition metals,

accordingly properties of zeolite can be modified by the type of cation. The chemical elements used normally in cation exchange are NH_4^+ , H^+ , tetramethylammonium (TMA^+), the rare-earth and noble metal ions, the alkaline (Na^+ , K^+ , Rb^+ , Cs^+) and alkaline earth (Mg^+ , Ca^+) ion and other nitrogen-containing organic cations [53-54]. It is quite pronounced that the different arrangement of tetrahedra give rise to myriads of open framework structures, which determine the pore structure, the size and shape of channels and cages with high surface area. Three dimensional frameworks ultimately consist of channels and interconnected voids or cages.

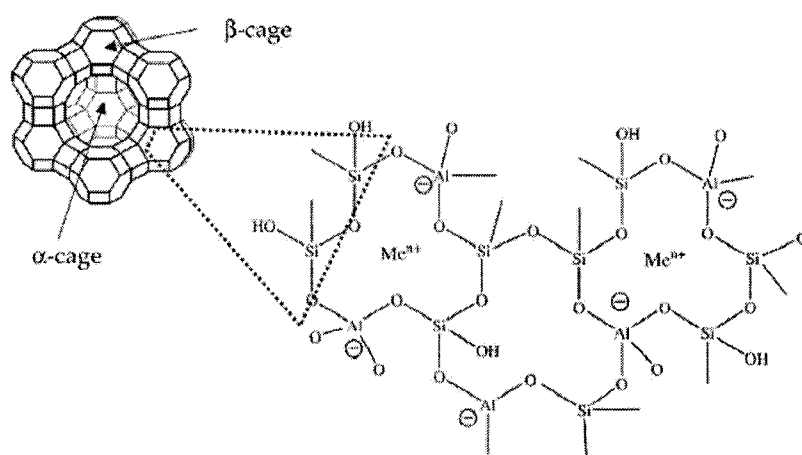


Figure 2.3. Illustration of three- and two-dimensional zeolite framework.
Source [57]: Trends in Analytical Chemistry, Vol. 25, No. 1, 2006 pp25

There are various factors influencing the characteristics of zeolite, to be exact, they extensively depend on the structure of framework, channel size and shape, the ordering and local environment of T-atoms and the size and location of cations within the framework [55-56]. It is therefore extremely

important to recognize the structural properties of zeolites in perception of phenomena associating with catalytic reactivity and adsorptive features as a diffusion medium, sorbent and molecular sieve.

Industrial applications of zeolites

A large number of zeolites have been proposed and 40 known natural zeolites and about 200 zeolites that are not naturally occurring have been synthesized with varied Si/Al ratios [58]. Of the great variety of zeolites, just a few types, mostly synthetic and synthetic-analog natural zeolites, are commercially found in industrial applications. For the industrial catalytic process, zeolites having medium to large pore size are of intense interest and such zeolites belong to a group of 10 or 12 member rings of oxygen atoms with relatively high Si/Al ratio [59]. In general, the pore structure differs considerably from one zeolite to another and its pore diameter is varied by the free aperture arising from 4, 6, 8, 10, 12 or 18 member rings of oxygen atoms. Extra-large pores that consist of more than 12 member rings and mesoporous zeolites have been recently synthesized [60-61]. Zeolites of high current interest in the major industrial process include zeolite Y and mordenite, which have a 12 member ring and zeolite ZSM-5, which has a 10 member ring system. Table 2.4 lists the pore diameters in zeolites and Figure 2.4 shows pictorial structures of selected zeolites.

Table 2.4. Pore Types and Diameters in Zeolites
 Source [62]: Chemical Reviews, Vol. 106, No. 3, 2006 pp 1079

Zeolite	Pore Type	Dimensions
Zeolite Y	Interconnected	7.4 Å diameter pore
	Spherical Supercage	11.8 Å diameter cavity
ZSM-5	Interconnected	5.5 Å x 5.6 Å opening
	Channels	5.1 Å x 5.5 Å opening
Mordenite	Interconnected	6.5 Å x 7.0 Å channel
	Channels	2.6 Å x 5.7 Å channel
Beta-Zeolite	Interconnected	7.6 Å x 6.4 Å channel
	Channels	5.5 Å x 5.5 Å channel
Zeolite A	Interconnected	4.1 Å diameter pore
	α -cage	11 Å diameter cavity
MCM-41	Mesoporous	3~10 nm

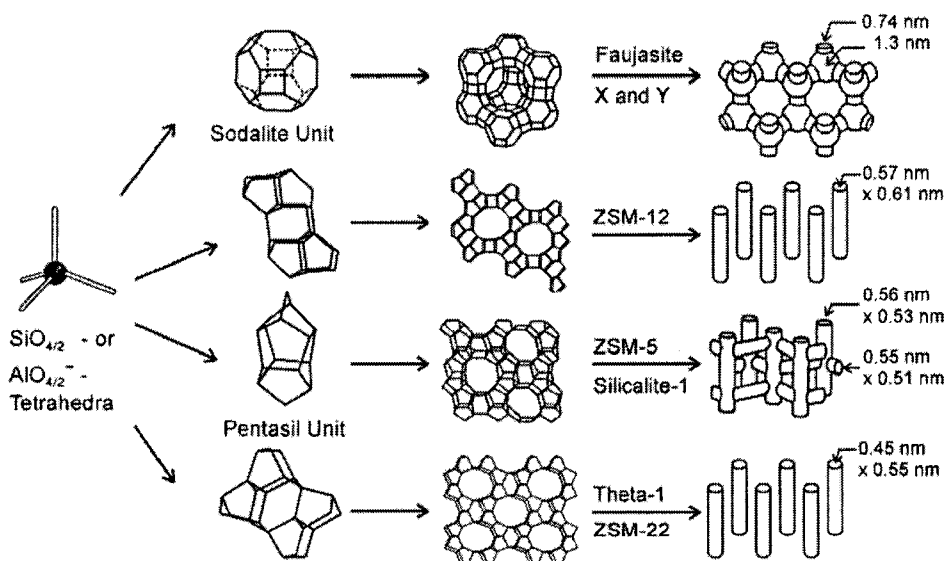


Figure 2.4. Framework structures of selected zeolites.
 Source [63]: Solid State Ionics Vol. 131, 2000 pp177.

Zeolites have been of great interest as catalysts and adsorptive materials for the last four decades, because of their high surface area, activity, confinement and unusual selectivity, frequently called molecular sieve property, mostly related to solid acid catalyzed processes, for example, isomerization, cracking, hydrocracking, etc [64-65]. The catalytic active sites of zeolite are originated from imbalanced charge in the framework between Si and Al ions that make them amphoteric, including Lewis- and Brønsted-acid sites [66]. All heterogeneous catalysis of zeolite takes place at acidic sites in the channels, cavities or cages formed by interconnected three dimensional frameworks [67-68]. The major commercial industrial processes based on zeolite catalysts are listed in Table 2.5.

Table 2.5. Major Commercial Process Based on Zeolite Catalysts
Source: Zeolite Catalysis: Principles and Applications, pp 241

Process	Zeolite	Products
Catalytic Cracking	Faujasite (Zeolite X or Y)	Gasoline, Fuel oil
Hydrocracking	Faujasite (Zeolite X or Y)	Kerosene, Jet fuel, BTX
Hydroisomerization	Mordenite	i-Hexane, Heptane
Iso/n-paraffin separation	Ca ⁺ - Zeolite A	Pure n-paraffin
Dewaxing	ZSM-5, Mordenite	Lubes
Olefin Drying	K ⁺ - Zeolite A	Polyolefin feed
Benzene Alkylation	ZSM-5	Styrene
Xylene Isomerization	ZSM-5	p-Xylene

Natural zeolite and its use in papermaking and paper coating

Natural zeolite has been practically used to control malodor arising from enclosed livestock-breeding spots, such as cat litter, pet shops, kennels and zoos. By and large, natural zeolite has all the advantages of inexpensive cost and abundant reserves, while it has relatively smaller channels, difficulty in purification and inconsistent properties compared with uniform synthetic zeolite. Due to high sorption capacity and its modification by selective cation-exchange [69], however, natural zeolite has been recently well demonstrated for the application of environmental remediation [70-71], especially adsorption process of organic and heavy metals [72] and gas separation [73].

Clinoptilolite, one of the most frequently occurring natural zeolite among more than 40 natural zeolite minerals, is a representative natural zeolite that has been thoroughly studied for modification of its chemical-physical properties [74-75]. Figure 2.5 shows clinoptilolite framework model. The structure of clinoptilolite has a rigid two-dimensional channel system that can be usually occupied by water, cations ion-exchanged and other organic molecules. Two cages in a three-dimensional network are created by intersections of interconnected channels and water and adsorptive materials freely go in and out of pores, without damage to the crystalline structure [76].

With regard to papermaking and coating, an interesting application of this natural zeolite has been announced with two potential uses; low-cost microparticle retention aid in papermaking and purified pigment for ink jet coating [77]. It was revealed that a highly purified clinoptilolite zeolite pigment makes it possible to significantly improve printing quality and economics in ink jet and digital printing and it also may be suitable as a

complementary pigment to make coated paper and paperboard for water-based gravure and flexography. The results of this work has been patented by Klass and Joyce [78-80].

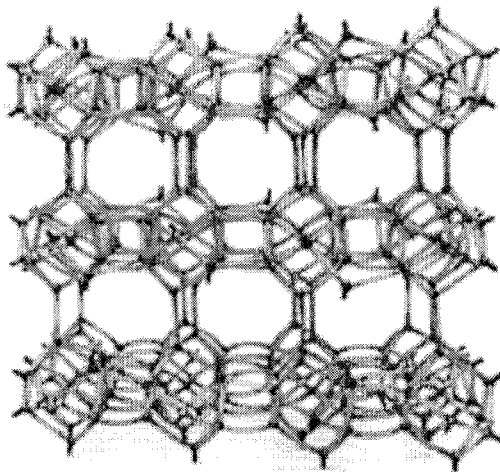


Figure 2.5. Framework structure of Clinoptilolite.
Source: <http://www.zeoponix.com/zeolite.htm>

Natural zeolite has also been tested as a retention aid in papermaking because it showed high self retaining characteristics in uncoated paper to get rid of print-thorough. The evaluation of retention effect was confirmed by comparing it to bentonite and silica used typically in microparticle retention systems and it was evident that natural zeolite performs outstandingly as a microparticle retention aid in both alkaline and acid papermaking furnishes. Another patent was issued from this line of work with clinoptilolite zeolite [81].

Photocatalytic Paper

Definition and overview

By Pelton, Geng and Brook [82], photocatalytic paper is defined as paper and non-woven fabrics that have a light-activated catalytic function to decompose organic pollutants and kill pathogens. Figure 2.6 illustrates briefly how photocatalytic paper functions. Since the first photoactive TiO_2 containing paper introduced by Matsubara et al. in 1995 [83], a few publications and patents have been announced as already summarized elsewhere [82]. H. Tanaka et al [84-88] have successfully prepared different types of photocatalytic paper composites with a dual polymeric retention system, using TiO_2 supported on the ceramic fibers. These were shown to remove effectively hazardous chemicals both bisphenol A in wastewater and indoor air pollutants such as acetaldehyde and toluene. The kinetic study of TiO_2 containing paper on the photooxidation of ketones was also performed in the gaseous phase and it was shown that water vapor tends to adsorb competitively with ketones and thereby, significantly affects the adsorption behavior on TiO_2 particles [89].

In addition, for a photocatalytic removal of nitrogen oxides (NO_x), different TiO_2 sheets have been prepared and reported that both photocatalytic papers combined with zeolite A [90] and treated with alkaline metal compounds including CaO , MgO , CaCO_3 , Al_2O_3 and Fe_2O_3 [91] were substantially effective for NO_x photodegradation. More recently, it was revealed that void structures of photocatalytic paper have considerable influence on the photocatalytic function [92].

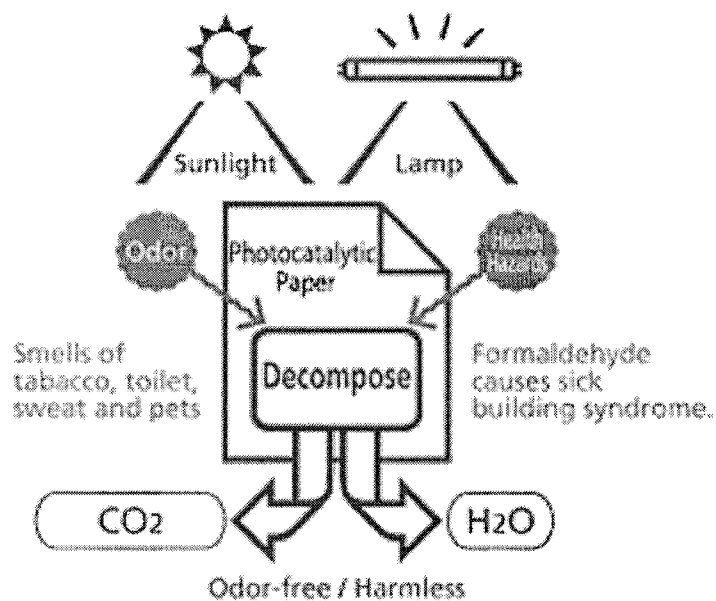


Figure 2.6. Photocatalysis process on photocatalytic paper.
 Source: http://web-japan.org/trends/07_sci-tech/sci080131.html

To the best of knowledge, commercial photocatalytic paper is developed and produced by three different companies, namely, Nippon Paper Group (Tokyo, Japan), Ahlstrom (Helsinki, Finland) and Ein Co. Ltd (Gifu, Japan). Nippon paper has announced the development of a new photocatalytic newsprint with an air purification effect [93] and more recently presented a photocatalytic coated paper based on TiO₂ converged technology [94]. Another Japanese company, Ein Co. Ltd. has patented [95] their own technique, specifically focused on environmental technology and developed a photocatalytic pulp, which can be applied for various types of products. Ahlstrom [96], on the other hand, has produced TiO₂ immobilized non-woven paper with an inorganic binder and N. Barka et al [97] has examined photocatalytic decomposition of Rhodamine B using coated TiO₂

photocatalyst on non-woven paper with an aqueous phase colloidal SiO_2 as an inorganic binder. As a result, they were determined the factors influencing the rate of photocatalytic degradation and their sensitivity on photocatalytic performance for the non-woven TiO_2 paper. Besides, A. Aguedach et al [98] also found that the photodegradation rate of azo dye, such as reactive black 5 (RB 5), is strongly affected by the ionic strength in dye solution when TiO_2 is coated on the non-woven paper with silica binder.

Preparation methods of photocatalytic paper

The approaches of the photocatalytic paper are largely classified into wet-end papermaking and paper coating. For wet-end papermaking, TiO_2 powders are deposited on the fibers with retention aids, which are chemicals, such as inorganic salts, natural or synthetic polymers, added to the papermaking stock to improve the retainability of fiber fines, mineral fillers and other additives [99]. It is thus important to retain TiO_2 (nano) particles in the paper sheet formed on the forming machine with a fast drainage process in using the traditional papermaking process. However, since it is normally possible to come about fiber-fiber or fines-fines flocculation by high molecular weight retention aids, it should be identified that TiO_2 particles are embedded in the fiber matrix as long as possible during the sheet formation. By the wet-end papermaking technique, the TiO_2 contents in photocatalytic paper are less likely to exist at the surface, more likely to be in its interior because drainage forces compel fillers to draw out into the fiber web.

In paper coatings, TiO_2 has been considered as an essential pigment to provide desirable optical properties, such as opacity and brightness, in

coating formulation generally mixing with other additives, which are principally used for improving the printability of coated paper. Genuinely, TiO_2 is the material that has two sides, but one set of properties and photoactivity, one side of intrinsic characteristics, has been an occasionally regarded factor that should be controlled for a quite long time, because it tends to deteriorate the quality of coating, printing and more seriously, paper itself by photocatalysis. Nonetheless, a number of TiO_2 coated samples focused on photocatalytic effect have been presented [90,100] using either paper or non-woven substrates, since coating readily increases the opportunity for contacting organic contaminants with TiO_2 particles as well as uniform distribution on the paper surface. In this sense, it would be interesting to see an air-purifying paper (Nippon Paper Industries) developed through the combination of pre-binding titania with an inorganic binder, which is a smaller inorganic material even than TiO_2 particles, prior to coating the substrate [101].

Applications of photocatalytic paper

It is generally conceded that photocatalytic paper is reasonably applicable to environmental and hygienic purposes, in short, degradation and disinfection. Moreover, photocatalytic paper, combined with high performance filter paper secures a healthful life in virtue of photodestructuring various pathogens and germs, hazardous organic molecules and obnoxious substances. The applications of photocatalytic paper based on either paper or non-woven substrate have been spreading to predominantly indoor air purification, sanitary product and food packaging.

The expanding applications of this unique paper are summarized in Table 2.6.

Table 2.6. The Expanding Applications of Photocatalytic Paper
Summarized from <http://www.ein.co.jp/en/paper/various.html>

Purpose	Function	Application
Indoor Air Purification	Purifying hazardous materials and germs floating in the air Relieving sick building syndrome (SBS)	Wallpaper, screen, lighting, sliding door paper, sliding screen paper
Hygiene (Individual & Public)	Disinfection Antimicrobial	Mask, paper diaper, tissue paper, hand towel, toilet sheet, poster/calendar, dust box, paper cover, etc.
Food Packaging	Resistant to food poisoning Disinfection & Antibacterial	Wrapping paper, paper cup, napkin, safe milk package, paper sheet for fresh fish, meat, uncooked gift, fruits, etc.

References

- [1] A. Mills, S.L. Hunte, "An overview of semiconductor photocatalysis", J. Photoch. Photobio. A 108 (1997) 1-35.
- [2] D. A. Tryk, A. Fujishima, K. Honda, "Recent topics in photoelectrochemistry: achievements and future prospects", Electrochim. Acta 45 (2000) 2363-2376.
- [3] N. Serpone, A. Salinaro, A. Emeline, V. Ryabchuk, "Turn overs and photocatalysis: A mathematical description", J. Photoch. Photobio. A 130 (2000) 83-94.
- [4] A. Fujishima, K. Hashimoto, H. Watanabe, "TiO₂ Photocatalysis: Fundamentals and Applications", BKC, Inc. Tokyo, Japan, 1997.

- [5] H. Kim, S. Lee, Y. Han, J. Park, "Preparation of dip-coated TiO₂ photocatalyst on ceramic foam pellets", *J. Mater. Sci.* 40 (2005) 5295-5298.
- [6] A. Fujishima, K. Honda, "Electrochemical Photolysis of Water at a Semiconductor Electrode", *Nature* 238 (1972) 37-38.
- [7] M. Ni, Michael K.H. Leung, Dennis Y.C. Leung, K. Sumathy, "A review and recent developments in photocatalytic water-splitting using TiO₂ for hydrogen production", *Renew. Sust. Energ. Rev.* 11 (2007) 401-425.
- [8] A. Fujishima, X. Zhang, D.A. Tryk, "Heterogeneous photocatalysis: From water photolysis to application in environmental cleanup", *Int. J. Hydrogen Energ.* 32 (2007) 2664-2672.
- [9] M. Gratzel, "Photoelectrochemical cells", *Nature* 414 (2001) 338-344.
- [10] M. Gratzel, "Dye-sensitized solar cells", *J. Photoch. Photobio. C* 4 (2003) 145-153.
- [11] L. Yang, Y. Lin, J. Jia et al., "Cauliflower-like TiO₂ rough spheres: Synthesis and applications in dye sensitized solar cells", *Micropor. Mesopor. Mat.* 112 (2008) 45-52.
- [12] H. Ekström, B. Wickman, M. Gustavsson et al., "Nanometer-thick films of titanium oxide acting as electrolyte in the polymer electrolyte fuel cell", *Electrochim. Acta.* 52 (2007) 4239-4235.
- [13] M. Gustavsson, H. Ekström, P. Hanarp et al., "Thin film Pt/TiO₂ catalysts for the polymer electrolyte fuel cell", *J. Power Sources* 163 (2007) 671-678.
- [14] A. Curulli, F. Valentini, G. Padeletti et al., "Smart (Nano) materials: TiO₂ nanostructured films to modify electrodes for assembling of new electrochemical probes", *Sensor. Actuat. B-Chem.* 111-112 (2005) 441-449.
- [15] L. Francioso, A.M. Taurino, A. Forleo, P. Siciliano, "TiO₂ nanowires array fabrication and gas sensing properties", *Sensor. Actuat. B-Chem.* 130 (2008) 70-76.
- [16] M.G. Manera, J. Spadavecchia, D. Buso et al., "Optical gas sensing of TiO₂ and TiO₂/Au nanocomposite thin films", *Sensor. Actuat. B-Chem.* 132 (2008) 107-115.

- [17] K. Sunada, Y. Kikuchi, K. Hashimoto, A. Fujishima, "Bactericidal and Detoxification Effects of TiO₂ Thin Film Photocatalyst", *Environ. Sci. Technol.* 32 (1998) 726-728.
- [18] G. Fu, P.S. Vary, C.-T. Lin, "Anatase TiO₂ Nanocomposites for Antimicrobial Coatings", *J. Phys. Chem. B* 109 (2005) 8889-8898.
- [19] K.S. Yao, D.Y. Wang, W.Y. Ho, J.J. Yan, K.C. Tzeng, "Photocatalytic bactericidal effect of TiO₂ thin film on plant pathogens", *Surf. Coat. Tech.* 201 (2007) 6886-6888.
- [20] C. Guillard, T.-H. Bui, C. Felix et al., "Microbiological disinfection of water and air by photocatalysis", *C. R. Chim.* 11 (2008) 107-113.
- [21] C.H. Ao, S.C. Lee, Y.Z. Yu, J.H. Xu, "Photodegradation of formaldehyde by photocatalyst TiO₂: effects on the presences of NO, SO₂ and VOCs", *Appl. Catal. B- Environ.* 54 (2004) 41-50.
- [22] J. Zhao, C. Chen, W. Ma, "Photocatalytic degradation of organic pollutants under visible light irradiation", *Top. Catal.* 35 (2005) 269-278.
- [23] A. Strini, S. Cassese, L. Schiavi, "Measurement of benzene, toluene, ethylbenzene and O-xylene gas phase photodegradation by titanium dioxides dispersed in cementitious materials using a mixed flow reactor", *Appl. Catal. B- Environ.* 61 (2005) 90-97.
- [24] L. Reijnders, "Hazard reduction for the application of titania nanoparticles in environmental technology", *J. Hazard. Mater.* 152 (2008) 440-445.
- [25] A.C. Rodrigues, M. Boroski, N.S. Shimada, et al., "Treatment of paper pulp and paper mill wastewater by coagulation-flocculation followed by heterogeneous photocatalysis" *J. Photoch. Photobio. A* 194 (2008) 1-10.
- [26] I.J. Ochuma, R.P. Fishwick, J. Wood, J.M. Winterbottom, "Photocatalytic oxidation of 2,4,6-trichlorophenol in water using a concurrent downflow contactor reactor", *J. Hazard. Mater.* 144 (2007) 627-633.
- [27] S. Doh, C. Kim, S. Lee, S. Lee, H. Kim, "Development of photocatalytic TiO₂ nanofibers by electrospinning and its application to degradation of dye

- pollutants", *J. Hazard. Mater.* 154 (2008) 118-127.
- [28] S. Malato, J. Blanco, D.C. Alarcón et al., "Photocatalytic decontamination and disinfection of water with solar collectors", *Catal. Today* 122 (2007) 137-149.
- [29] C. Euvananont, C. Junin, K. Inpor, P. Limthongkul, C. Thanachayanont, "TiO₂ optical coating layers for self-cleaning applications", *Ceram. Int.* 34 (2008) 1067-1071.
- [30] O. Carp, C.L. Huisman, A. Reller, "Photoinduced reactivity of titanium dioxide", *Prog. Solid State Chem.* 32 (2004) 33-177.
- [31] M.R. Hoffmann, S.T. Martin, W. Choi, D.W. Bahnemann, "Environmental applications of semiconductor photocatalysis", *Chem. Rev.* 95 (1995) 69-96.
- [32] A.L. Linsebigler, G. Lu, J.T. Yates Jr., "Photocatalysis on TiO₂ surfaces: Principles, Mechanisms, and Selected Results", *Chem. Rev.* 95 (1995) 735-758.
- [33] A. Fujishima, T.N. Rao, D.A. Tryk, "Titanium dioxide photocatalysis", *J. Photoch. Photobio. C* 1 (2000) 1-21.
- [34] T.L. Thompson, J.T. Yates Jr., "Surface science studies of the photoactivation of TiO₂-New photochemical processes", *Chem. Rev.* 106 (2006) 4428-4453.
- [35] M.A. Fox, M.T. Dulay, "Heterogeneous Photocatalysis", *Chem. Rev.* 93 (1993) 341-357.
- [36] U. Diebold, "The surface science of titanium dioxide", *Surf. Sci. Rep.* 48 (2003) 53-229.
- [37] C.N.R Rao, K.J. Rao, "Phase transitions in solids", McGraw-Hill, New York, 1978.
- [38] U.I. Gaya, A.H. Abdullah, "Heterogeneous photocatalytic degradation of organic contaminants over titanium dioxide: A review of fundamentals, progress and problems", *J. Photoch. Photobio C* 9 (2008) 1-12.
- [39] K. Kim, E. Lee, Y. Kim et al., "A relation between the non-stoichiometry

and hydroxyl radical generated at photocatalytic TiO₂ on 4CP decomposition", *J. Photoch. Photobio. A* 159 (2003) 301-310.

[40] J. Clarke, R.R. Hill, D.R. Robert, "Primary Processes in the Catalytic Photooxidation of *p*-Cresol", *J. Chem. Tech. Biotechnol.* 68 (1997) 397-404.

[41] X. Yang, N. Tamai, "How fast is interfacial hole transfer? In situ monitoring of carrier dynamics in anatase TiO₂ nanoparticles by femtosecond laser spectroscopy", *Phys. Chem. Chem. Phys.* 3 (2001) 3393-3398.

[42] M. Sleiman, P. Conchon, C. Ferronato, J.-M. Chovelon, "Iodosulfuron degradation by TiO₂ photocatalysis: Kinetic and reactional pathway investigations", *Appl. Catal. B-Environ.* 71 (2007) 279-290.

[43] J. Zhao, X. Yang, "Photocatalytic oxidation for indoor air purification: a literature review", *Buil. Environ.* 38 (2003) 645-654.

[44] V. Augugliaro, M. Litter, L. Palmisano, J. Soria, "The combination of heterogeneous photocatalysis with chemical and physical operations: A tool for improving the photoprocess performance", *J. Photoch. Photobio C* 7 (2006) 127-144.

[45] J.D. Peel, "Paper science and paper manufacturing", Angus Wilde Publications Inc. Vancouver, Canada, 1999.

[46] G. Buxbaum, G. Pfaff, "Industrial Inorganic Pigments", Wiley-VCH, Weinheim, Germany 3rd Ed. 2005.

[47] D.W. Breck, "Zeolite Molecular Sieves: Structure, Chemistry and Use", Wiley, New York (1974).

[48] J.V. Smith, "Origin and structure of zeolites in Zeolite Chemistry and Catalysis", J.A. Rabo Ed. ACS Monogr. 171 (1976) 1.

[49] R. Szostak, "Molecular Sieves Principles of Synthesis and Identification", Van Nostrand Reinhold, New York, Chap. 1 (1989).

[50] S. Bhatia, "Zeolite Catalysis Principles & Applications", 1st Ed., CRC Press Inc. (1990).

[51] S. Hashimoto, "Zeolite photochemistry: impact of zeolites on

photochemistry and feedback from photochemistry to zeolite science", *J. Photoch. Photobio. C* 4 (2003) 19-49.

[52] M.G. Valdés, A.I. Pérez-Cordoves, M.E. Díaz-García, "Zeolites and zeolite-based materials in analytical chemistry", *Trends Anal. Chem.* 25 (2006) 24-30.

[53] E.M. Flanigen, "Zeolites and Molecular Sieves an Historical Perspective", *Stud. Surf. Sci. Catal.* 58 (1991) 13-34.

[54] A. Dyer, "An Introduction to Zeolite Molecular Sieve", Wiley, New York (1988).

[55] T. Frising, P. Leflaive, "Extraframework cation distribution in X and Y faujasite zeolites: A review", *Micropor. Mesopor. Mat. In press* (2008).

[56] Y. Ma, W. Tong, H. Zhou, S.L. Suib, "A review of zeolite-like porous materials", *Micropor. Mesopor. Mat.* 37 (2000) 243-252.

[57] P.K. Dutta, Y. Kim, "Photochemical processes in zeolites: new developments", *Curr. Opin. Solid St. M.* 7 (2003) 483-490.

[58] W.M. Meier, D.H. Olson, C. Baerlocher, "Atlas of Zeolite Structure Types", 4th Ed. Elsevier (1996).

[59] C.N. Satterfield, "Heterogeneous Catalysis in Industrial Practice", 2nd Ed., McGraw Hill International, (1993).

[60] J.S. Beck, J.C. Vartuli, W.G. Roth et al. "A New Family of Mesoporous Molecular Sieves Prepared with Liquid Crystal Templates", *J. Am. Chem. Soc.* 114 (1992) 10834-10843.

[61] M. Ziolk, "Catalytic liquid-phase oxidation in heterogeneous system as green chemistry goal-advantages and disadvantages of MCM-41 used as catalyst", *Catal. Today* 90 (2004) 145-150.

[62] G. Sartori, R. Maggi, "Use of Solid Catalysts in Friedel-Crafts Acylation Reactions", *Chem. Rev.* 106 (2006) 1077-1104.

[63] J. Weitkamp, "Zeolites and catalysis", *Solid State Ionics* 131 (2000) 175-188.

- [64] K. Tanabe, W.F. Hölderich, "Industrial application of solid acid-base catalysts", *Appl. Catal. A* 181 (1999) 399-434.
- [65] R.J. Schmidt, "Industrial catalytic processes-phenol production", *Appl. Catal. A-Gen.* 280 (2005) 89-103.
- [66] A. Corma, "Inorganic Solids Acids and Their Use in Acid-Catalyzed Hydrocarbon Reactions", *Chem. Rev.* 95 (1995) 559-614.
- [67] A. Corma, "State of the art and future challenges of zeolites as catalyst", *J. Catal.* 216 (2003) 298-312.
- [68] T. L. M. Maesen, R. Krishna, J.M. van Baten, et al., "Shape-selective n-alkane hydroconversion at exterior zeolite surfaces", *J. Catal.* 256 (2008) 95-107.
- [69] G. Rodríguez-Fuentes, "Design and development of new zeolitic materials based on natural clinoptilolite", *Stud. Surf. Sci. Catal.* 170 (2007) 2074-2079.
- [70] R.S. Bowman, "Review: Application of surfactant-modified zeolites to environmental remediation", *Micropor. Mesopor. Mat.* 61 (2003) 43-56.
- [71] C.R. Oliveira, J. Rubio, "New basis for adsorption of ionic pollutants onto modified zeolites", *Miner. Eng.* 20 (2007) 552-558.
- [72] S.E. Bailey, T.J. Olin, R. M. Bricka, D.D. Adrian, "A review of potentially low-cost sorbents for heavy metals", *Wat. Res.* 33 (1999) 2469-2479.
- [73] M.W. Ackley, S.U. Rege, H. Saxena, "Review: Application of natural zeolites in the purification and separation of gases", *Micropor. Mesopor. Mat.* 61 (2003) 25-42.
- [74] A. Lam, A. Rivera, G. Rodríguez-Fuentes, "Theoretical study of metronidazole adsorption on clinoptilolite", *Micropor. Mesopor. Mat.* 49 (2001) 157-162.
- [75] A. Lam, L.R. Sierra, G. Rojas et al., "Theoretical study of physical adsorption of aspirin on natural clinoptilolite", *Micropor. Mesopor. Mat.* 23 (1998) 247-252.

- [76] P. Kowalczyk, M. Sprynskyy, A.P. Terzyk et al., "Porous structure of natural and modified clinoptilolites", *J. Colloid. Interf. Sci.* 297 (2006) 77-85.
- [77] C.P. Klass, "New modified natural zeolite: An effective ink jet coating pigment, and an affordable microparticle retention aid", Paper 360^o, August 2007.
- [78] L. Pal, "Effect of Modified Clay- ZEOLITE PIGMENT on the Viscoelastic, Optical, and Printing Properties of a LWC Gravure Coating", Masters Thesis, Western Michigan University, April 2003.
- [79] M. Padigala, "Application of Porous Media for Inkjet Coatings", Masters Thesis, Western Michigan University, August 2002.
- [80] C.P. Klass, M.K. Joyce, "High performance purified natural zeolite pigment for papermaking and paper coating", US 6616748, September 2003.
- [81] C.P. Klass, M.D. Sikora, "High performance natural zeolite microparticle retention aid for papermaking", US 7201826, April 2007.
- [82] R. Pelton, X. Geng, M. Brook, "Photocatalytic paper from colloidal TiO₂-factor fantasy", *Adv. Colloid. Interfac.* 127 (2006) 43-53.
- [83] H. Matsubara, M. Takada, S. Koyama, K. Hashimoto A. Fujishima, "Photoactive TiO₂ containing paper: Preparation and its photocatalytic activity under weak UV light illumination", *Chem. Letters* (1995) 767-768.
- [84] Y. Iguchi, H. Ichiura, T. Kitaoka, H. Tanaka, "Preparation and characteristics of high performance paper containing titanium dioxide photocatalyst supported on inorganic fiber matrix", *Chemosphere* 53 (2003) 1193-1199.
- [85] S. Fukahori, H. Ichiura, T. Kitaoka, H. Tanaka, "Capturing of bisphenol A photodecomposition intermediates by composite TiO₂-zeolite sheets", *Appl. Catal. B: Environ.* 46 (2003) 453-462.
- [86] H. Ichiura, T. Kitaoka and H. Tanaka, "Removal of indoor pollutants under UV irradiation by a composite TiO₂-zeolite sheet prepared using a papermaking technique", *Chemosphere* 50 (2003) 79-83.

- [87] S. Fukahori, H. Ichiura, T. Kitaoka, H. Tanaka, "Photocatalytic decomposition of bisphenol A in water using composite TiO₂-Zeolite sheets prepared by a papermaking technique", *Environ. Sci. Technol.* 37 (2003) 1048-1051.
- [88] H. Ichiura, T. Kitaoka, H. Tanaka, "Preparation of composite TiO₂-zeolite sheets using a papermaking technique and their application to environmental improvement: Part I. Removal of acetaldehyde with and without UV irradiation", *J. Mater. Sci.* 37 (2002) 2937-2941.
- [89] C. Raillard, V. Hequet, P. Le Cloirec, J. Legrand, "Kinetic study of ketones photocatalytic oxidation in gas phase using TiO₂-containing paper: effect of water vapor", *J. Photochem. Photobiol. A: Chem.* 163 (2004) 425-431.
- [90] H. Ichiura, T. Kitaoka, H. Tanaka, "Preparation of composite TiO₂-zeolite sheets using a papermaking technique and their application to environmental improvement: Part II. Effect of zeolite coexisting in the composite sheet on NO_x removal", *J. Mater. Sci.* 38 (2003) 1611-1615.
- [91] H. Ichiura, T. Kitaoka and H. Tanaka, "Photocatalytic oxidation of NO_x using composite sheets containing TiO₂ and a metal compound", *Chemosphere* 51 (2003) 855-860.
- [92] S. Fukahori, Y. Iguchi, H. Ichiura, T. Kitaoka, H. Tanaka, H. Wariishi, "Effect of void structure of photocatalyst paper on VOC decomposition", *Chemosphere* 66 (2007) 2136-2141.
- [93] Nippon Paper Group, "Nippon Paper Industries Develops Photocatalytic Paper with Air Purification Effect", <http://www.npg.com/e/news/news05101901.html>, Oct. 2005.
- [94] H. Fujiwara, "Application of Nanotechnology in Pulp and Paper in Japan", *Proceedings of the TAPPI 2006 International Conference on Nanotech.* Atlanta, pp 62-66.
- [95] S. Nishbori, "Photocatalytic pulp composition", US Patent 6419792, July 2002.
- [96] Ahlstrom, Photocatalytic media, <http://www.ahlstrom.com/index.asp?id=02CCFAD536644D13BFB7E705C9A87673&data=1,00308B787886459385F296A5AFD4FA74,15C24462F0B44B5F9>

7AD0C82B5156B4D&tabletarget=data_1&laytmp=ahlstrom06

[97] N. Barka, S. Qourzal, A. Assabbane, A. Nounah, Y. Ait-Ichou, " Factors influencing the photocatalytic degradation of Rhodamine B by TiO₂ coated non-woven paper", J. Photoch. Photobio. A 195 (2008) 346-351.

[98] A. Aguedach, S. Brosillon, J. Morvan, El K. Lhadi, "Infl uence of ionic strength in the adsorption and during photocatalysis of reactive black 5 azo dye on TiO₂ coated on non woven paper with SiO₂ as a binder", J. Hazard. Mater. 150 (2008) 250-256.

[99] W.E. Scott, "Pri nciples of Wet End Chemistry", Atlanta, GA: TAPPI Press, 1996

[100] A. Aguedach, S. Brosillon, J. Morvan, EK Lhadi, " Photocatalytic degradation of azo-dyes reactive black 5 and reactive yellow 145 in water over a newly deposited titanium dioxide", Appl. Catal. B: Environ. 57 (2005) 55-62.

[101] Air-Purifying Paper,
http://web-japan.org/trends/07_sci-tech/sci080131.html, Jan. 2008.

CHAPTER III

RESEARCH SCOPE AND OBJECTIVES

The current study is focused on: 1) synthesizing colloidal nano-titania and its supported zeolite, 2) characterizing as-prepared materials and evaluating their photocatalytic efficiency, and 3) preparing photocatalytic paper of developed zeolite-based nano-TiO₂ and investigating its potential for photodecomposition of organic contaminants.

This research was principally carried out in two ways: The first was to synthesize, to characterize and to optimize the optical and photocatalytic properties of the titania nanocrystalline material from sol-gel derived TiO₂ colloidal nanoparticles, and the second aimed to prepare, to estimate the suitability of natural zeolite microparticle systems, and to develop a novel zeolite-based nanosized TiO₂ photocatalytic paper for disinfection and toxin passivation in packaging.

The outlines of the objectives of this research are as follows:

1. To study sol-gel synthetic routes to obtain high photoactive TiO₂ nanopowders from colloidal titania nano sol,
2. To optimize the effect of crystalline phase, which influences the optical properties, as well as the photocatalytic activity, of polycrystalline TiO₂ nanoparticles,
3. To determine the availability of natural zeolite for retaining TiO₂ in a fiber matrix, when it is used in a microparticle retention system for wet-end papermaking technique,

4. To characterize the newly developed natural zeolite-TiO₂ hybrid material,
and
5. To investigate the photoactivity and physical properties of novel photocatalytic paper made by using as-prepared TiO₂ nanoparticles-supported on natural zeolite.

CHAPTER IV

EXPERIMENTALS

Materials

Titanium tetra-isopropoxide (TTIP 99%), ACS reagent grade 2-propanol and hydrochloric acid (HCl) were used as received from Aldrich in the preparation of sol-gel derived TiO₂ colloids. Natural zeolite (clinoptilolite, ZOBRITE™) was provided by ZO mineral partners. The pulp used for the photocatalytic paper was bleached softwood northern kraft pulp and all of the pulps were refined to a Canadian Standard Freeness (CSF) of approximately 430 ml according to Technical Association of the Pulp and Paper Industry (TAPPI) test methods T 227 [1] and T 248 [2]. Cationic starch and cationic polyacrylamide (C-PAM, Core Shell 61607; NALCO) were also used as flocculants in natural zeolite microparticle retention systems. Nanosized P25 bicrystalline TiO₂ (Degussa, 22 nm, 50 m²/g, 70% anatase and 30% rutile), which is the most commonly referred to photocatalytic material, was employed as a comparative specimen as a photocatalysis agent. Non-woven photocatalytic paper was purchased from Ahlstrom (France, BR 1048-075, 75g/m²).

Synthesis of Photocatalytic Materials

TiO₂ colloidal nanoparticles

Colloidal TiO₂ particles were prepared by the acid catalyzed hydrolysis of titanium tetra-isopropoxide (TTIP 99%, Aldrich) dissolved in 2-propanol with vigorous stirring for 4-5 hrs to further peptization, based on

the design of experiments established with 3 factors and 2 levels. All reagents were used as received and detailed experimental conditions are given in Table 4.1.

Table 4.1. Experimental Factors for TiO₂ Colloidal Nanoparticles

Run #	Factors		
	TTIP (M)	HCl (M)	Peptization Temp (C)
1	0.2	0.1	0
2	0.5	0.1	0
3	0.2	0.2	0
4	0.5	0.2	0
5	0.2	0.1	Room
6	0.5	0.1	Room
7	0.2	0.2	Room
8	0.5	0.2	Room

Zeolite-based photocatalyst

A few nanometers sized TiO₂ colloidal nanoparticles were made thorough a sol-gel synthetic route in which acid catalyzed hydrolysis of titanium tetra-isopropoxide dissolved in 2-propanol. Briefly, in a typical synthesis of zeolite-based TiO₂ photocatalyst, 10 ml of 0.5 M TTIP solution in 2-propanol was added slowly drop by drop to 2 ml of 0.1M HCl in 88 ml of 2-propanol under vigorous stirring at 0°C. Continuous stirring was carried out for 4-6 hrs to further peptization, and the obtained particle size in a transparent TiO₂ sol was 2-3 nm on an average. Natural zeolite was

subsequently mixed thoroughly with as-prepared titania sol by stirring and removed completely from the solvent by evaporation. TiO₂ impregnated natural zeolite was then collected and dried at 110°C followed by post-calcination at 300°C to 800°C to induce the crystallinity of TiO₂ on zeolite.

Photocatalytic Papermaking

Determination of TiO₂ retention

A dynamic drainage device [3], typically called a Britt Jar (Electrocraft, Motomatic II), was used to simulate the main and interactive factors in microparticle retention systems involving cationic starch and polyacrylamide and to determine the effect of natural zeolite for TiO₂ retention in the fiber matrix. As indicated in TAPPI test method T261 [4], paper stock was prepared with 500 mL of 0.5% pulp consistency and filler retention was tested at 750 rpm repetitively at each Britt Jar run with varying dosing level of retention aids based on the design of experiments. A 2³ factorial model was designed in this study and variables and levels are listed in Table 4.2. The amount of TiO₂ loaded to paper stock was fixed at 10% of pulp consistency. The TiO₂ filler retention was determined by the following formula [5];

$$R_{\text{TiO}_2} (\%) = \left(1 - \frac{M_w}{M_H} \right) \times 100 \quad (4.1)$$

where R_{TiO_2} is the retention rate of TiO₂ nanoparticles, M_w is the solid weight of filtrate in the drainage and M_H is the original solid weight of the pulp slurry stock, respectively. The main effects and interaction factors were analyzed to identify the most significant factors influencing TiO₂ retention in

the pulp using MINITAB 14 software (Minitab Institute, USA).

Table 4.2. Factors and Levels for the 2³ Factorial Design in TiO₂ Retention Test

Factor		Level	
Symbol	Variable*	-	+
A	Natural Zeolite (%)	0	2
B	Cationic Starch (%)	0	0.5
C	Cationic Polyacrylamide (%)	0	0.1

* weigh percent versus 0.3% pulp contents

* Basis on 10% TiO₂ addition level

Preparation of photocatalytic paper

Photocatalytic papers of various TiO₂ photocatalysts with approximate 100 g/m² basis weight were prepared according to TAPPI test methods T 205 [6]. The pulp was mechanically refined to a Canadian Standard Freeness (CSF) of approximately 430 ml as formally designated in TAPPI test methods T 227 [7] and T 248 [8], prior to be blended with other materials. As-prepared zeolite-based TiO₂ was added to the pulp suspension with stirring, followed by the addition of cationic starch and cationic polyacrylamide (C-PAM) for the enhancement of retention. In the case of P25 containing paper, natural zeolite was combined with pulp suspension at the last step of dosing. Optimum levels of each retention aid were determined from the Britt Jar experiments. The addition level of each retention aid was 10% photocatalyst, 0.5% cationic starch, 0.1% C-PAM and, when needed, 2% natural zeolite in that order versus 0.3% pulp consistency (3 g dry pulp/L). All lab-made sheets were uniformly formed on a 200 wire mesh in a standard handsheet forming

machine and dried under standard conditions given in TAPPI T 402 [9] for at least 24 hrs before it was used for the photocatalysis.

Characterization of Photocatalyst-Based Materials

Crystallographic Examination

The X-ray diffraction (XRD) analysis was performed with a Diano X-ray Diffractometer at room temperature using 20 Kw Cu-K α radiation ($\lambda=0.15418$ nm) to survey the crystal structure, approximate crystalline size and integrity of raw natural zeolite and TiO₂ nanoparticles. All peaks were identified using MDI Jade 5.0 software (Materials Data Inc. USA). The average crystallite size of the samples was roughly calculated using the Scherrer equation [10] based on the X-ray line broadening technique as follows;

$$t = \frac{0.9\lambda}{B\cos\theta_B} \quad (4.2)$$

where t is the diameter of the particle, λ is the wavelength of X-rays, B is the full width of diffraction lines at half of maximum intensity (radians), and θ_B is the diffraction angle corresponding to the maximum peak.

The crystalline phase fraction was also calculated by the following formula, which has been described elsewhere [11].

$$W_R = \frac{1}{\left[1 + 0.8\left(\frac{I_A}{I_R}\right)\right]} \quad (4.3)$$

where W_R is the percentage of rutile phase, and I_A and I_R are the intensities of

anatase (101) and rutile (110) diffraction, respectively.

Particle size measurement

The particle size distribution of the colloidal samples was obtained by a Dynamic Light Scattering (DLS) particle size analyzer (NICOMP, $\lambda=632.8$ nm, He-Ne laser). Transmission electron microscope (TEM) images were taken with a JEOL transmission electron microscope (JEM-1230) to confirm the accuracy of DLS values for colloids. The samples for TEM measurement were prepared by dropping a tiny amount of each sample using a micropipette on a Formvar/carbon-coated copper grid (01814F, Ted Pella) and drying in air for at least 1 hour before imaging. Three typical regions of each sample were imaged at 300,000~500,000X magnification.

Optical properties of TiO₂ nanoparticles

The optical properties of the TiO₂ nanopowders deposited on the paper were characterized with regard to opacity, brightness and CIEL*a*b* values and each optical property was tested by an opacimeter (BNL-2 Opacimeter, Diano Corp.), a Brightimeter (Brightimeter Micro S-5, Technidyne Corp.) and an X-rite 530 SpectroDensitometer, respectively. All of the measurements were repeated 10 times for each sample and the average values were calculated and reported.

Morphology of photocatalytic papers

The surface morphologies of various photocatalytic handsheets including example of commercial photocatalytic paper (Ahlstrom, France, BR

1048-075, 75g/m²) were observed by scanning electron microscopy (SEM, Akashi ISI-DS 130) after gold sputtering on the specimen. The voltage set to accelerate electrons was 12 kV and three typical SEM images were taken at 50~1000X magnification in each sample under vacuum.

Evaluation of Photocatalytic Activity

To investigate the photoreactivity of photocatalytic material and its lab-made photocatalytic handsheets, toluene was chosen as a representative compound among various indoor VOC chemicals. Photocatalytic decomposition of gas-phase toluene was carried out in a 1L glass photoreactor under UV light irradiation (EIKO blacklight lamp, 4W, $\lambda=365\text{nm}$) with circular photocatalyst handsheet (11.29cm in diameter). Specifically, in the TiO₂ nanoparticles experiments, 0.1 g of each TiO₂ powder sample was deposited on the filter paper substrate (Whatman Qualitative, Grade #2) instead of placing on the photocatalytic handsheet. For the quantitative analysis of varying toluene concentrations through the entire experimental time, regardless of UV irradiation, gas samples were withdrawn from a sampling port attached to the reactor and injected into the Gas Chromatograph (GC, SRI 8610C) equipped with a Flame Ionization Detector (FID) and a 30m x 0.25 mm fused silica capillary column (Quadrex Corp.). All samples were tested three times to verify the photodegradation effect and the results were within 5% of standard deviations.

References

- [1] TAPPI test method T 227 om-99, Freeness of pulp (Canadian Standard Method)
- [2] TAPPI test method T 248 sp-00, Laboratory beating of pulp (PFI mill method)
- [3] TAPPI test method T 248 sp-00, Laboratory beating of pulp (PFI mill method)
- [4] TAPPI test method T 261 cm-00, Fines fraction by weight of paper stock by wet screening
- [5] J.D. Peel, "Paper science and paper manufacturing", Angus Wilde Publications Inc. Vancouver, Canada, 1999.
- [6] TAPPI test method T 205 sp-02, Forming handsheets for physical tests of pulp
- [7] TAPPI test method T 227 om-99, Freeness of pulp (Canadian Standard Method)
- [8] TAPPI test method T 248 sp-00, Laboratory beating of pulp (PFI mill method)
- [9] TAPPI test method T402 sp-98, Standard conditioning and testing atmospheres for paper, board, pulp handsheets, and related products
- [10] B.D. Cullity, "Elements of X-ray diffraction", Menlo Park, CA: Addison-Wesley Publishing Company, 1978, p 98-106.
- [11] C. Kim, I. Kwon, B. Moon, et al., "Synthesis and particle size effect on the phase transformation of nanocrystalline TiO₂", Mater. Sci. Eng. 27 (2007) 1343-1346.

CHAPTER V

SYNTHETIC BEHAVIOR AND PHOTOCATALYTIC ACTIVITY OF NANOCRYSTALLINE TiO₂ FROM SOL-GEL DERIVED COLLOIDS

Seonghyuk Ko, Pnina Ari-Gur and Paul D. Fleming

Department of Paper Engineering, Chemical Engineering and Imaging

*Department of Mechanical and Aeronautical Engineering

Western Michigan University

The characteristics of TiO₂ nanoparticles in a sol-gel synthetic route, from the colloidal to nanopowder, were investigated based on a factorial experimental design. The as-prepared nanosized TiO₂ was characterized by dynamic light scattering (DLS), transmission electron microscopy (TEM), and X-ray diffraction (XRD). Various initial sizes of colloidal nanoparticles ranging between 2.5±0.1 nm and 14.3±0.9 nm were synthesized. It was revealed that the different passages exist between the disparately synthesized colloidal particles on the crystalline phase transformation and particle growth along with annealing temperatures. The photocatalytic activity of pure anatase TiO₂ nanoparticles prepared from optimal synthetic colloids was better than that of commercially available Degussa P25 TiO₂ in toluene removal.

Keywords: TiO₂ nanoparticles, design of experiment, sol-gel, photocatalytic activity, crystalline phase

Introduction

Recently, nanocrystalline TiO₂ has received enormous attention as the

most promising photocatalytic material, as it is photosensitive, inexpensive, non-toxic and chemically stable [1-4]. Of the three main crystalline phases of TiO₂, anatase, rutile and brookite, it is also generally well known that anatase TiO₂-based photocatalyst is more effective than the other phases in decomposing harmful organic compounds [5-6]. Referring to the physical properties of TiO₂ in terms of crystalline structures, there is no wonder that anatase will be transformed to rutile with increase of temperature, because the surface free energy has to be minimized to become thermodynamically stable and rutile is the most stable among the three main phases [6-7] at high temperature. With the level of nanometer scale of particle size, photocatalytic activity is enhanced due to not only the large surface-to-volume ratio, but also band gap widening by the quantum size effect [8-9]. For these reasons, proper control of the size at the level of nano and crystalline structure of TiO₂ in the process of preparation is essential for photocatalytic characteristics.

TiO₂ nanoparticles have been prepared successfully through a variety of methods, such as the sol-gel process [10-11], solvothermal treatments [12], laser pyrolysis [13], hydrothermal method [14], reverse microemulsion method [15], and flame synthesis [16]. Among all synthetic methods, the sol-gel process is still considered as one of the most attractive methods, due to such unique advantages as low-temperature processing, simple, convenient and great flexibility at the stage of preparing TiO₂ samples, either powder or film, with high purity [17]. However, it is recognized as one of the main drawbacks that sol-gel derived TiO₂ is amorphous and needs further heat treatment to obtain crystallization, which can be also accompanied by particle size growth [18]. It is, therefore of practical significance to not only explore

the mechanism of phase transformation for initial colloids to post-synthesized TiO₂ nanoparticles in a sol-gel synthetic route, but also to study the particle growth accompanying the phase transition, in order to modulate properly the particle size and crystalline type, and eventually optimize the photocatalytic activity. In the present study, colloidal titania nanoparticles were prepared by the sol-gel process, according to a design of experiments and the resultant TiO₂ nanoparticles were systematically characterized from primitive colloids to solid nanoparticles with its photocatalytic activity. As a result, by comparing to well-known commercially available Degussa P25 TiO₂, higher photocatalytic effects were achieved with optimal synthetic colloidal-prepared samples.

Experimental

Colloidal TiO₂ particles were prepared by the acid catalyzed hydrolysis of titanium tetra-isopropoxide (TTIP 99%, Aldrich) dissolved in 2-propanol with a vigorous stirring for 4-5 hrs to further peptization, based on the design of experiments established with 3 factors and 2 levels. All reagents were used as received and detailed experimental conditions are given in Table 5.1.

In order to investigate the phase transformation and particle size change of TiO₂ nanostructures, along with different annealing temperatures, nanocrystalline TiO₂ powder samples were prepared by evaporating solvent from colloidal suspensions, without any heating (at room temperature), followed by post-calcination in air.

The particle size distribution of the colloidal samples was obtained by

Dynamic Light Scattering (DLS) particle size analyzer (NICOMP, $\lambda=632.8$ nm, He-Ne laser). Transmission electron micrograph (TEM) images were taken with a JEOL transmission electron microscope (JEM-1230) to confirm the accuracy of DLS values for colloids. The samples for TEM measurement were prepared by dropping a tiny amount of each sample using a micropipette on a Formvar/carbon-coated copper grid (01814F, Ted Pella) and drying in air for at least 1hr before imaging. Three typical regions of each sample were imaged at 500,000X magnification. The X-ray diffraction (XRD) analysis was performed with a Diano X-ray Diffractometer using Cu-K α radiation ($\lambda=0.15418$ nm).

To evaluate the photoreactivity, photocatalytic decomposition of gas-phase toluene was carried out in a 1L glass photoreactor under UV light irradiation (EIKO blacklight lamp, 4W, $\lambda=365$ nm). 0.1 g of each TiO₂ powder sample, deposited on the filter paper substrate (Whatman Qualitative, Grade #2), was used in the removal of toluene. During the irradiation, a gas sample was withdrawn from a sampling port attached to the reactor and injected into the Gas Chromatography (GC, SRI 8610C) equipped with a Flame Ionization Detector (FID) and a 30 m x 0.25 mm fused silica capillary column (Quadrex Corp.). Degussa P25 TiO₂, which is the most commonly used for photocatalysis, was employed as a reference for comparison..

Results and Discussion

Table 5.1 gives the factors and levels used for synthesizing colloidal titania nanoparticles with the particle size measured by the DLS technique as a response on this experimental design. Hereafter, colloidal samples will be

denoted as DOE Run #, like DOE#2, according to the number of the experimental run. The colloidal particles obtained from entire runs were in the range of 2~14nm size. It was found that the peptization temperature is significant to determine the size of nanoparticles and the smallest colloidal nanoparticles are produced in 0.5M TTIP and 0.1M HCl under 0°C. Considering the titanium alkoxide goes through hydrolysis, polymerization and condensation to determine the particle size during the sol-gel process [19], it should be noted that the temperature for these reactions is a critical factor in determining the colloidal particle size. Representative TEM images of the as-prepared TiO₂ shown in Figure 5.1 unveil that the titania particles in Figure 5.1(A) are distinctly smaller than those of Figure 5.1(B), resulting from DOE #5, which is consistent with the DLS measurements (See more data in appendix).

Table 5.1. Experimental Factors for TiO₂ Colloidal Nanoparticles and Their Particle Size

Run #	Factors			Response
	TTIP (M)	HCl (M)	Peptization Temp (°C)	Particle Size (nm)
1	0.2	0.1	0	6.5 ± 0.1
2	0.5	0.1	0	2.5 ± 0.1
3	0.2	0.2	0	3.1 ± 0.2
4	0.5	0.2	0	5.0 ± 0.2
5	0.2	0.1	Room	8.5 ± 0.5
6	0.5	0.1	Room	4.0 ± 0.3
7	0.2	0.2	Room	14.3 ± 0.9
8	0.5	0.2	Room	6.8 ± 0.5

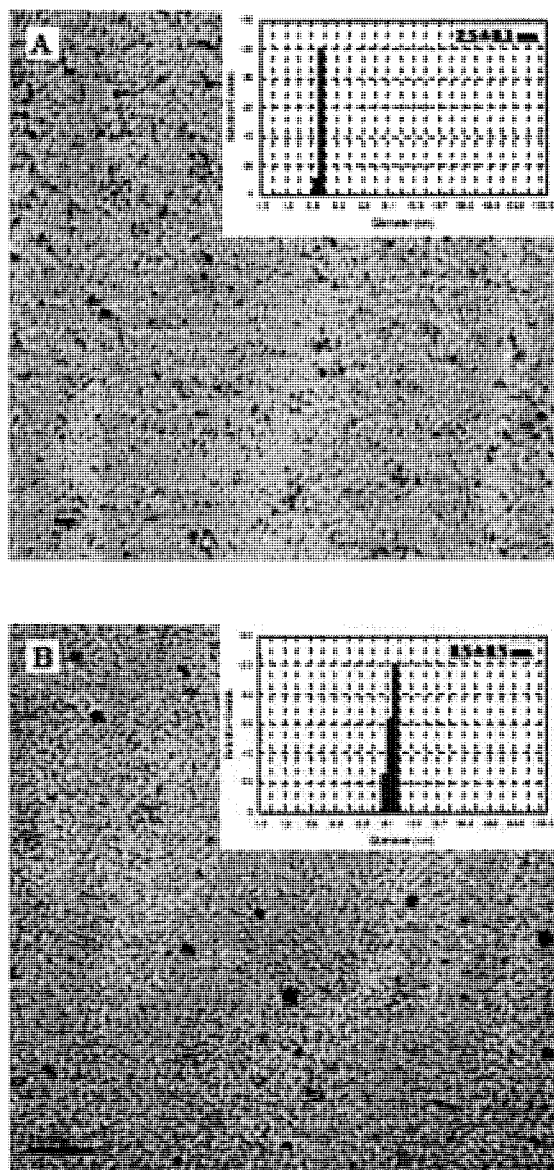


Figure 5.1. Representative TEM images of TiO₂ colloidal nanoparticles and DLS particle diameter distribution (the upper insert); (A) DOE #2, scale bar=10nm, (B) DOE #5, scale bar=50nm.

Figure 5.2 shows XRD patterns of TiO₂ nanoparticles annealed at different temperatures ranging from 300°C to 800°C in order to investigate phase transformation and particle size change as well. DOE #2 and #5

colloidal samples in Table 1 were chosen for this study named as powder A and B. Diffraction peaks correspond to a reference pattern (ICDD 21-2172) of crystalline titanium dioxide. The average single particle size of the prepared TiO₂ was calculated from the X-ray line broadening technique using the Scherrer equation [20]. As seen in Figure 5.2, both of the samples have only the anatase phase up to 500°C annealing temperature. However, they show different trends of phase transition above 600°C, which was the temperature the rutile phase appears slightly in powder B. It is evident that the behavior of crystalline phase transformations, which include transformation sequence and starting point of change, varied with primary size of colloidal nanoparticles. The anatase phase was completely transformed to a rutile phase at 800°C of annealing temperature in both of the powders.

The correlation of phase transition with particle size change as a function of annealing temperature is shown in Figure 5.3. The rutile weight fraction was calculated by the following formula [21].

$$W_R = \frac{1}{\left[1 + 0.8 \left(\frac{I_A}{I_R}\right)\right]} \quad (5.1)$$

where W_R is the rutile weight fraction and I_A and I_R are the diffraction peak intensities of anatase (101) and rutile (110), respectively. On the basis of the Scherrer equation [20], single particle size of DOE #2 has been roughly estimated and conspicuously increased to about 16.4 nm maximum in anatase phase from 2.5 nm colloidal particles. Indeed, it is a general tendency that not only TiO₂ particle growth, but crystalline structure also changes from

amorphous to anatase, then into rutile, as annealing temperature increases [6].

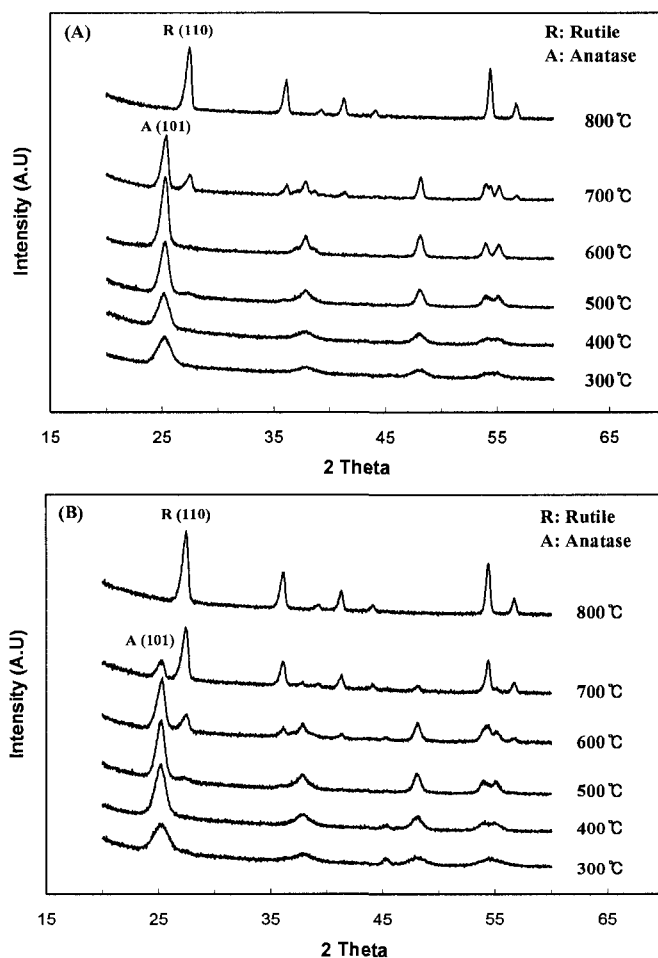


Figure 5.2. XRD diffraction patterns of as-prepared TiO₂ nanoparticles; (A) DOE #2, (B) DOE #5.

It is also makes it possible to weigh a coarsening mechanism, when the colloidal material evolved into a crystalline phase for different types of powder TiO₂ nanoparticles. Banfield et al. reported that different coarsening pathways exist between different particle sizes in thermal stability of

nanoparticle phase transformations [22-23], and thus, it is entirely noticeable that the nature of primary colloidal particles definitely affects both the particle propagation and features of crystalline structure transformations.

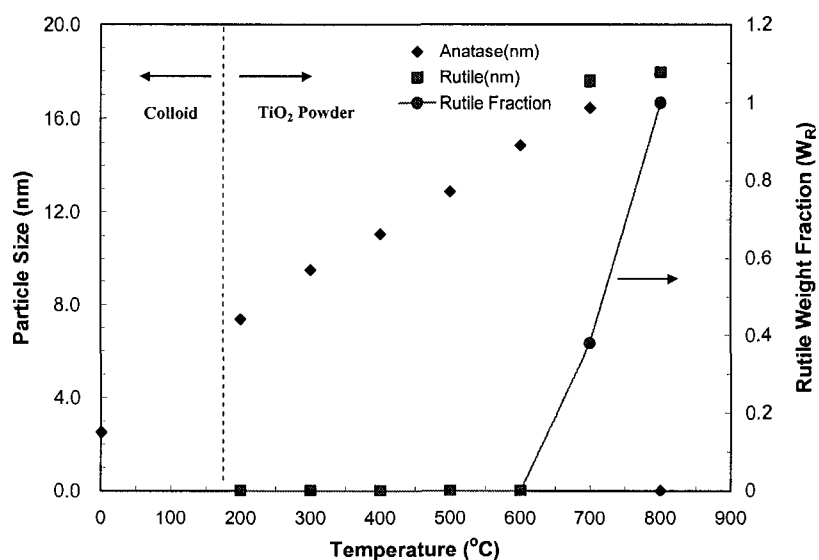


Figure 5.3. The relationship of particle growth and rutile weight fraction as a function of annealing temperature.

For the photocatalytic activity, toluene was used as a model compound to compare as-prepared TiO₂ with commercial Degussa P25 TiO₂, which consists of 70% anatase and 30% rutile phase and the results are shown in Figure 5.4. DOE #2 sample annealed at 600°C, which has only anatase phase of about 14.8 nm, was chosen for this work. As observed in Fig. 4, photoactivity of as-prepared TiO₂ surpasses that of the P25 TiO₂. According to previous reports [24-25], the degree of anatase crystallinity is positively correlated with the efficiency of the titania for photocatalytic degradation of organic pollutants in that fewer defects in the crystalline frame contribute to

prohibition of recombination of photosensitized electron-hole pairs. Moreover, it has been revealed that the photoactivity of Degussa P25 is mainly attributed to the anatase phase resulting from the undesirable fact that the anatase grains have been separated from the rutile grains [26]. Accordingly, it is more evident that as-prepared anatase TiO_2 was highly crystallized with less defects, resulting in enhancement of photocatalytic activity. Consequently, based on these facts, this result supports the conclusion that the photocatalytic effect is synergistically enhanced with the degree of crystallization and nanosized particles for pure anatase nanocrystalline titania in toluene decomposition.

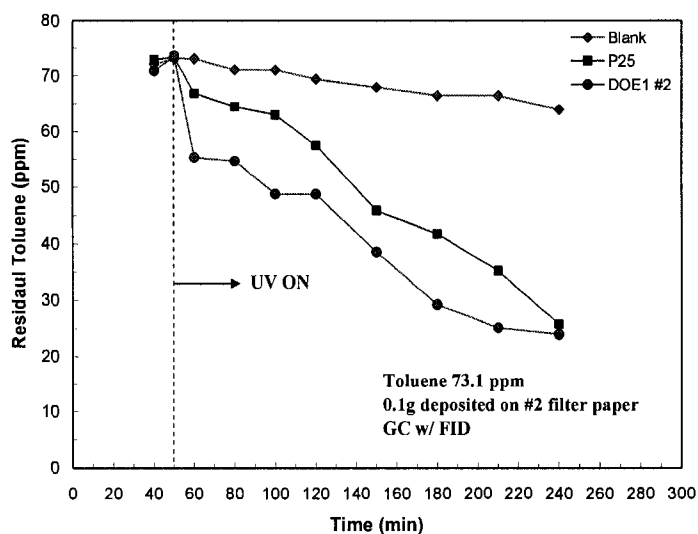


Figure 5.4. Photodegradation of gaseous toluene under UV irradiation.

Conclusions

The synthetic characteristics of nanosized TiO_2 have been studied from sol-gel derived colloidal nanoparticles prepared through the experimental

design approach. A few nanometers size of colloidal samples, which are in the range of 2.5 nm to 14.3 nm determined predominantly by media temperature, were synthesized followed by annealing at various temperatures. The evolution of crystalline phases and growth showed different-behavior sequences with different primary sizes of colloidal nanoparticles and it was confirmed that varying primitive properties of TiO₂ colloidal particles has an impact on the behavior of the crystalline phase transition and coarsening mechanisms as well. The photocatalytic activity of the selected as-prepared TiO₂ nanoparticles, which are comprised of only anatase phase, was more potent compared to that of Degussa P25 TiO₂ in toluene decomposition on a paper substrate.

References

- [1] M.R. Hoffmann, S.T. Martin, W. Choi, D.W. Bahnemann, "Environmental applications of semiconductor photocatalysis", *Chem. Rev.* 95 (1995) 69-96.
- [2] A.L. Linsebigler, G. Lu, J.T. Yates Jr., "Photocatalysis on TiO₂ surfaces: Principles, Mechanisms, and Selected Results", *Chem. Rev.* 95 (1995) 735-758.
- [3] A. Fujishima, T.N. Rao, D.A. Tryk, "Titanium dioxide photocatalysis", *J. Photoch. Photobio. C* 1 (2000) 1-21.
- [4] T.L. Thompson, J.T. Yates Jr., "Surface science studies of the photoactivation of TiO₂-New photochemical processes", *Chem. Rev.* 106 (2006) 4428-4453.
- [5] M.A. Fox, M.T. Dulay, "Heterogeneous Photocatalysis", *Chem. Rev.* 93 (1993) 341-357.
- [6] A. Fujishima, K. Hashimoto, H. Watanabe, "TiO₂ Photocatalysis: Fundamentals and Applications", BKC, Inc. Tokyo, Japan, 1997.

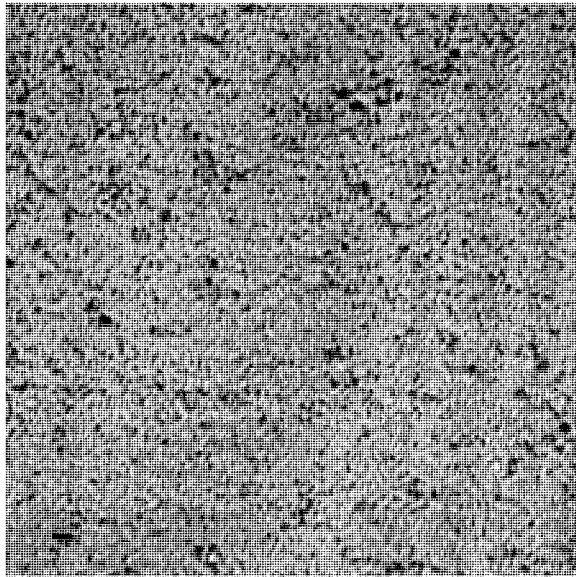
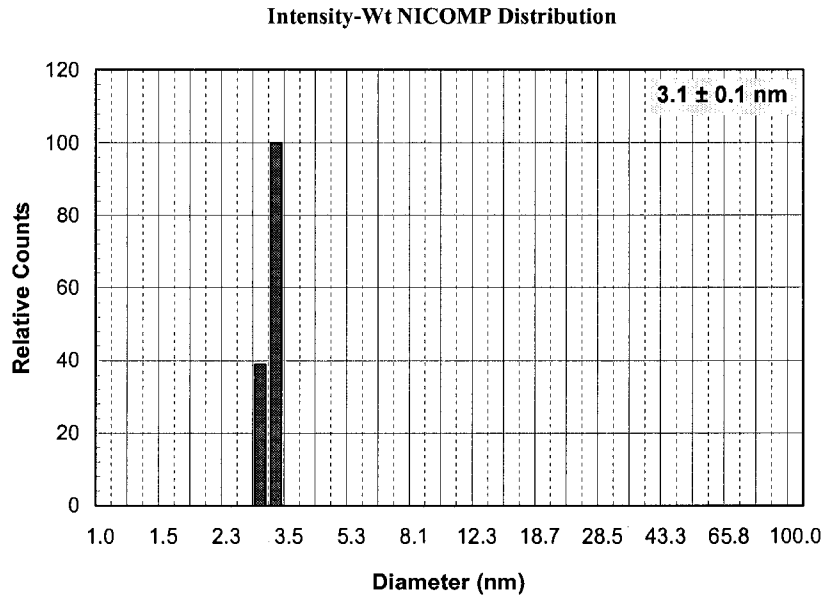
- [7] G. Buxbaum, G. Pfaff, "Industrial Inorganic Pigments", Wiley-VCH, Weinheim, Germany 3rd Ed. 2005.
- [8] M. Anpo, M. Takeuchi, "The design and development of highly reactive titanium oxide photocatalysts operating under visible light irradiation", *J. Catal.* 216 (2003) 505-516.
- [9] K. M. Reddy, C. V. G. Reddy, S.V. Manorama, "Preparation, Characterization, and Spectral Studies on Nanocrystalline Anatase TiO₂", *J. Solid State Chem.* 158 (2001) 180-186.
- [10] L. Cao, A. Huang, F.-J. Spiess, S.L. Suib, "Gas-Phase Oxidation of 1-Butane Using Nanoscale TiO₂ Photocatalysts", *J. Catal.* 188 (1999) 48-57.
- [11] J. Zhu, J. Zhang, F. Chen, K. Iino, M. Anpo, "High activity TiO₂ photocatalysts prepared by a modified sol-gel method: characterization and their photocatalytic activity for the degradation of XRG and X-GL", *Top. Catal.* 35 (2005) 261-268.
- [12] C. Kim, B. Moon, J. Park, S. Chung, S. Son, "Synthesis of nanocrystalline TiO₂ in toluene by a solvothermal route", *J. Cryst. Growth* 254 (2003) 405-410.
- [13] M. Scarisoreanu, Morjan, R. Alexandrescu, et al., "Effects of some synthesis parameters on the structure of titania nanoparticles obtained by laser pyrolysis", *Appl. Surf. Sci.* 253 (2007) 7908-7911.
- [14] P.D. Cozzoli, A. Kornowski, H. Weller, "Low-Temperature Synthesis of Soluble and Processable Organic-Capped Anatase TiO₂ Nanorods", *J. Am. Chem. Soc.* 125 (2003) 14539-14548.
- [15] M. Lee, S. Park, G. Lee, C. Ju, S. Hong, "Synthesis of TiO₂ particles by reverse microemulsion method using nonionic surfactants with different hydrophilic and hydrophobic group and their photocatalytic activity", *Catal. Today* 101 (2005) 283-290.
- [16] Y. Zhao, C. Li, X. Liu, et al., "Synthesis and optical properties of TiO₂ nanoparticles", *Mater. Lett.* 61 (2007) 79-83.
- [17] R.A. Caruso, M. Antonietti, "Sol-Gel Nanocoating: An Approach to the preparation of Structured Materials", *Chem. Mater.* 13 (2001) 3272-3282.

- [18] K. I. Hadjiivanov, D. G. Klissurski, "Surface chemistry of titania (anatase) and titania-supported catalysts", *Chem. Soc. Rev.* 25 (1996) 61-69.
- [19] L. L. Hench, J. K. West, "The Sol-Gel Process", *Chem. Rev.* 90 (1990) 33-72.
- [20] B.D. Cullity, "Elements of X-ray diffraction", Menlo Park, CA: Addison-Wesley Publishing Company, 1978, p 98-106.
- [21] C. Kim, I. Kwon, B. Moon, et al., "Synthesis and particle size effect on the phase transformation of nanocrystalline TiO₂", *Mater. Sci. Eng.* 27 (2007) 1343-1346.
- [22] A. A. Gribb, J. F. Banfield, "Particle size effects on transformation kinetics and phase stability in nanocrystalline TiO₂", *Am. Mineral* 82 (1997) 717-728.
- [23] H. Zhang, J. F. Banfield, "Phase transformation of nanocrystalline anatase-to-rutile via combined interface and surface nucleation", *J. Mater. Res.* 15 (2000) 437-448.
- [24] H. Kominami, J. Kato, S. Murakami, et al., "Sol-gel syntheses of semiconductor photocatalysts of ultra-high activities", *Catal. Today* 84 (2003) 181-189.
- [25] J.-G. Yu, H.-G. Yu, B. Cheng, X.-J. Zhao, J. C. Yu, W.-K. Ho, "The Effects of Calcination Temperature on the Surface Microstructure and Photocatalytic Activity of TiO₂ Thin Films Prepared by Liquid Phase Deposition", *J. Phys. Chem. B* 107 (2003) 13871-13879.
- [26] Z. Zhang, C.C. Wang, R. Zakaria, J.Y. Ying, "Role of Particle Size in Nanocrystalline TiO₂-Based Photocatalysts", *J. Phys. Chem.* 102 (1998) 10871-10878.

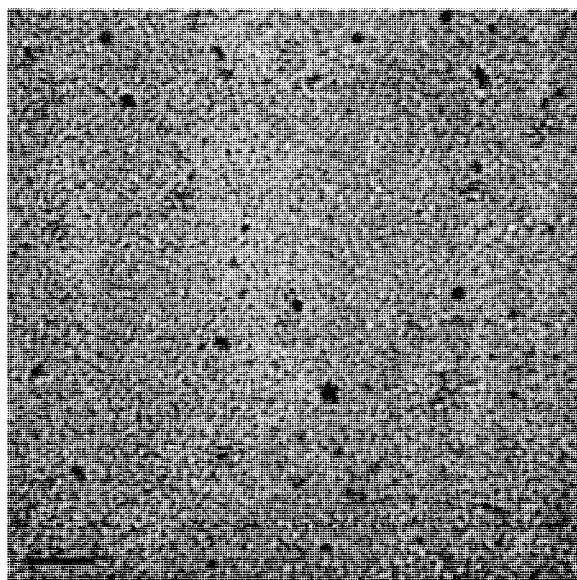
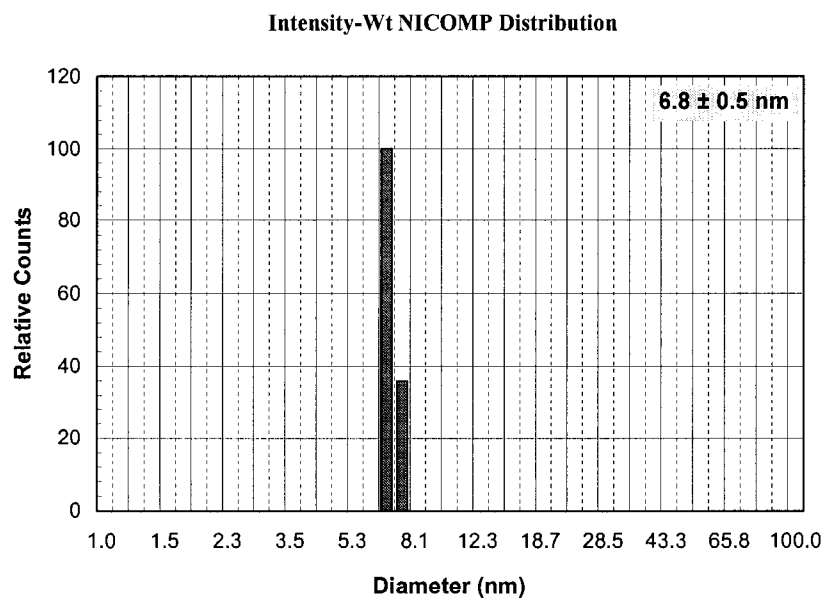
Appendix

DLS Distribution and TEM Image of Colloidal TiO₂ Nanoparticles

DOE 1 Run #3



DOE 1 Run #8



CHAPTER VI

OPTIMIZATION OF OPTICAL PROPERTIES AND PHOTOCATALYTIC ACTIVITY OF POLYCRYSTALLINE TiO₂ NANOPARTICLES TOWARD PHOTOCATALYTIC PAPER

Seonghyuk Ko, Margaret K. Joyce and Paul D. Fleming
Department of Paper Engineering, Chemical Engineering and Imaging
Western Michigan University, Kalamazoo, Michigan, USA

Nanocrystalline TiO₂ has attracted much attention both as a photocatalytic agent and an opacifying pigment, due to its photosensitivity, high refractive index, non-toxicity and chemical stability. Recently, its applications have been extended to a photocatalytic paper that can effectively decompose toxins and kill pathogens. Herein, we have investigated the effect of the crystalline phase of TiO₂ nanoparticles to optimize the optical properties, as well as photocatalytic activity, as it is deposited onto a paper substrate. Six different crystallite fractions of anatase and rutile were prepared for this study. The structural change and particle size were characterized by X-ray diffraction (XRD). Optical properties including opacity, brightness and CIEL*a*b* values were tested using a BNL Dyano 10 Opacimeter, Technidyne Brightimeter and X-rite 530 SpectroDensitometer. Photocatalytic activity was evaluated by measuring toluene removal, using gas chromatography (GC). It was found that a specific ratio of two different crystalline phases exists to ensure relatively higher optical properties and photoactivity as well, and consequently, the optimum value of phase fraction was in the range of 0.48 rutile:0.52 anatase and 0.71rutile:0.29anatase.

Keyword: nanocrystalline TiO₂, optical property, photocatalysis, photocatalytic paper

Introduction

Titanium dioxide (TiO₂) has been largely used for an opacifying pigment and photocatalytic agent [1]. Due to unique optical properties of a high refractive index and whiteness, TiO₂ has long been engaged in such applications, requiring high opacity and brightness as coatings, paints, plastics, ink and paper [2]. In addition, during the last two decades, especially as a photocatalytic semiconductor material, nanocrystalline TiO₂ has drawn enormous attentions as it is photosensitive, inexpensive, non-toxic and chemically stable [3-6] and these benefits have led to its wide applications, for example, solar cell [7-8], optical sensors [9], hygienic products [10] and extensive environmental cleanup for both air pollutants [11-12] and wastewater [13-14].

Of a variety of TiO₂-based applications, there has been growing interest in recent years to extend the application and value of functional paper, named as photocatalytic paper, which is defined as paper that has a light-activated catalytic function to decompose organic pollutants and kill pathogens [15]. Since the first photoactive TiO₂ containing paper introduced by Matsubara et al. in 1995 [16], a few publications and patents have been announced as already summarized elsewhere [15]. H. Tanaka's research group has successfully prepared different types of photocatalytic paper composites with a dual polymeric retention system using, TiO₂ supported on the inorganic fibers [17-19]. These were found to remove hazardous chemicals

both bisphenol A in wastewater and indoor air pollutants such as acetaldehyde and toluene. In addition, the void structure effect has recently been investigated and a kinetic study of TiO₂ containing paper on the VOC decomposition with photocatalytic activity has been reported [20-21].

TiO₂ is well known to have three main crystalline structures, which have different optical and physical properties, namely anatase, brookite and rutile [1]. Due to its higher surface area, anatase has higher photoactivity and also, anatase is transformed to rutile with an increase in temperature, because the surface free energy has to be minimized to become thermodynamically stable and rutile is the most stable at high temperature among three main phases [22]. As noticed, different structures govern dissimilar optical and physical properties, which lead to different applications by definition. Indeed, TiO₂ is a material that highly depends on its crystalline phase to determine its pigment and photocatalyst properties.

It would not be an overstatement to say that photocatalytic paper will be possibly applicable to innovative applications, for example, antimicrobial food packaging, bioactive conjugated catalytic paper, as well as toxin passivation and deodorizing paper. To the best of our knowledge, all previous attempts [15-20] have been performed by using only anatase TiO₂, due to its strong photooxidation capability among the three main different crystalline phases. However, rutile TiO₂ has the relative advantage of optical and photosensitivity, because of its exceptionally high refractive index and smaller band gap energy, which provides better visible light absorption efficiency. It is, therefore, very necessary to explore the optimum combination of bicrystallite TiO₂ to impart essential optical properties, while maintaining

the high photocatalytic function in the photocatalytic papers. To date, very little has been done in this direction.

The purpose of the present study is to optimize the ratio of crystalline phases of polycrystalline TiO₂ nanoparticles to assign required optical properties, such as opacity, brightness and L*a*b* values, and simultaneously to ensure higher photocatalytic activity. Six TiO₂ nanoparticles varying in different crystalline fractions of anatase and rutile were used as after deposition onto filter paper. Structural change and optical analyses of TiO₂ were conducted by XRD, BNL Dyano 10 Opacimeter, Technidyne Brightimeter and X-rite 530 SpectroDensitometer, while at the same time photocatalytic activity was evaluated with toluene decomposition. In the end, the optimal ranges of crystalline phase fraction for influencing both the optical properties and photocatalytic activity are suggested in detail.

Experimental

Sample preparation

Nanophase Degussa P25 TiO₂, which is the most commonly referred material in the field of photocatalysis, was used for this study. P25 TiO₂ is a bicrystalline phase of 70% anatase and 30% rutile in itself with about 20nm of average single particle size (surface area; 50m²/g). Crystalline phase modulation was accomplished by heat treatment of the P25 TiO₂, due to the fact that anatase transformed to a rutile phase, which is more thermodynamically stable, along with heating. The heat treatment of the TiO₂ powder was performed in air for 4hrs at different temperatures ranging from 500C to 800C and lastly, six different TiO₂ nanoparticles with varying

fractions of crystal morphologies were obtained.

Characterization of TiO₂

To investigate the structural transition of TiO₂, X-ray diffraction (XRD) measurements were performed with a Diano X-ray Diffractometer at room temperature using a 20Kw Cu-K α radiation ($\lambda=0.15418$ nm). The average crystallite size of the samples was calculated from X-ray line broadening technique using the Scherrer equation [23] as follows;

$$t = \frac{0.9\lambda}{B\cos\theta_B} \quad (6.1)$$

where t is the diameter of the particle, λ is the wavelength of X-rays, B is the full width of diffraction lines at half of maximum intensity (radians), and θ_B is the diffraction angle corresponding to the maximum peak.

The crystalline phase fraction was also calculated by the following formula, which has been described elsewhere [24].

$$W_R = \frac{1}{\left[1 + 0.8\left(\frac{I_A}{I_R}\right)\right]} \quad (6.2)$$

where W_R is the percentage of rutile phase, and I_A and I_R are the intensities of anatase (101) and rutile (110) diffraction, respectively. In each case, the baseline amount was subtracted from the peak intensities and the lowest intensity value of each series was taken to be the baseline for that sample.

The optical properties of the TiO₂ deposited onto the paper were

characterized with respect to opacity, brightness and CIEL*a*b* values and each optical property was tested with an Opacimeter (BNL-2 Opacimeter, Diano Corp.), Brightimeter (Brightimeter Micro S-5, Technidyne Corp.) and X-rite 530 SpectroDensitometer, respectively. All of the measurements were tested 10 times for each sample and the average values were calculated and reported.

Evaluation of photocatalysis

To evaluate the photoreactivity, photocatalytic decomposition of gas-phase toluene was carried out in a 1L glass photoreactor under UV light irradiation (EIKO blacklight lamp, 4W, $\lambda=365\text{nm}$). 0.1 g of each TiO_2 powder sample deposited on the filter paper substrate (Whatman Qualitative, Grade #2) was used in the removal of toluene. For the quantitative analysis of toluene concentration, during the irradiation, gas samples were withdrawn from a sampling port attached to the reactor and injected into the Gas Chromatograph (GC, SRI 8610C) equipped with a Flame Ionization Detector (FID) and a 30m x 0.25 mm fused silica capillary column (Quadrex Corp.).

Results and Discussion

XRD patterns and crystalline phase transition

Figure 6.1 shows XRD patterns for the P25 TiO_2 nanoparticles annealed at different temperatures. Diffraction peaks obviously correspond to a reference pattern (ICDD 21-2172) of crystalline titanium dioxide. It is evident that P25 is comprised of anatase and rutile phases and the crystallite structure transformed to rutile from anatase along with heat treatment. As observed in

Figure 6.1, nothing happens to the crystalline phase at a temperature of 500 °C. The diffraction intensity of the rutile phase increased at 600°C and the anatase phase completely disappeared at 800°C of heat treatment.

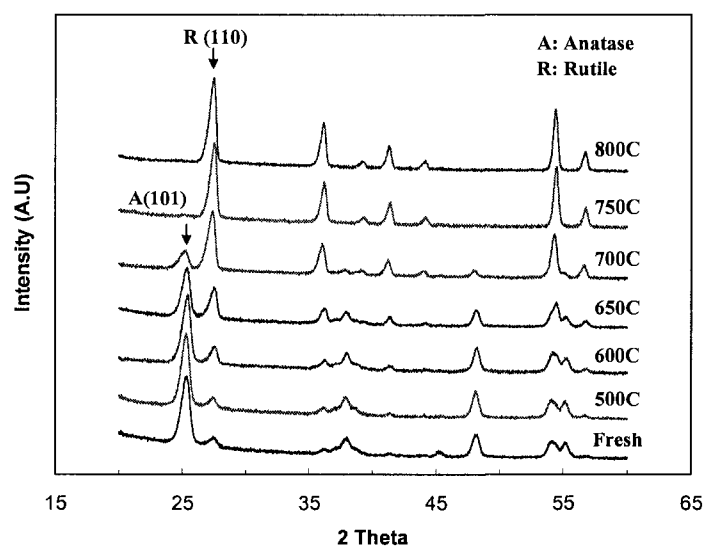


Figure 6.1. XRD patterns of phase modulated P25 TiO₂ nanoparticles.

The change in phase fraction at the different annealing temperatures is shown in Figure 6.2. With the intensity of each diffraction peak, the phase fraction has been numerically determined, which was in the range of 30% to 100% rutile phase. Based on the Scherrer equation, which has been used to roughly estimate the size of nanoparticles, the average particle size was maintained at around 20 nm through the entire range of the heat treatment.

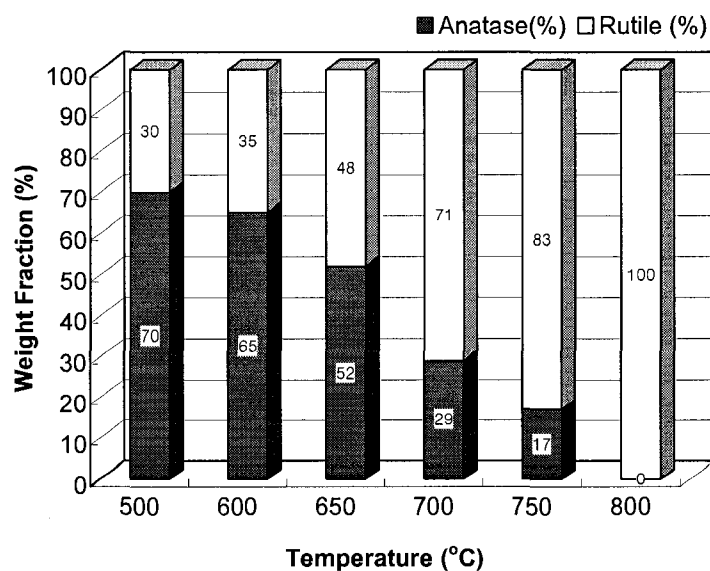


Figure 6.2. Crystallite fractions of TiO₂ nanoparticles annealed at varied temperature.

Optical properties

Opacity, brightness and CIEL*a*b* values were examined from the point of view of paper coating and wet-end paper making applications and the results are shown in Figure 6.3 and Figure 6.4. Figure 6.3 shows opacity and brightness as function of rutile weight fraction. In general, it was highly expected that the pure rutile phase would give the best opacity and brightness, due to its higher refractive index and better ability to reflect radiation in comparison to the anatase form. As seen in Figure 6.3, however, proper ratios of the two crystal forms, anatase and rutile, exist in TiO₂. More exactly, the optimal fraction of the two crystalline phases was 0.29 anatase and 0.71 rutile for both enhanced opacity and brightness.

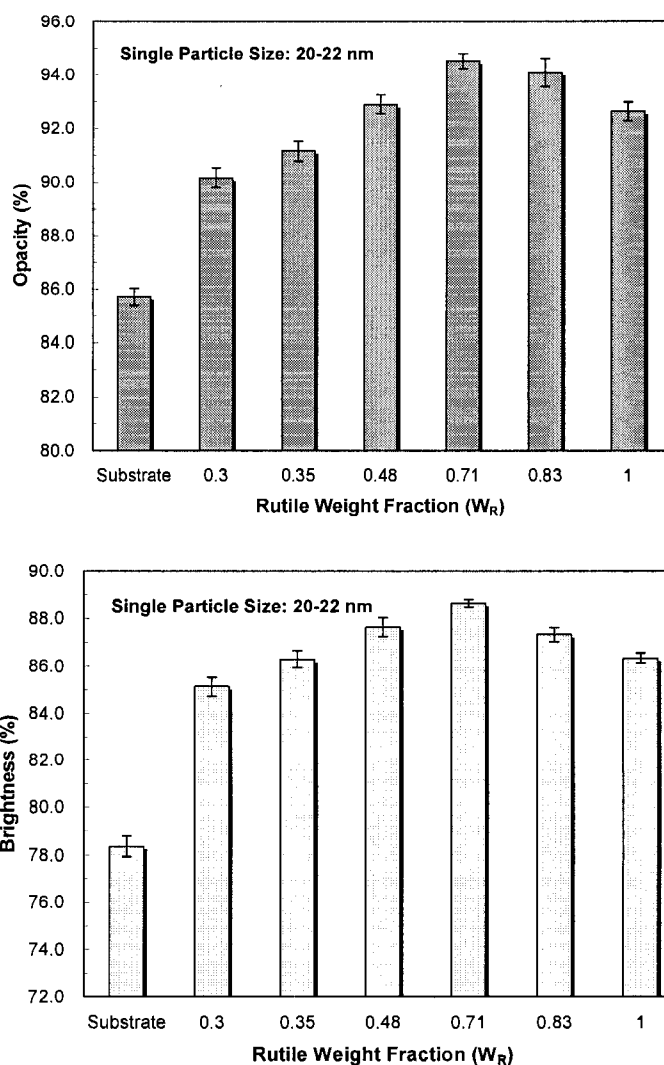


Figure 6.3. Opacity and brightness of TiO_2 nanoparticles according to different rutile fractions.

Notably, opacity is a function of refractive index relative to the air in the case of paper sheet, in other words, the greater the differences in refractive index, the higher amount of light scattering. It is also known that light scattering occurring in particles is attributed to direct reflection and diffraction as well [2]. Y. Deng et al [25]., recently, reported that light

scattering efficiency of a biphasic pigment increased by reflection and refraction of light at the grain boundaries between crystals of different phases, which have different refractive indices. From the fact that anatase is the more UV region sensitive phase in terms of UV reflectance with higher surface area, it is understood that combinations with anatase could make it possible for optical properties to be strengthened due to synergetic effects of refraction, reflection and diffraction between two phases in light scattering. Figure 6.4 shows CIEL*a*b* values of TiO₂ nanoparticles, which is the most complete color model used conventionally to describe all the colors visible to the human eye. All trends of CIEL*a*b* values were in good accordance with the results of opacity and brightness, which means appropriate anatase to rutile ratios will serve more sensibly neutral base color based on high whiteness.

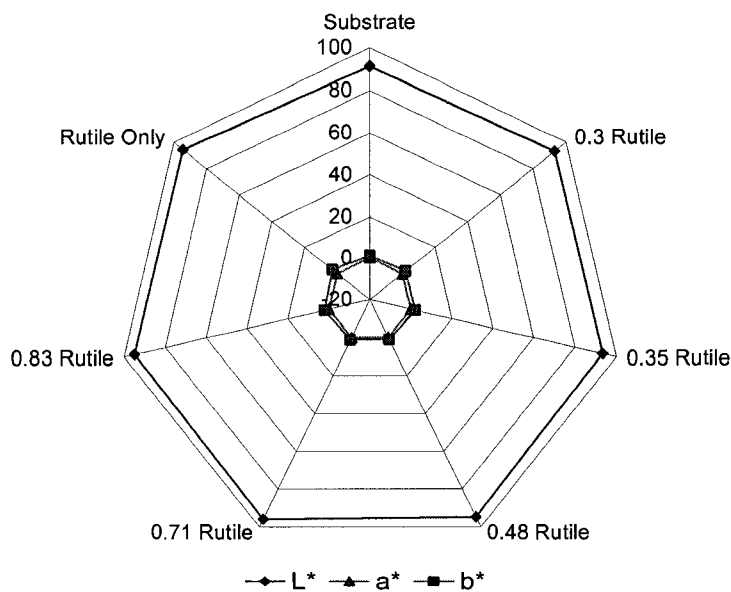


Figure 6.4. Diagram of CIEL*a*b* values of TiO₂ nanoparticles with different rutile weight fraction.

Photocatalytic activity

For the photocatalytic activity, toluene was used as a model compound to investigate the effect of phase transformation. Figure 6.5 shows toluene removal of phase modulated TiO₂ nanoparticles according to different rutile contents ranging from 0.3 to 1.0 weight fraction. As observed in Figure 5, residual toluene is increasing gradually by small gaps to 0.48 rutile fraction, while removal efficiency of toluene drops rapidly at 0.71 rutile and only 25% of initial toluene removed from the rutile phase only. It is highly probable that rutile TiO₂ has low photooxidation capability, because rutile has a low level conduction band, which has not enough reducing potential to produce a superoxide (O₂^{·-}) from molecular oxygen (O₂). It has been found that superoxide is as important as the holes and hydroxyl radicals in breaking down organic compounds [1]. As a result, photocatalytic activity is strongly dependent on the anatase phase and it is more worthwhile that rutile will be inducted as a photocatalytic inhibitor to apply where needed to protect from photodecomposition.

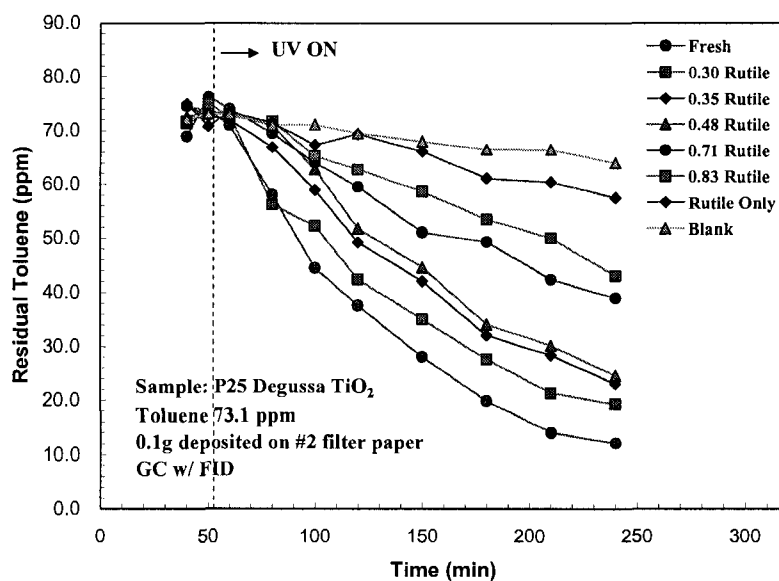


Figure 6.5. Photodegradation of toluene with varied crystalline phase of TiO₂ nanoparticles under UV irradiation.

Conclusion

We present here the results of measurements of optical properties and photocatalytic activity that allow us to optimize the effect of polycrystalline phases of TiO₂ nanoparticles from the point of view of principal crystal structures, anatase and rutile. Six different fractions of crystal structure of TiO₂, which are in the range of 0.7 anatase: 0.3 rutile to only rutile phase, were prepared from P25 Degussa TiO₂ by means of heat treatment at 500 °C-800 °C. For the optical properties, opacity, brightness and CIEL*a*b* values were tested and 0.71 rutile/0.29 anatase phase composition of TiO₂ was definitely superior to the others, even though pure rutile has the higher refractive index. The photocatalytic activity of the as-modulated TiO₂ nanoparticles was gradually decreased along with decreasing contents of anatase phase and photoactivity dropped largely from beyond 0.48 rutile ratio in toluene

decomposition. Accordingly, it is obviously shown that there is an optimal range of anatase and rutile crystalline phases that possesses both better optical properties and photocatalytic activity. Consequently, it makes practically possible an optimal range of TiO₂ phase fractions in the range of 0.48 rutile:0.52 anatase and 0.71 rutile:0.29 anatase.

References

- [1] A. Fujishima, K. Hashimoto, H. Watanabe, "TiO₂ Photocatalysis: Fundamentals and Applications", Tokyo, Japan, 1997
- [2] G. Buxbaum, G. Pfaff G, "Industrial Inorganic Pigments", Wiley-VCH, Weinheim, Germany 3rd Ed. 2005
- [3] M. R. Hoffmann, S. T. Martin, W. Choi, D. W. Bahnemann, "Environmental applications of semiconductor photocatalysis", Chem. Rev. 95 (1995) 69-96.
- [4] A. L. Linsebigler, G. Lu, J. T. Yates Jr., "Photocatalysis on TiO₂ surfaces: Principles, Mechanisms, and Selected Results", Chem. Rev. 95 (1995) 735-758.
- [5] A. Fujishima, T. N. Rao, D.A. Tryk, "Titanium dioxide photocatalysis", J. Photoch. Photobio. C 1 (2000) 1-21.
- [6] T.L. Thompson, J.T. Yates Jr., "Surface science studies of the photoactivation of TiO₂-New photochemical processes", Chem. Rev. 106 (2006) 4428-4453.
- [7] M. Gratzel, "Photoelectrochemical cells", Nature 414 (2001) 338-344.
- [8] M. Gratzel, "Dye-sensitized solar cells", J. Photoch. Photobio. C 4 (2003) 145-153.
- [9] A. Curulli, F. Valentini, G. Padeletti et al., "Smart (Nano) materials: TiO₂ nanostructured films to modify electrodes for assembling of new electrochemical probes", Sensor. Actuat. B-Chem. 111-112 (2005) 441-449.

- [10] K. Sunada, Y. Kikuchi, K. Hashimoto, A. Fujishima, "Bactericidal and Detoxification Effects of TiO₂ Thin Film Photocatalyst", *Environ. Sci. Technol.* 32 (1998) 726-728.
- [11] C. H. Ao, S. C. Lee, Y. Z. Yu, J. H. Xu, "Photodegradation of formaldehyde by photocatalyst TiO₂: effects on the presences of NO, SO₂ and VOCs", *Appl. Catal. B- Environ.* 54 (2004) 41-50.
- [12] A. Strini, S. Cassese, L. Schiavi, "Measurement of benzene, toluene, ethylbenzene and O-xylene gas phase photodegradation by titanium dioxides dispersed in cementitious materials using a mixed flow reactor", *Appl. Catal. B- Environ.* 61 (2005) 90-97.
- [13] A.C. Rodrigues, M. Boroski, N. S. Shimada, et al., "Treatment of paper pulp and paper mill wastewater by coagulation-flocculation followed by heterogeneous photocatalysis" *J. Photoch. Photobio. A* 194 (2008) 1-10.
- [14] I. J. Ochuma, R. P. Fishwick, J. Wood, J.M. Winterbottom, "Photocatalytic oxidation of 2,4,6-trichlorophenol in water using a concurrent downflow contactor reactor", *J. Hazard. Mater.* 144 (2007) 627-633.
- [15] R. Pelton, X. Geng, M. Brook, "Photocatalytic paper from colloidal TiO₂-factor or fantasy", *Adv. Colloid. Interfac.* 127 (2006) 43-53.
- [16] H. Matsubara, M. Takada, S. Koyama, K. Hashimoto A. Fujishima, "Photoactive TiO₂ containing paper: Preparation and its photocatalytic activity under weak UV light illumination", *Chem. Letters* (1995) 767-768.
- [17] Y. Iguchi, H. Ichiura, T. Kitaoka, H. Tanaka, "Preparation and characteristics of high performance paper containing titanium dioxide photocatalyst supported on inorganic fiber matrix", *Chemosphere* 53 (2003) 1193-1199.
- [18] S. Fukahori, H. Ichiura, T. Kitaoka, H. Tanaka, "Capturing of bisphenol A photodecomposition intermediates by composite TiO₂-zeolite sheets", *Appl. Catal. B: Environ.* 46 (2003) 453-462.
- [19] H. Ichiura, T. Kitaoka and H. Tanaka, "Removal of indoor pollutants under UV irradiation by a composite TiO₂-zeolite sheet prepared using a papermaking technique", *Chemosphere* 50 (2003) 79-83.

- [20] C. Raillard, V. Hequet, P. Le Cloirec, J. Legrand, "Kinetic study of ketones photocatalytic oxidation in gas phase using TiO₂-containing paper: effect of water vapor", *J. Photochem. Photobiol. A: Chem.* 163 (2004) 425-431.
- [21] S. Fukahori, Y. Iguchi, H. Ichiura, T. Kitaoka, H. Tanaka, H. Wariishi, "Effect of void structure of photocatalyst paper on VOC decomposition", *Chemosphere* 66 (2007) 2136-2141.
- [22] C. N. R Rao, K. J. Rao, "Phase transitions in solids", McGraw-Hill, New York, 1978.
- [23] B. D. Cullity, "Elements of X-ray diffraction", Menlo Park, CA: Addison-Wesley Publishing Company, 1978, p 98-106.
- [24] C. Kim, I. Kwon, B. Moon, et al., "Synthesis and particle size effect on the phase transformation of nanocrystalline TiO₂", *Mater. Sci. Eng.* 27 (2007) 1343-1346.
- [25] K. Nelson, Y. Deng, "Effect of polycrystalline structure of TiO₂ particles on the light scattering efficiency", *J. Colloid. Interf. Sci.* 319 (2008) 130-139.

CHAPTER VII

PREPARATION AND STUDY OF VOC REMOVAL OF NANO TITANIA PHOTOCATALYTIC PAPER USING A NATURAL ZEOLITE MICROPARTICULATE SYSTEM

Seonghyuk Ko, Jan Pekarovic and Paul D. Fleming
Department of Paper Engineering, Chemical Engineering and Imaging
Western Michigan University, Kalamazoo MI 49008, USA

Nanosized TiO₂ photocatalytic papers were successfully prepared using a natural zeolite microparticle retention system in papermaking. Applying a factorial experimental design, natural zeolite is evidently confirmed as the most significant and interactive factor for increasing the TiO₂ retention rate in paper stock. The photocatalysis of as-prepared sheets was evaluated with toluene as one representative VOC among indoor pollutants. Under UV irradiation, it was shown to very effectively remove gaseous toluene by photodecomposition, assisted by absorption. It was revealed that natural zeolite plays an important role in both increasing retention rate of TiO₂ nanoparticles and enhancing photocatalytic efficiency of the paper. It is indeed sensible that the photocatalytic paper can be potentially applied for the environmental purification as well as antimicrobial passivation.

Keyword: nanosized TiO₂, photocatalytic paper, natural zeolite, VOC, photocatalysis, experimental design

Introduction

Since the pioneer discovery of TiO₂ photoelectrochemical water splitting and hydrogen production using light in 1972 [1], the Fujishima-Honda effect, there have been huge breakthroughs, both scientifically and practically, in various applications of semiconductor photocatalysis. Examples include solar cells [2-3], optical sensors [4], hygienic products [5] and extensive environmental cleanup for both air pollutants [6-7] and wastewater [8-9], which is often referred to as Light Cleaning [10]. In particular, among the possible photocatalytic semiconductor materials, nanocrystalline TiO₂ has drawn enormous attention because it is photosensitive, inexpensive, non-toxic and chemically stable [11-14].

Photocatalysis occurs when a photocatalyst such as titanium dioxide, also known as titania, is exposed to photons with at least as much energy as the band gap energy of the photocatalyst. When the band gap energy is exceeded, the material forms electron-hole pairs, which are sets of negatively charged electrons and positively charged vacancies, where the electrons used to be. In general, the holes react with H₂O to form hydroxyl (OH[•]) radicals, which lead to an oxidation reaction of a variety of contaminants, such as environmental pollutants and microorganisms. In other words, the oxidizing power of these radicals is the means by which organic chemicals are degraded during photocatalysis, whether in aqueous and gaseous media.

As an effective means of decomposing organic compounds as well as microorganisms, TiO₂ photocatalyst makes possible an innovative novel paper product, which is called photocatalytic paper [15], for toxin passivation, deodorizing and disinfection. Photocatalytic papers may also be able to be

more emphasized for environmental purifications. Moreover, as the time for staying indoors increases more and more nowadays, indoor air quality has become a concern and it is important that it be kept as clean as possible. It is well known that volatile organic compounds (VOCs) are representative of indoor air pollutants and, according to the EPA, VOCs are known to cause negative health effects, with multiple symptoms such as headache, nausea, conjunctiva irritation, dyspnea, allergic skin and emesis, etc. In particular, a large number of hazardous chemicals and the high risk for exposure to those chemicals in new houses and new buildings are the main causes of the serious sick building syndrome (SBS), which is commonly used to demonstrate that any uncomfortable symptoms pose a threat of occupants' [16] health.

As one of promising technologies for VOC removal, there have been numerous studies on photocatalytic oxidation with different TiO_2 system and different chemicals, as already reviewed by S. Wang et al [17]. Despite many studies reported, few publications and patents have been found regarding photocatalytic paper for VOC removal [15]. H. Tanaka et al [18-20] have successfully prepared different types of photocatalytic paper composites with a dual polymeric retention system, using TiO_2 supported on the ceramic fiber matrix. These were found to remove hazardous chemicals both bisphenol A in wastewater and indoor air pollutants such as acetaldehyde and toluene. In addition, the void structure effect has recently been investigated and a kinetic study of TiO_2 containing paper on the VOC decomposition with photocatalytic activity [21-22] has been reported.

In the present study, nanosized TiO_2 photocatalytic paper was

successfully prepared by a natural zeolite microparticulate system based on the factorial experimental design and the ability of VOC removal was investigated with as-fabricated photocatalytic handsheets. For this purpose, retention of TiO₂ nanoparticles was tested primarily with the dynamic drainage jar (Britt Jar™) and the effect of natural zeolite in terms of retention was confirmed. Factors influencing retention of TiO₂ nanoparticles will be discussed via statistical analysis tools. TiO₂ nanoparticles used in this study were characterized by TEM and XRD and photocatalytic performance was carried out by toluene decomposition with a gas chromatograph.

Experimental

Materials

The pulps used for the retention were bleached hardwood and softwood northern kraft pulp and softwood bleached kraft pulp. These were also used for producing the photocatalytic handsheets. All of the pulps were refined to a Canadian Standard Freeness (CSF) of approximately 430 ml according to Technical Association of the Pulp and Paper Industry (TAPPI) test methods T 227[23] and T 248[24]. Nanosized bicrystalline TiO₂ (Degussa P25, 22 nm, 50 m²/g, 70% anatase and 30% rutile), which is the most commonly discussed photocatalytic material, was employed as the photocatalytic agent. Natural zeolite (clinoptilolite, ZOBRITE™), provided by ZO mineral partners, was used for a TiO₂ supporter and retention aid as well. Cationic starch and cationic polyacrylamide (C-PAM, Core Shell 61607; NALCO) were used as flocculants in natural zeolite microparticle retention systems.

Characterization of TiO₂ nanoparticles

The X-ray diffraction (XRD) analysis was performed with a Diano X-ray Diffractometer at room temperature using 20 Kw Cu-K α radiation ($\lambda=0.15418$ nm) to investigate the crystal structure and approximate particle size of TiO₂ nanoparticles. The morphology and accurate size of TiO₂ particles was obtained with transmission electron microscope (TEM, JEOL JEM-1230). The samples for TEM imaging were prepared by dropping a tiny amount of TiO₂ dispersed in 2-propanol on a Formvar/carbon-coated copper grid (01814F, Ted Pella). Three typical regions of each sample were imaged at 300,000X magnification.

Retention of TiO₂

A dynamic drainage device, typically called a Britt Jar (Electrocraft, Motomatic II), was used to simulate the main and interactive factors in microparticle retention systems involving cationic starch and polyacrylamide and to determine the effect of natural zeolite for the TiO₂ retention in the fiber matrix. As indicated in TAPPI test method T261 [25], paper stock was prepared with 500 mL of 0.5% pulp consistency and filler retention was tested at 750 rpm repetitively at each Britt Jar run with varying dosing levels of retention aids based on the 2³ factorial experimental design. The amount of TiO₂ loaded to paper stock was fixed at 10% of pulp consistency. The TiO₂ filler retention was determined by following formula [26];

$$R_{\text{TiO}_2}(\%) = \left(1 - \frac{M_w}{M_H}\right) \times 100 \quad (7.1)$$

where R_{TiO_2} is the retention rate of TiO_2 nanoparticles, M_W is the solid weight of filtrate in the drainage and M_H is the original solid weight of the pulp slurry stock, respectively. Main effect and interaction factors were analyzed to identify the most significant factors influencing TiO_2 retention in the pulp using MINITAB 14 software (Minitab Institute, USA).

Preparation of photocatalytic paper

Determined optimum levels of each retention aid, from the Britt Jar experiments, and pulp stock for the handsheet were blended with 10% nano TiO_2 , 0.5% cationic starch, 0.1% C-PAM and 2% natural zeolite in that order. A 0.3% pulp consistency slurry was applied for stock preparation and at last 5 photocatalytic handsheets of approximate $100g/m^2$ of base weight were obtained according to TAPPI test method T 205 [27]. All handsheets were dried under standard conditions given in TAPPI T 402 [28] for at least 24hrs prior to perform photocatalysis.

Evaluation of photocatalysis

To investigate VOC removal with handmade photocatalytic paper, toluene was chosen for this study as a model compound among various indoor VOC chemicals. Photocatalytic decomposition of gas-phase toluene was carried out in a 1L glass photoreactor under UV light irradiation (EIKO blacklight lamp, 4W, $\lambda=365nm$) with circular TiO_2 handsheet (11.29cm in diameter). For the quantitative analysis of toluene concentration, during the irradiation, gas samples were withdrawn from a sampling port attached to the reactor and injected into the Gas Chromatograph (GC, SRI 8610C)

equipped with a Flame Ionization Detector (FID) and a 30m x 0.25 mm fused silica capillary column (Quadrex Corp.).

Results and Discussion

TiO₂ photocatalyst characterization

Figure 7.1 shows XRD pattern of the P25 TiO₂ nanoparticles used for this study. Diffraction peaks obviously correspond to a reference pattern (ICDD 21-2172) of crystalline titanium dioxide. It is evident that P25 has bicrystalline structure comprising of anatase and rutile phases. The primary single particle size was estimated at about 22 nm from the X-ray line broadening technique using the Scherrer equation [29].

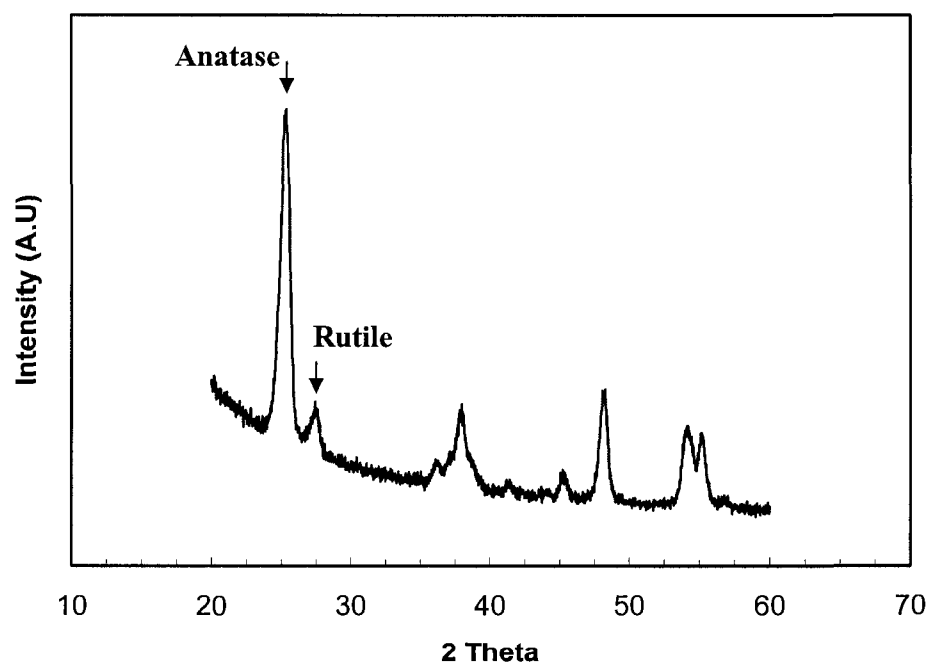


Figure 7.1. XRD pattern of Degussa P25 TiO₂ powder.

Figure 7.2 gives representative TEM images of the P25 TiO₂ powder.

As seen in Figure 7.2, two different sizes of grains are observed in their agglomerations among the particles. The smaller particles appear to be approximately 20 nm as shown more clearly in Figure 7.2(B) and the larger particles estimated to be about 50 nm in diameter. Since the anatase phase is predominant in the XRD pattern of Figure 7.1, it may be concluded that the smaller particles are anatase, while the larger particles are rutile, which is quite compatible with other observations [30]. It also should be noted that two phases in P25 TiO₂ exist separately in highly close proximity, for this phenomenon, photocatalytic activity of P25 TiO₂ may mainly be contributed to the anatase phase.

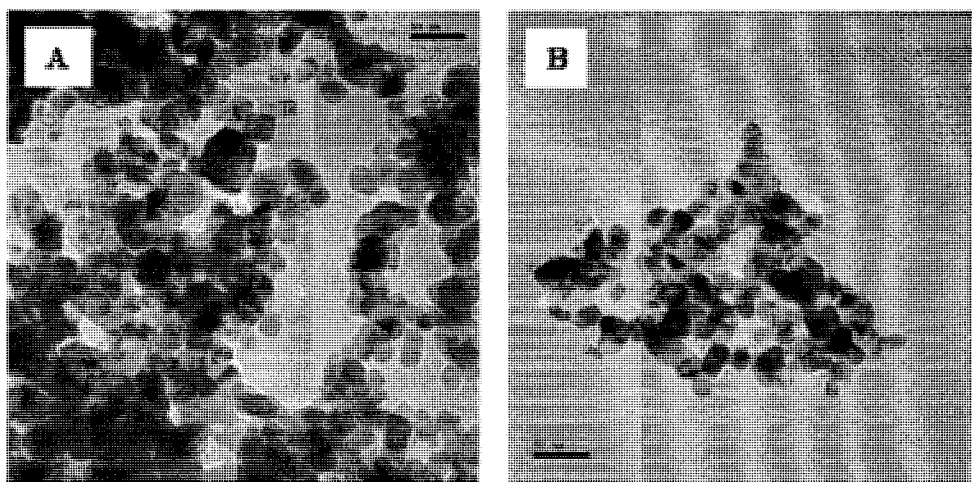


Figure 7.2. Representative TEM images of P25 TiO₂ nanoparticles; scale bar=50nm.

TiO₂ retention

A factorial experiment is quite effective to determine the most significant factors and reasonable to illustrate the main effects and

interactions of factors, because all levels of given factors correlated with every other factor in the experiments and all data are used in computing for both effects [31]. The 2³ factorial model was designed in this study and variables and levels are listed in Table 7.1. In a typical microparticulate retention system [32], the level of dosing of additives, cationic compounds and silica or bentonite clay, may affect retention of filler and fines and thus, it is necessary for the statistical experimental design to choose all of contents as operating variables, cationic starch, cationic PAM and natural zeolite, which is substituted for silica and bentonite clay.

Table 7.1. Factors and Levels for the 2³ Factorial Experimental Design

Factor		Level	
Symbol	Variable*	-	+
A	Natural Zeolite (%)	0	2
B	Cationic Starch (%)	0	0.5
C	Cationic Polyacrylamide (%)	0	0.1

* weigh percent versus 0.3% pulp contents

* Basis on 10% TiO₂ addition level

A set of 8 experiments were carried out and the results are shown in Figure 7.3. As fundamental of microparticle effects in fiber matrix, it was observed that there are significant differences in TiO₂ retention between with and without natural zeolite, and therefore, it is obvious and confirmed that natural zeolite definitely improves the TiO₂ retention with other cationic aids. The microparticle system readily makes it possible to achieve high retention and good formation because of decreased fiber-to-fiber flocculation resulting

from presenting microparticles between fiber and fiber. Natural zeolite microparticle retention aid has already been patented [33] by C.P. Klass and M.D. Sikora and has, in part, inspired this study. Conspicuously, as notated within Figure 7.3, it is interestingly revealed that natural zeolite may fairly act as a supporting substrate for TiO_2 , because retention values are relatively higher than those for the presence of cationic additives with no natural zeolite. In the end, dosing levels of retention additives were determined for further preparation of photocatalytic paper.

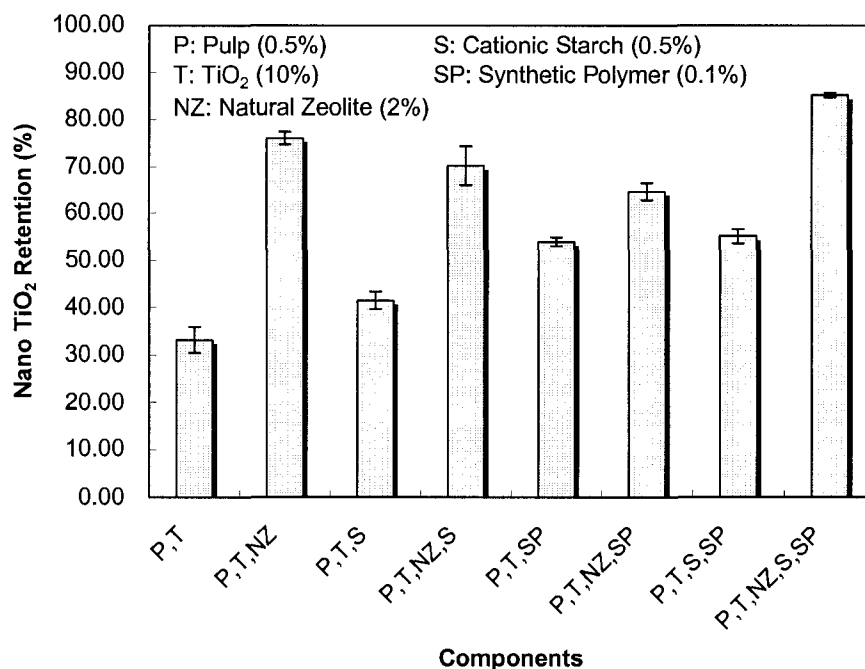


Figure 7.3. TiO_2 retention values in bleached softwood pulp with varying retention aids; CSF=430 ml, 750rpm

Figure 7.4 shows main factor effects and interactions of the experimental variables. As expected in Figure 7.3, it was verified that natural

zeolite decisively affects the retention of TiO_2 nanoparticles and C-PAM is also notable for retaining TiO_2 in the pulp. For the interaction plot, natural zeolite interacted sensitively with the different levels of addition of two other variables and is as distinct from that of other factors, while cationic starch shows insignificant interaction effects, implying just little contribution on the TiO_2 retention made by cationic starch without natural zeolite and C-PAM. Natural zeolite, therefore, proved to play an important role not only in microparticle retention system, but as a means of supporting titania.

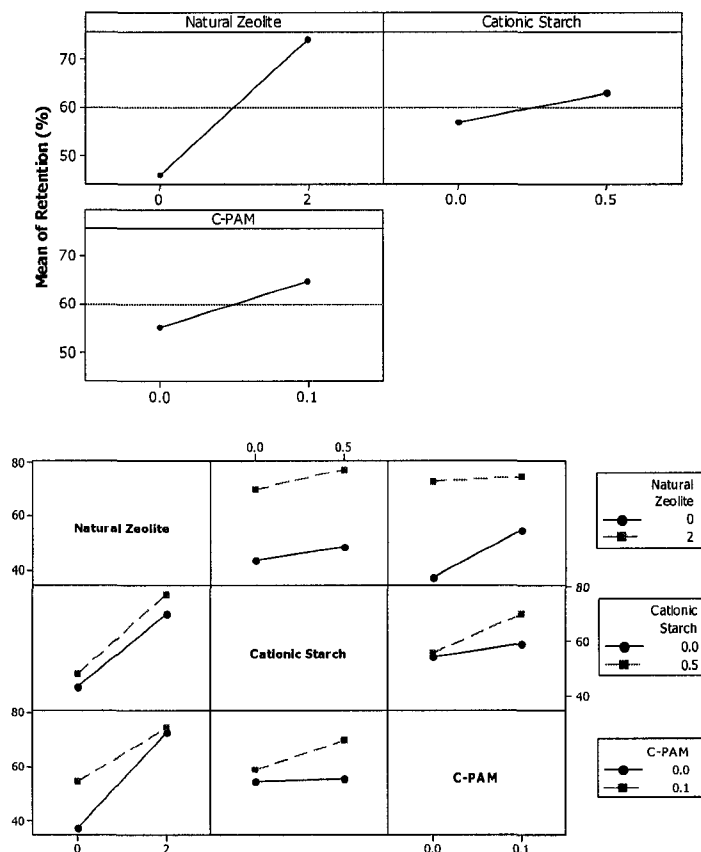


Figure 7.4. Main effect and interaction plot for TiO_2 retention (%) in natural zeolite microparticle system.

Photocatalytic activity

Figure 7.5 illustrates the toluene removal of photocatalytic paper prepared using a natural zeolite microparticle retention system. The concentration of gaseous toluene was 73.1 ppm and the photocatalytic test was performed under UV irradiation for 5 hrs after an initial stabilization time of 1hr. Prior to assessment of photocatalytic activity, blank tests were conducted with pure paper sheets, which had no TiO₂ and zeolite to exclude toluene oxidation in bulk by UV. In parallel with this, the variation of toluene concentration caused by both absorption and adsorption was also examined with 10% TiO₂ photocatalytic paper without UV.

As seen in Figure 7.5, toluene adsorbed steadily for almost 4hrs by natural zeolite followed by a period of stabilization of residual toluene. The last adsorption efficiency was about 25% of initial toluene and it seems reasonable to assume that it may happen largely because of zeolite pores and will effectively contribute to assisting the photocatalytic reaction. On the photocatalytic handsheets, toluene was decomposed continuously during the entire UV irradiation time in both samples having different contents of TiO₂. Residual toluene decreases progressively with slow decomposition rate in the 10% TiO₂ sheet, while toluene was removed more effectively for the 20% TiO₂ sheet and the efficiency achieved was almost 87%, which is probably due to the repetition of adsorption and photodecomposition of adsorbate between zeolite and TiO₂ nanoparticles when the photocatalytic sheets were under UV irradiation. In consequence, it is concluded that photocatalytic paper has become more influential in its potential of photocatalytic performance through the desired intent that natural zeolite takes effect not only as a

retention aid for the TiO₂ nanoparticles via both binder and supporter itself in the microparticle system, but also as adsorbent material being performance enhancing in photocatalytic decomposition as well.

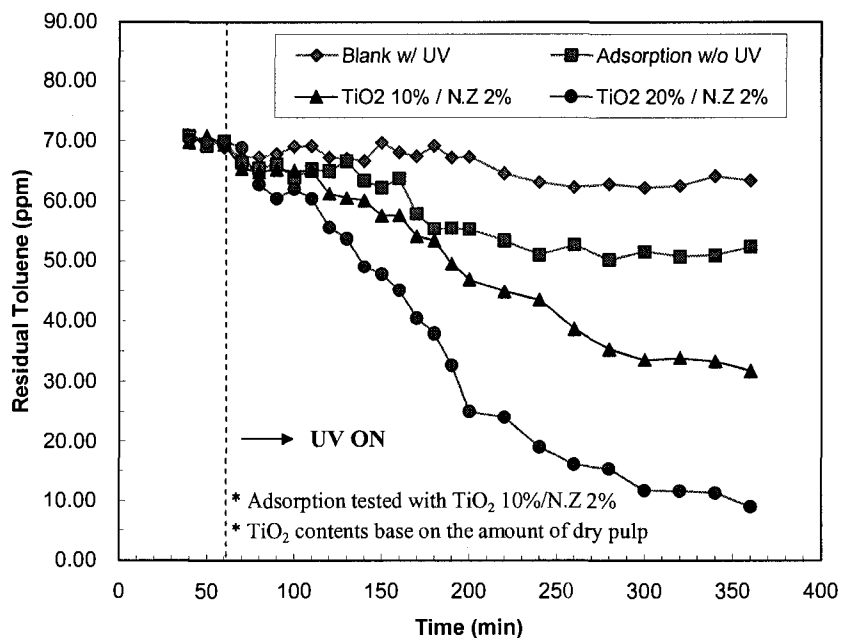


Figure 7.5. Photodecomposition of gaseous toluene by nano TiO₂ photocatalytic sheets.

Conclusion

Photocatalytic paper from nanosized TiO₂ was prepared using a natural zeolite microparticle retention system in papermaking and was investigated for VOC removal by prototype photocatalytic sheets. The retention of TiO₂ nanoparticles was outstandingly improved by addition of natural zeolite and, according to analysis of factorial experimental design, natural zeolite was shown to be the primary main effect factor affecting retention in paper stock and is vigorously interactive with sequential

additives of C-PAM and cationic starch. With the latent capability to adsorb contaminant due to natural zeolite, as-prepared photocatalytic papers were very effective in removing gaseous toluene, which is one of main indoor pollutants, and its ultimate removal efficiency was about 87%. Therefore, it should be pointed out that natural zeolite makes possible improving the retention of TiO₂ nanoparticles as both a microparticle retention aid and supporter, as well as enhancing the photocatalytic performance resulting from capturing the pollutant temporarily and photodecomposition under UV. In conclusion, the TiO₂ photocatalytic paper can be effectively fabricated with natural zeolite and it possesses high photodecomposition ability for organic contaminants.

References

- [1] A. Fujishima, K. Honda, "Electrochemical Photolysis of Water at a Semiconductor Electrode", *Nature* 238 (1972) 37-38.
- [2] M. Gratzel, "Photoelectrochemical cells ", *Nature* 414 (2001) 338-344.
- [3] M. Gratzel, " Dye-sensitized solar cells", *J. Photoch. Photobio. C* 4 (2003) 145-153.
- [4] A. Curulli, F. Valentini, G. Padeletti, et al., "Smart (Nano) materials: TiO₂ nanostructured films to modify electrodes for assembling of new electrochemical probes", *Sensor. Actuat. B-Chem.* 111-112 (2005) 441-449.
- [5] K. Sunada, Y. Kikuchi, K. Hashimoto, A. Fujishima, "Bacterial and Detoxification Effects of TiO₂ Thin Film Photocatalyst", *Environ. Sci. Technol.* 32 (1998) 726-728.
- [6] C.H. Ao, S.C. Lee, Y.Z. Yu, J.H. Xu, "Photodegradation of formaldehyde by photocatalyst TiO₂: effects on the presences of NO, SO₂ and VOCs", *Appl.*

Catal. B- Environ. 54 (2004) 41-50.

[7] A. Strini, S. Cassese, L. Schiavi, "Measurement of benzene, toluene, ethylbenzene and O-xylene gas phase photodegradation by titanium dioxides dispersed in cementitious materials using a mixed flow reactor", Appl. Catal. B- Environ. 61 (2005) 90-97.

[8] A. C. Rodrigues, M. Boroski, N.S. Shimada, et al., "Treatment of paper pulp and paper mill wastewater by coagulation-flocculation followed by heterogeneous photocatalysis" J. Photoch. Photobio. A 194 (2008) 1-10.

[9] I.J. Ochuma, R.P. Fishwick, J. Wood, J.M. Winterbottom, "Photocatalytic oxidation of 2,4,6-trichlorophenol in water using a concurrent downflow contactor reactor", J. Hazard. Mater. 144 (2007) 627-633.

[10] A. Fujishima, K. Hashimoto, H. Watanabe, "TiO₂ Photocatalysis: Fundamentals and Applications", BKC, Inc. Tokyo, Japan, 1997.

[11] M. R. Hoffmann, S. T. Martin, W. Choi, D. W. Bahnemann, "Environmental applications of semiconductor photocatalysis", Chem. Rev. 95 (1995) 69-96.

[12] A.L. Linsebigler, G. Lu, J.T. Yates Jr., "Photocatalysis on TiO₂ surfaces: Principles, Mechanisms, and Selected Results", Chem. Rev. 95 (1995) 735-758.

[13] A. Fujishima, T. N. Rao, D. A. Tryk, "Titanium dioxide photocatalysis", J. Photoch. Photobio. C 1 (2000) 1-21.

[14] T. L. Thompson, J. T. Yates Jr., "Surface science studies of the photoactivation of TiO₂-New photochemical processes", Chem. Rev. 106 (2006) 4428-4453.

[15] R. Pelton, X. Geng, M. Brook, "Photocatalytic paper from colloidal TiO₂-fact or fantasy", Adv. Colloid. Interfac. 127 (2006) 43-53.

[16] B. Wang, T. Takigawa, Y. Yamasaki, et al., "Symptom definitions for SBS (sick building syndrome) in residential dwellings", Int. J. Hyg. Environ. Health, 211 (2008) 114-120.

[17] S Wang, H. M. Ang, M. O. Tade, "Volatile organic compounds in indoor environment and photocatalytic oxidation: State of the art", Environ.

International, 33 (2007) 694-705.

[18] Y. Iguchi, H. Ichiura, T. Kitaoka, H. Tanaka, "Preparation and characteristics of high performance paper containing titanium dioxide photocatalyst supported on inorganic fiber matrix", *Chemosphere* 53 (2003) 1193-1199.

[19] S. Fukahori, H. Ichiura, T. Kitaoka, H. Tanaka, "Capturing of bisphenol A photodecomposition intermediates by composite TiO₂-zeolite sheets", *Appl. Catal. B: Environ.* 46 (2003) 453-462.

[20] H. Ichiura, T. Kitaoka, H. Tanaka, "Removal of indoor pollutants under UV irradiation by a composite TiO₂-zeolite sheet prepared using a papermaking technique", *Chemosphere* 50 (2003) 79-83.

[21] C. Raillard, V. Hequet, P. Le Cloirec, J. Legrand, "Kinetic study of ketones photocatalytic oxidation in gas phase using TiO₂-containing paper: effect of water vapor", *J. Photochem. Photobiol. A: Chem.* 163 (2004) 425-431.

[22] S. Fukahori, Y. Iguchi, H. Ichiura, T. Kitaoka, H. Tanaka, H. Wariishi, "Effect of void structure of photocatalyst paper on VOC decomposition", *Chemosphere* 66 (2007) 2136-2141.

[23] TAPPI test method T 227 om-99, Freeness of pulp (Canadian Standard Method)

[24] TAPPI test method T 248 sp-00, Laboratory beating of pulp (PFI mill method)

[25] TAPPI test method T 261 cm-00, Fines fraction by weight of paper stock by wet screening

[26] J.D. Peel, "Paper science and paper manufacturing", Angus Wilde Publications Inc. Vancouver, Canada, 1999.

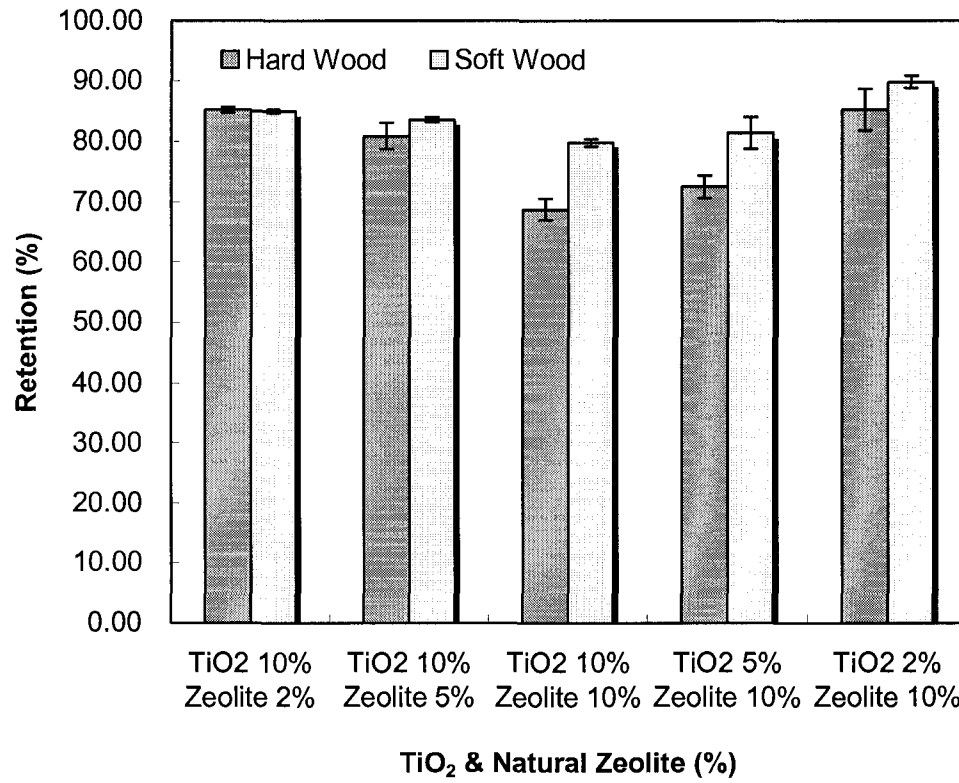
[27] TAPPI test method T 205 sp-02, Forming handsheets for physical tests of pulp

[28] TAPPI test method T402 sp-98, Standard conditioning and testing atmospheres for paper, board, pulp handsheets, and related products

- [29] B.D. Cullity, "Elements of X-ray diffraction", Menlo Park, CA: Addison-Wesley Publishing Company, 1978, p 98-106.
- [30] T. Ohno, K. Sarukawa, K. Tokieda, M. Matsumura, "Morphology of a TiO₂ Photocatalyst (Degussa, P-25) Consisting of Anatase and Rutile Crystalline Phases", J. Catal., 203 (2001) 82-86.
- [31] C.R. Hicks, N.V. Ternner Jr., "Fundamental Concepts in the Design of Experiments", 5th Ed. New York: Oxford University Press, 1999, p 133-137.
- [32] W.E. Scott, "Principles of Wet End Chemistry", Atlanta, GA: TAPPI Press, 1996.
- [33] C.P. Klass, M.D. Sikora, "High performance natural zeolite microparticle retention aid for papermaking", PN: US 7201 826 B2, 2007

Appendices

A. The Effect of TiO₂ and Natural Zeolite Contents on Retention Rate

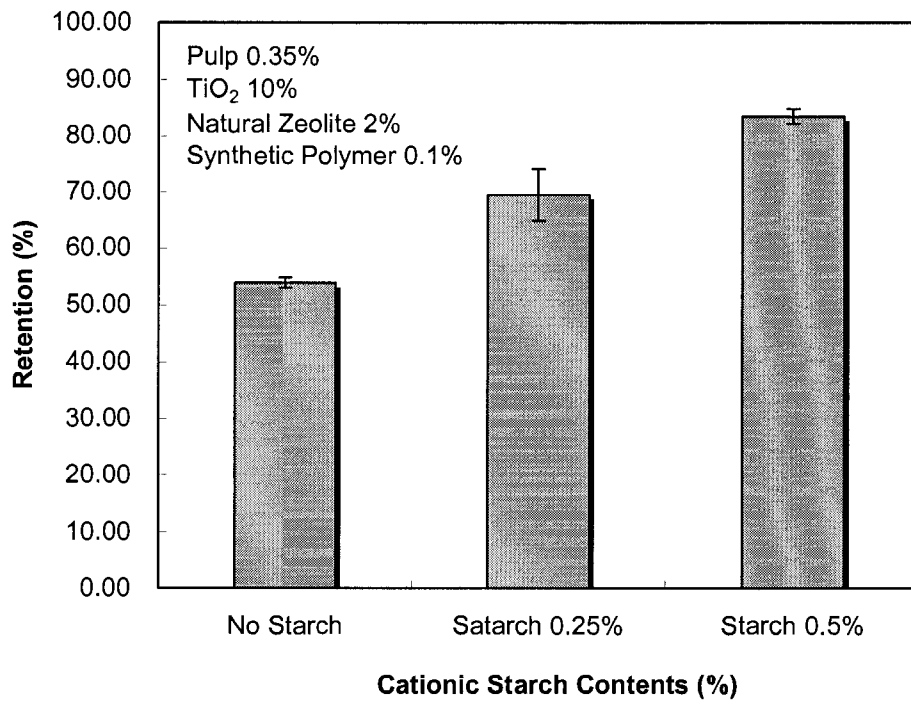


Pulp: 0.35% consistency

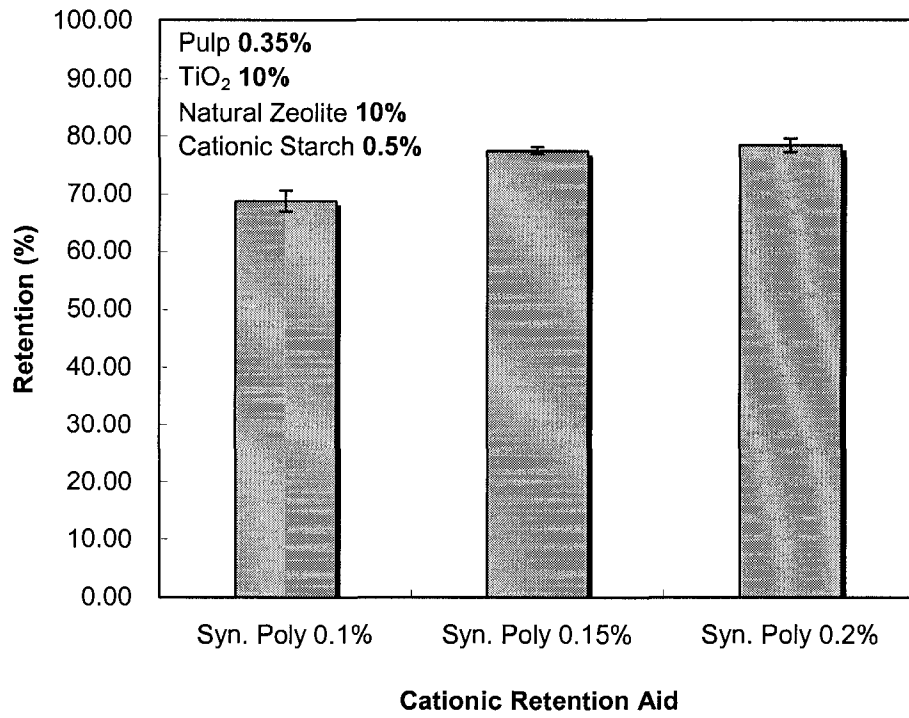
Cationic Starch: 0.5%

Cationic Polyacrylamide: 0.1%

B. The Effect of Cationic Starch Contents on TiO₂ Retention Rate



C. The Effect of Cationic Polymer (C-PAM) on TiO₂ Retention Rate



CHAPTER VIII

NATURAL ZEOLITE-BASED NANO TiO₂ PHOTOCATALYTIC PAPER: PREPARATION, CHARACTERIZATION AND PHOTOCATALYSIS ASSESSMENT

Seonghyuk Ko, Pnina Ari-Gur, Margaret Joyce and Paul D. Fleming
Department of Paper Engineering, Chemical Engineering and Imaging
Western Michigan University, Kalamazoo MI 49008, USA

A novel paper with high photocatalytic performance was successfully fabricated, using natural zeolite (clinoptilolite)-based nanosized TiO₂. Photocatalytic materials, from sol-gel derived TiO₂ colloids, incorporated into zeolite, have been designed, prepared and characterized. Resultant pre-matured anatase TiO₂ on zeolite particles were readily used in photocatalytic paper, which revealed zeolite-TiO₂ particles dispersed on a dense network of fibers with microvoids. Zeolite-based TiO₂ paper presented here decomposed gaseous toluene very effectively with UV irradiation and the removal efficiency was more competent than that of a group of comparisons with Degussa P25 TiO₂ paper and commercially available photocatalytic paper. It indeed is reasonably worthwhile that the outstanding findings provide us an in-depth view of the possibility of innovative photocatalytic paper being used for breaking down toxins and possibly microorganisms as well.

Keywords: natural zeolite, clinoptilolite, nanosized TiO₂, photocatalytic paper, photocatalysis

Introduction

Titanium dioxide (TiO_2) has been largely used for an opacifying pigment and photocatalytic agent [1]. Due to unique optical properties of a high refractive index and whiteness, TiO_2 has long been engaged in such applications requiring high opacity and brightness as coatings, paints, plastics, ink and paper [2]. In particular, since an epoch-making discovery of TiO_2 photoelectrochemical water splitting and hydrogen production using light in 1972 [3], as it is called Fujishima-Honda effect, there have been huge breakthroughs, both scientifically and practically, in various applications of semiconductor photocatalysis, for example, solar cells [4-5], optical sensors [6], hygienic products [7] and extensive environmental cleanup for both air pollutants [8-9] and wastewater [10-11], which is often referred to as "Light Cleaning" [1]. For these wide applications, nanocrystalline TiO_2 has been unchallenged among other semiconductor materials because of its photosensitivity, low cost, non-toxicity and chemical stability [12-15].

Encouraging as an effective means of decomposing organic compounds, as well as microorganisms, TiO_2 photocatalyst makes it possible to design an innovative novel paper product, which is called photocatalytic paper for toxin passivation, deodorizing and disinfection. Photocatalytic paper can be defined as smart paper that has light-activated catalytic function to decompose organic pollutants and kill pathogens and would be also specifically emphasized on two possible applications, antimicrobial active and VOC removable paper [16]. In recent years, food-borne microbial outbreaks have promoted developing the next generation of materials that incorporates anti-bacterial properties in active food packaging [17]. This is an

advanced packaging system functionalized by an interacting package component with a food product to satisfy desired demands for fresh-like foods, safe from pathogens [18]. More recently, a new bioactive paper and its packaging has been designed and developed to detect and deactivate any pathogens, such as E.coli and salmonella, borne by food, air and water [19].

In addition, as the time for staying indoors increases more and more these days, indoor air quality has become a bigger concern and it is more import for it to be kept as clean as possible. It is well known that volatile organic compounds (VOCs) are representative of indoor air pollutants and, according to the EPA, VOCs are known to cause negative health effects with such multiple symptoms as headache, nausea, conjunctiva irritation, dyspnea, allergic skin and emesis, etc. Among promising technologies for VOCs removal, there have been numerous studies on photocatalytic oxidation with different TiO₂ system and different chemicals were already reviewed by S. Wang et al [20]. Despite lots of studies reported, however, only a few publications and patents have been found regarding photocatalytic paper for VOC removal [16]. H. Tanaka et al [21-23] have successfully prepared different types of photocatalytic paper composites with a dual polymeric retention system, using TiO₂ supported on the inorganic fibers. These were found to remove hazardous chemicals both bisphenol A in wastewater and indoor air pollutants, such as acetaldehyde and toluene. In addition, the void structure effect has recently been investigated and a kinetic study of TiO₂ containing paper on the VOC decomposition with photocatalytic activity [24-25] has been reported.

As is often the case, it is of particular interest to immobilize nanosized

TiO₂ particles on such supporting or anchoring materials as silica [26-27], glass bead [28], alumina [29], fiberglass [30], clay [31] or zeolite [32-33], with the ultimate aim of intact photoactivity and further into the enhancement of photocatalytic efficiency. Of various supports, zeolites have been more favorable to be used in supporting TiO₂, due to their unique crystal structures and uniform pores and channels, which lead to large surface area and induce synergetic adsorption affects of organic matters in turn. A great deal of previous works has been performed in synthetic zeolites, for instance, HZSM-5 [34], Y zeolite [35] and MCM-41 zeolite [36], because of relatively larger surface area and supercages in infrastructure enabling entrapment of TiO₂ nanoparticles.

As distinct from synthetic zeolites, however, natural zeolite provides significant advantages of cost effectiveness, natural abundance and easier accessibility. Surprisingly, though, relatively few studies have been devoted to an anchoring and incorporation of TiO₂ on the natural zeolite. Moreover, our previous study revealed that natural zeolite plays important roles between fibers and TiO₂ particles not only as an effective microparticle retention aid, but as photocatalytic activity enhancer as well in photocatalytic paper [37]. It is worthwhile, thus, to investigate the integration of natural zeolite and nanosized TiO₂ and to evaluate the photocatalytic activity of photocatalytic paper containing as-prepared natural zeolite-based nano TiO₂. Such studies have not, so far, been noticed, nor, to our knowledge, have they been researched in detail in the area of photocatalytic paper.

The present study aims to synthesize, to characterize nano TiO₂-natural zeolite hybrid material from sol-gel derived nano titania colloids [38]

and to develop novel photocatalytic paper using natural zeolite-based TiO₂ nanoparticles retention system in papermaking. Photocatalytic activity on VOC decomposition was assessed with gaseous toluene, and to compare photocatalytic activity, two different types of photocatalytic papers were also tested, a commercial photocatalytic non-woven paper and representative sample paper prepared in the lab, using Degussa P25 TiO₂, which is the most referred for photocatalysis. In the end, the phenomenon of improving photocatalytic property will be discussed along with the photodegradation efficiency. The physical properties of both as-prepared zeolite-based TiO₂ nanoparticles and its photocatalytic paper will also be reported.

Experimental

Materials

Titanium tetra-isopropoxide (TTIP 99%), ACS reagent grade 2-propanol and hydrochloric acid (HCl) were used as received from Aldrich in the preparation of sol-gel derived TiO₂ colloids. Natural zeolite (clinoptilolite, ZOBRITE™) was favorably presented by ZO mineral partners [39]. The pulp used for the photocatalytic paper was bleached softwood northern kraft pulp and as retention aids in papermaking, cationic starch and cationic polyacrylamide (C-PAM, Core Shell 61607; NALCO) were used in a natural zeolite microparticle system. Nanosized P25 TiO₂ (Degussa, 22 nm, 50 m²/g, 70% anatase and 30% rutile), which is the most commonly referred photocatalytic material, was employed in comparative specimen as a photocatalysis agent. Non-woven photocatalytic paper was purchased from Ahlstrom (France, BR 1048-075, 75g/m²).

Combination of TiO₂ and natural zeolite

A few nanometers size of TiO₂ colloidal nanoparticles were prepared thorough a sol-gel synthetic route in which acid catalyzed hydrolysis of titanium tetra-isopropoxide dissolved in 2-propanol was carried out. Briefly, in a typical synthesis of zeolite-based TiO₂ photocatalyst [38], 10 ml of 0.5 M TTIP solution in 2-propanol was added slowly dropwise to 2 ml of 0.1M HCl in 88 ml of 2-propnol under vigorous stirring at 0°C and kept stirring for 4-6 hrs to further peptization, thereby obtained particle size in a transparent TiO₂ sol was 2-3 nm on an average (Figure 5.1(A)). Natural zeolite was subsequently mixed thoroughly with as-prepared titania sol by stirring. The solvent was removed completely by evaporation. TiO₂ impregnated natural zeolite was then collected and dried at 110°C followed by post-calcination at 300°C to 800°C to induce the crystallinity of TiO₂ on zeolite. TiO₂ contents in the final forms were adjusted to be in the same ratio of when zeolite is used in microparticle filler retention system in the papermaking technique [37]. Specifically, its corresponding ratio was 5TiO₂/1Natural Zeolite, designated here afterwards 5T/NZ, 3T/NZ and 1T/NZ were additionally prepared for comparison.

Preparation of photocatalytic paper

Photocatalytic papers of varied TiO₂ photocatalyst with approximate 100 g/m² of basis weight were prepared according to Technical Association of the Pulp and Paper Industry (TAPPI) test methods T 205 [40]. The pulp was mechanically refined to a Canadian Standard Freeness (CSF) of approximately 430 ml according to TAPPI test methods T 227 [41] and T 248

[42] prior to blending with other materials. As-prepared zeolite-based TiO₂ was added to the pulp suspension with stirring followed by adding cationic starch and cationic polyacrylamide (C-PAM) as retention aids. In the event of P25 containing paper, natural zeolite was combined with the pulp suspension at the last step of dosing. The addition level of each retention aid was 10% photocatalyst, 0.5% cationic starch, 0.1% C-PAM and in case of need, 2% natural zeolite in that order versus 0.3% pulp consistency (3 g dry pulp/L). All handsheets were uniformly formed on a 200 wire mesh in a standard handsheet forming machine and dried under standard conditions given in TAPPI T 402 [43] for at least 24 hrs before it was used for the photocatalysis.

Characterization

Photocatalytic materials and their handsheets prepared in this study were meticulously characterized with an X-ray diffractometer (XRD), transmission electron microscope (TEM) and scanning electron microscope (SEM). The X-ray diffraction (XRD) analyses was carried out using a Diano X-ray Diffractometer at room temperature using 20 Kw Cu-K α radiation ($\lambda=0.15418$ nm) to survey the crystal structures and integrity of raw natural zeolite and TiO₂ nanoparticles. All peaks were identified using MDI Jade 5.0 software (Materials Data Inc. USA). The morphology and accurate size of TiO₂ loaded natural zeolite was obtained with TEM (JEOL JEM-1230) and three typical regions of each sample were taken. The surface morphology of zeolite-based TiO₂ paper was observed by SEM (Akashi ISI-DS 130) after gold sputtering on the specimen.

Evaluation of photocatalytic activity

To assess the photocatalytic performance of the handmade photocatalytic papers, toluene was chosen for this study as a model compound among various indoor VOC chemicals. Photocatalytic decomposition of gas-phase toluene was carried out in a 1L glass photoreactor under UV light irradiation (EIKO blacklight lamp, 4W, $\lambda=365\text{nm}$) with a circular photocatalyst handsheet (11.29cm in diameter). For the quantitative analysis of varying toluene concentration through the entire experimental time, regardless of UV irradiation, gas samples were withdrawn from a sampling port attached to the reactor and injected into the Gas Chromatograph (GC, SRI 8610C) equipped with a Flame Ionization Detector (FID) and a 30m x 0.25 mm fused silica capillary column (Quadrex Corp.). All samples were tested three times to verify the photodegradation effect and the results were within 5% of standard deviations.

Results and Discussion

Characterization of zeolite-based TiO_2

Figure 8.1 shows the XRD patterns of TiO_2 -supported natural zeolite annealed at different temperatures ranging from 300°C to 800°C in order to investigate crystal structural changes. Diffraction peaks were identified apparently using XRD patterns processing software and it is obviously observed that the TiO_2 crystalline phase is maintained clearly through annealing temperatures, without phase transition from anatase to rutile, even after heating to 800°C. One of the outstanding features observed in XRD results is that zeolite structure had not been damaged and isolated from TiO_2

crystallization indicating that as-prepared colloidal TiO₂ nanoparticles were effectively loaded to natural zeolite and well-combined into thermally stable zeolite-based TiO₂. The crystal size of anatase TiO₂ over natural zeolite was estimated to 13nm based on the FWHM (full width at half maximum intensity).

Figure 8.2 gives the TEM images of zeolite-based TiO₂ nanoparticles. Three different samples were imaged at 300,000~500,000X magnification. As seen in Figure 8.2(A), a myriad of colloidal nanoparticles were loaded onto a mostly zeolite surface due to its smaller pore size than TiO₂ colloids, namely, natural zeolite has generally 0.4-0.7 nm of pore size [44] while as-prepared TiO₂ colloidal nanoparticles were about 2-3 nm. Figure 8.2(B) and (C) displays distinctly different sizes of grains as the form of zeolite surrounded by TiO₂ implying TiO₂ nanoparticles were gradually evolved from amorphous TiO₂ on the surface of zeolite. It is also observed that TiO₂ particles crystallized on zeolite are decidedly different in their size; specifically it appears to be approximately 10 nm at 600°C calcination in Figure 8.2(B), where as the larger particles shown in Figure 8.2(C) are estimated to be about 15 nm in diameter, which is consistent with the single particle size calculated from X-ray diffraction peaks in Figure 8.1. It is, therefore, evident that zeolite provides sufficient support, not only to hold tightly TiO₂ nanoparticles, but also to function as adsorption sites enabling an increase in photodegradation efficiency for organic materials.

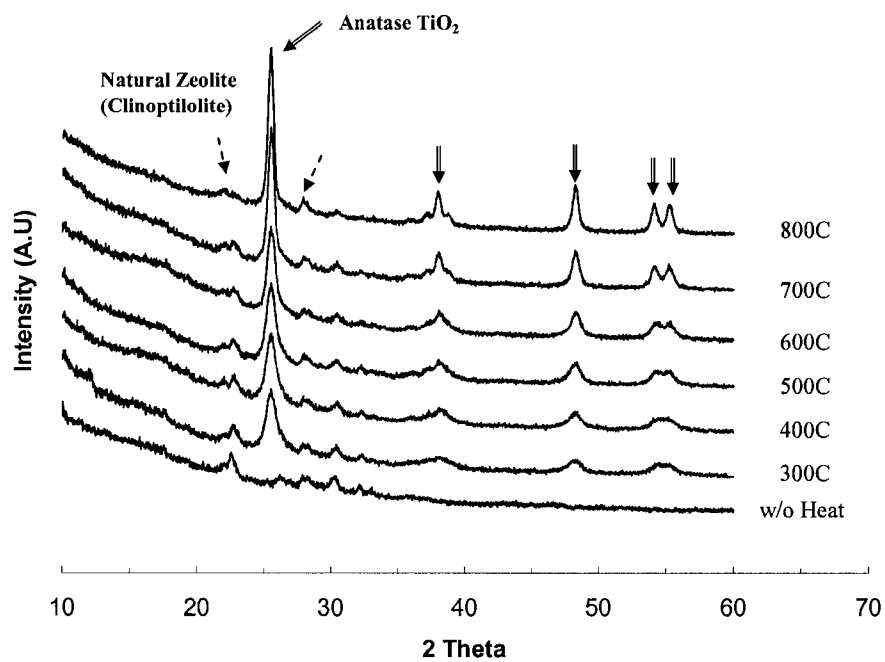


Figure 8.1. XRD patterns of natural zeolite-based TiO₂ with varying calcination temperature.

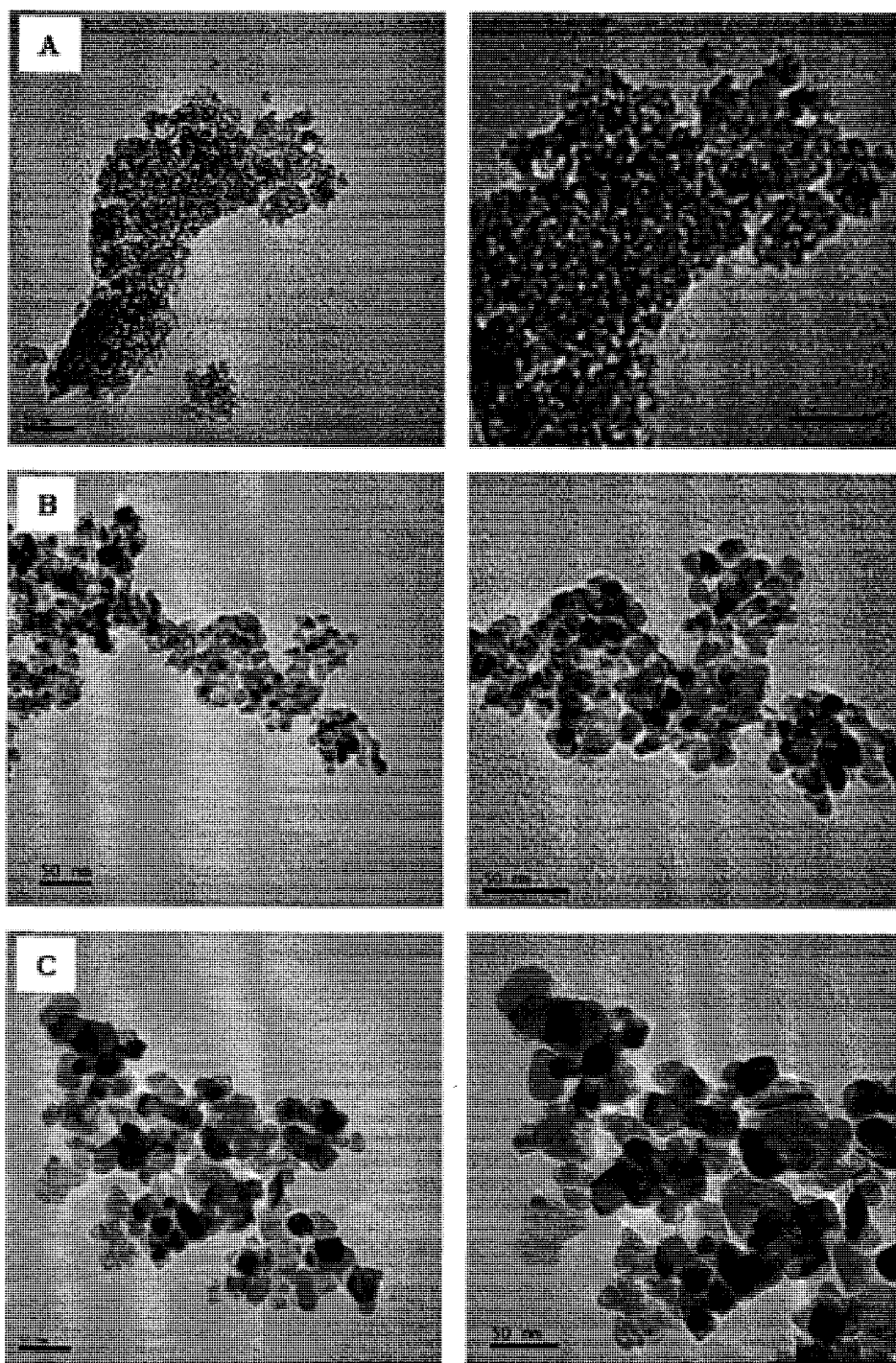


Figure 8.2. Representative TEM images of TiO_2 nanoparticles on natural zeolite at different calcination temperature; (A) no calcination, (B) 600 °C and (C) 800 °C, scale bar = 50nm.

Morphology of photocatalytic paper

The surface morphology of photocatalytic papers was observed by scanning electron microscopy (SEM) and images are shown in Figure 8.3. One commercial and two lab-made photocatalytic papers using P25 TiO₂ and zeolite-based TiO₂ were tested with a blank sample, which contains neither TiO₂ nor zeolite. Fine particles were well-dispersed over the fibers and the pulps, except for the Ahlstrom sample shown in Figure 8.3(D), form highly dense fiber network structures, resulting from well-fibrillated internally and flexible fibers. Zeolite-based TiO₂ paper presents the most uniformly arranged microvoids in the fiber matrix, whereas the Ahlstrom sample has a somewhat loose configuration and it was found to contain many large pores between its non-woven fibers.

The upper images in each photograph in Figure 8.3 were to identify particles retained on the fibers within the microvoids. Although seen in partial agglomerates of particles, it is apparent that TiO₂-based particles are fairly attached to the inner microvoid fibers. In considering that the performance of TiO₂ paper is positively affected by the void structure [25], it makes possible the better photocatalytic performance in the zeolite-based TiO₂ paper, which is composed of properly distributed microvoids and confined zeolite-TiO₂ powders inside of voids.

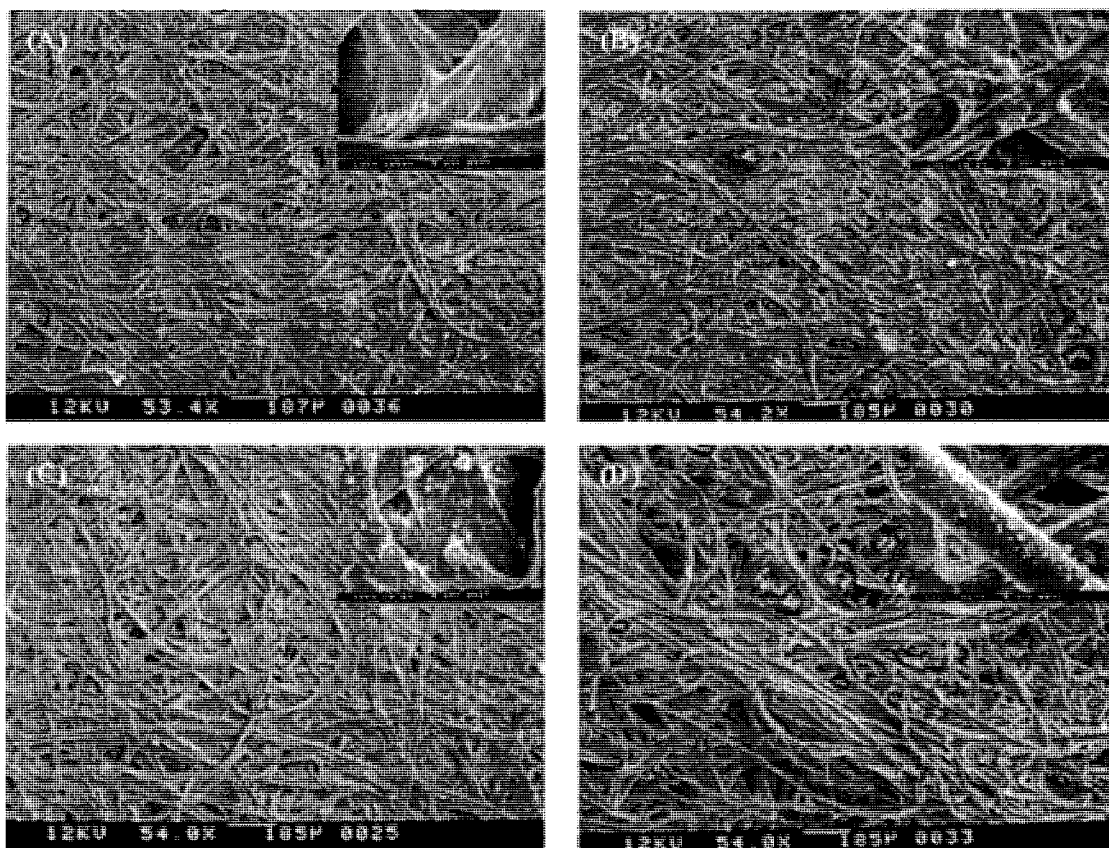


Figure 8.3. SEM images of photocatalytic papers; (A) blank sheet, (B) P25 TiO₂/natural zeolite sheet, (C) natural zeolite-based nano TiO₂ paper and (D) Ahlstrom sample.

Evaluation of photocatalytic activity

Figure 8.4 illustrates the photodecomposition performance of photocatalytic papers prepared using zeolite-based TiO_2 synthesized with varying TiO_2 weight contents in a typical microparticle retention system. The concentration of gaseous toluene was 73.1 ppm and a constant specific time was given to allow initial adsorption, which occurred commonly after injection of toluene into the reactor. After it leveled off, photocatalysis was subsequently performed under UV irradiation for 5 hrs. To exclude the effect of adsorption without UV and oxidation in bulk by UV, both of blank and adsorption test were carried out prior to photocatalytic activity and the results are shown with photocatalysis in Figure 8.4.

As seen in the adsorption profile, toluene adsorbed steadily for almost 4hrs by natural zeolite followed by a period of stabilization of residual toluene. The last adsorption efficiency was about 30% of initial toluene and it seems reasonable to assume that it may happen mostly by zeolite pores in the layered fiber matrix and will effectively contribute to assist the photocatalytic reaction. On the photocatalytic handsheets, toluene was decomposed continuously during the entire UV irradiation time in both samples made from different contents of TiO_2 over zeolite. Residual toluene is decreasing progressively with a slow decomposition rate in 1 TiO_2 /natural zeolite sheet, while toluene is removed more rapidly at both 3 TiO_2 /NZ and 5 TiO_2 /NZ with small gap between those TiO_2 sheets and efficiency achieved was almost 95%, which is seen due to the repetition of adsorption by zeolite and photodecomposition of adsorbate by TiO_2 nanoparticles when the photocatalytic sheets were under UV irradiation.

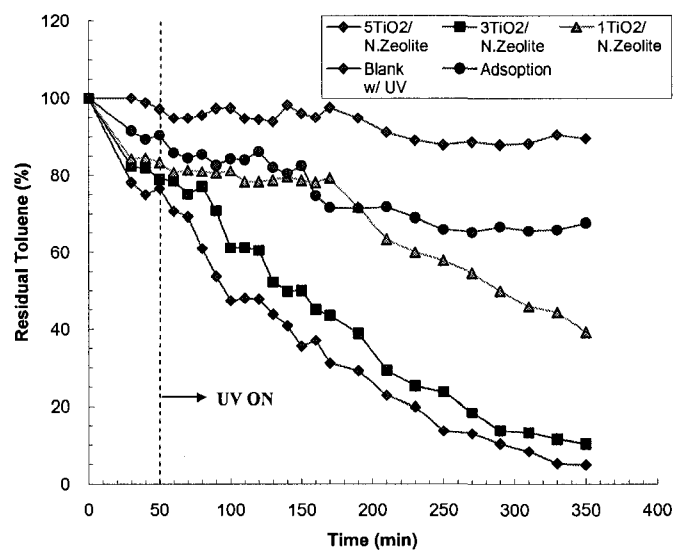


Figure 8.4. Decomposition of gaseous toluene on photocatalytic papers under UV irradiation.

As a comparison, one commercial and one hand made photocatalytic paper using Degussa P25 TiO₂ were evaluated for photodecomposition of toluene and the results are shown in Figure 8.5. It is observed that the immediate decrease in residual toluene with the Ahlstrom sample at the first point of examination. This phenomenon is caused probably by the mutual effect of its highly spotted macrovoids, as seen in Figure 8.3, and high adsorption capacity of SiO₂ used in this photocatalytic paper as a binder with TiO₂ and non-woven fibers. In spite of a striking adsorption property, however, it showed quite poor photocatalytic performance with regard to only photodegradation effect under UV, to be exact, only about 20% of toluene that disappeared totally was by photocatalysis activated by UV. As for photocatalysis itself, it also was interesting to observe that the other

samples made using a different type of TiO_2 exhibited a better capability to photodecompose the toluene, ostensibly, even though the commercial one shows higher removal efficiency than that of P25 TiO_2 paper. However, a remarkable fact is that zeolite-based TiO_2 papers display steep removal profiles, indicating conspicuously high photocatalytic activity and, in this regard, pre-loaded TiO_2 on zeolite is much more effective than when TiO_2 is used separately in papermaking with zeolite. These results are presumably attributed to multiple synergy effects with proper microvoids made in fiber-fiber connections, anatase-crystallized TiO_2 and zeolite, more exactly, paper detains the contaminants within the microvoids and zeolite subsequently traps the organic materials and also suppress the recombination of electron-hole pairs on the TiO_2 surface [45], thereby enhancing the photocatalytic activity.

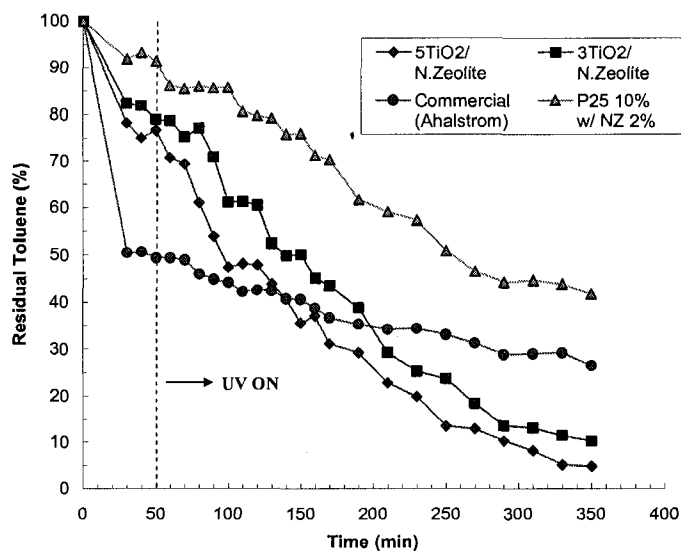


Figure 8.5. Comparison of toluene photodegradation by different types of photocatalytic papers.

Conclusion

Nanosized TiO₂-supported natural zeolite photocatalytic papers were prepared using a microparticle retention system, with cationic starch and cationic polyacrylamide in papermaking. TiO₂ loaded on zeolite was well-matured from sol-gel derived colloids to about 10-13 nm size of anatase crystalline phase at the surface of zeolite. Fibers formed a closely-packed network, creating microvoids, and zeolite-based TiO₂ particles were attached on the web of fibers. As with the photocatalytic performance, photocatalytic paper using pre-synthesized zeolite-nano TiO₂ was definitely superior to the others in toluene removal, which were employed for a comparison including Degussa P25 TiO₂ and Ahlstrom photocatalytic paper as representative selections of current commercially available active TiO₂ and photocatalytic paper, respectively. It was noteworthy that photocatalytic paper, based on zeolite-TiO₂ hybrid materials, achieves the desired impact of robust photocatalytic efficiency, due to the reciprocal effect with order of confinement of organic contaminant in microvoids between fiber networks, its further adsorption on zeolite and subsequent photodecomposition of adsorbate by TiO₂ nanoparticles. Notably, the results presented in this study have offered unique insights into the novel photocatalytic paper, which has sufficient photocatalytic potential to completely remove toxins, and microorganism as well.

References

- [1] A. Fujishima, K. Hashimoto and H. Watanabe, "TiO₂ Photocatalysis: Fundamentals and Applications", BKC, Inc. Tokyo, Japan, 1997.

- [2] G. Buxbaum, G. Pfaff, "Industrial Inorganic Pigments", Wiley-VCH, Weinheim, Germany 3rd Ed. 2005.
- [3] A. Fujishima, K. Honda, "Electrochemical Photolysis of Water at a Semiconductor Electrode", *Nature* 238 (1972) 37-38.
- [4] M. Gratzel, "Photoelectrochemical cells", *Nature* 414 (2001) 338-344.
- [5] M. Gratzel, "Dye-sensitized solar cells", *J. Photoch. Photobio. C* 4 (2003) 145-153.
- [6] A. Curulli, F. Valentini, G. Padeletti et al., "Smart (Nano) materials: TiO₂ nanostructured films to modify electrodes for assembling of new electrochemical probes", *Sensor. Actuat. B-Chem.* 111-112 (2005) 441-449.
- [7] K. Sunada, Y. Kikuchi, K. Hashimoto, A. Fujishima, "Bactericidal and Detoxification Effects of TiO₂ Thin Film Photocatalyst", *Environ. Sci. Technol.* 32 (1998) 726-728.
- [8] C. H. Ao, S. C. Lee, Y. Z. Yu, J. H. Xu, "Photodegradation of formaldehyde by photocatalyst TiO₂: effects on the presences of NO, SO₂ and VOCs", *Appl. Catal. B- Environ.* 54 (2004) 41-50.
- [9] A. Strini, S. Cassese, L. Schiavi, "Measurement of benzene, toluene, ethylbenzene and O-xylene gas phase photodegradation by titanium dioxides dispersed in cementitious materials using a mixed flow reactor", *Appl. Catal. B- Environ.* 61 (2005) 90-97.
- [10] A. C. Rodrigues, M. Boroski, N. S. Shimada, et al., "Treatment of paper pulp and paper mill wastewater by coagulation-flocculation followed by heterogeneous photocatalysis" *J. Photoch. Photobio. A* 194 (2008) 1-10.
- [11] I. J. Ochuma, R. P. Fishwick, J. Wood, J. M. Winterbottom, "Photocatalytic oxidation of 2,4,6-trichlorophenol in water using a concurrent downflow contactor reactor", *J. Hazard. Mater.* 144 (2007) 627-633.
- [12] M. R. Hoffmann, S. T. Martin, W. Choi, D. W. Bahnemann, "Environmental applications of semiconductor photocatalysis", *Chem. Rev.* 95 (1995) 69-96.

- [13] A. L. Linsebigler, G. Lu, J. T. Yates Jr., "Photocatalysis on TiO₂ surfaces: Principles, Mechanisms, and Selected Results", *Chem. Rev.* 95 (1995) 735-758.
- [14] A. Fujishima, T. N. Rao, D. A. Tryk, "Titanium dioxide photocatalysis", *J. Photochem. Photobiol. C* 1 (2000) 1-21.
- [15] T. L. Thompson, J. T. Yates Jr., "Surface science studies of the photoactivation of TiO₂-New photochemical processes", *Chem. Rev.* 106 (2006) 4428-4453.
- [16] P. Appendini, J. H. Hotchkiss, "Review of antimicrobial food packaging", *Innova. Food Sci. Emerg. Technol.* 3 (2002) 113-126.
- [17] M. Ozdemir, J. D. Floros, "Active Food Packaging Technologies", *Crit. Rev. Food Sci. Nutri.* 44 (2004) 185-193.
- [18] SENTINEL Bioactive Paper Network, <http://www.bioactivepaper.ca>
- [19] S Wang, H. M. Ang, M. O. Tade, "Review: Volatile organic compounds in indoor environment and photocatalytic oxidation: State of the art", *Environ. International* 33 (2007) 694-705.
- [20] R. Pelton, X. Geng, M. Brook, "Photocatalytic paper from colloidal TiO₂-fact or fantasy", *Adv. Colloid. Interfac.* 127 (2006) 43-53.
- [21] Y. Iguchi, H. Ichiura, T. Kitaoka, H. Tanaka, "Preparation and characteristics of high performance paper containing titanium dioxide photocatalyst supported on inorganic fiber matrix", *Chemosphere* 53 (2003) 1193-1199.
- [22] S. Fukahori, H. Ichiura, T. Kitaoka, H. Tanaka, "Capturing of bisphenol A photodecomposition intermediates by composite TiO₂-zeolite sheets", *Appl. Catal. B: Environ.* 46 (2003) 453-462.
- [23] H. Ichiura, T. Kitaoka and H. Tanaka, "Removal of indoor pollutants under UV irradiation by a composite TiO₂-zeolite sheet prepared using a papermaking technique", *Chemosphere* 50 (2003) 79-83.
- [24] C. Raillard, V. Hequet, P. Le Cloirec, J. Legrand, "Kinetic study of ketones photocatalytic oxidation in gas phase using TiO₂-containing paper: effect of water vapor", *J. Photochem. Photobiol. A: Chem.* 163 (2004) 425-431.

- [25] S. Fukahori, Y. Iguchi, H. Ichiura, T. Kitaoka, H. Tanaka, H. Wariishi, "Effect of void structure of photocatalyst paper on VOC decomposition", *Chemosphere* 66 (2007) 2136-2141.
- [26] H.-J. Kim, Y.-G. Shul, H. Han, "Photocatalytic properties of silica-supported TiO₂", *Top. Catal.* 35 (2005) 287-293.
- [27] L. Zou, Y. Luo, M. Hooper, E. Hu, "Removal of VOCs by photocatalysis process using adsorption enhanced TiO₂-SiO₂ catalyst", *Chem. Eng. Proc.* 45 (2006) 959-964.
- [28] C.-S. Chiou, J.-L. Shie, C.-Y. Chang, C.-C. Liu, C.-T. Chang, "Degradation of di-n-butyl phthalate using photoreactor packed with TiO₂ immobilized on glass beads", *J. Hazard. Mater.* 137 (2006) 1123-1129.
- [29] S. Sakthivel, M.V. Shankar, M. Palanichami, B. Arabindoo, V. Murugesan, "Photocatalytic decomposition of leather dye Comparative study of TiO₂ supported on alumina and glass beads", *J. Photoch. Photobio. A* 148 (2002) 153-159.
- [30] H. Yu, S.C. Lee, J. Yu, C.H. Ao, "Photocatalytic activity of dispersed TiO₂ particles deposited on glass fibers", *J. Mol. Catal. A-Chem.* 246 (2006) 206-211.
- [31] L.M. Daniel, R.L. Frost, H. Zhu, "Laponite-supported titania photocatalysts", *J. Colloid Interf. Sci.* 322 (2008) 190-195.
- [32] N. Dubey, S.S. Rayalu, N.K. Labhsetwar et al., "Photocatalytic properties of zeolite-based materials for the photoreduction of methyl orange", *Appl. Catal. A-Gen.* 303 (2006) 152-157.
- [33] W. Panpa, P. Sujaridworakun, S. Jinawath, "Photocatalytic activity of TiO₂/ZSM-5 composites in the presence of SO₄²⁻ ion", *Appl. Catal. B-Environ.* 80 (2008) 271-276.
- [34] M. Noorjahan, V.D. Kumari, M. Subrahmanyam, P. Boule, "A novel and efficient photocatalyst: TiO₂-HZSM-5 combine thin film", *Appl. Catal. B-Environ.* 47 (2004) 209-213.
- [35] S. Anandan, M. Yoon, "Review: Photocatalytic activities of the nano-sized TiO₂-supported Y-zeolites", *J. Photoch. Photobio. C* 4 (2003) 5-18.

- [36] X. Wang, W. Lian, X. Fu, J-M. Basset, F. Lefebvre, " Structure, preparation and photocatalytic activity of titanium oxides on MCM-41 surface", J. Catal. 238 (2006) 13-20.
- [37] S. Ko, J. Pekarovic, P.D. Fleming, " Preparation and Study of VOC Removal of Nano Titania Photocatalytic Paper using a Natural Zeolite Microparticulate Retention System", Prepared for Chemosphere.
- [38] S. Ko, P. Ari-Gur, P.D. Fleming, "Synthetic Behavior and Photocatalytic Activity of Nanocrystalline TiO₂ from Sol-Gel Derived Colloids", Submitted to Materials Letters.
- [39] ZO Minerals Partners, LTD, San Antonio, Texas 78205
- [40] TAPPI test method T 205 sp-02, Forming handsheets for physical tests of pulp
- [41] TAPPI test method T 227 om-99, Freeness of pulp (Canadian Standard Method)
- [42] TAPPI test method T 248 sp-00, Laboratory beating of pulp (PFI mill method)
- [43] TAPPI test method T402 sp-98, Standard conditioning and testing atmospheres for paper, board, pulp handsheets, and related products
- [44] F. Li, Y. Jiang, L. Yu, Z. Yang, T. Hou, S. Sun, " Surface effect of natural zeolite (clinoptilolite) on the photocatalytic activity of TiO₂", Appl. Surf. Sci. 252 (2005) 1410-1416.
- [45] R. Chatti, S.S. Rayalu, N. Dubey, N. Labhsetwar, S. Devotta, "Solar-based photoreduction of methyl orange using zeolite supported photocatalytic materials", Sol. Energ. Sol. C 91 (2007) 180-190.

CHAPTER IX

CONCLUSION

Paper I: The synthetic characteristics of nanosized TiO₂ have been studied from sol-gel derived colloidal nanoparticles prepared through the experimental design approach. A few nanometer size of colloidal samples, which are in the range of 2.5 nm to 14.3 nm, determined predominantly by media temperature, were synthesized followed by annealing at varied temperatures. The evolution of crystalline phases and growth showed different-behavior sequences with different primary size of colloidal nanoparticles and it was confirmed that varying primitive properties of TiO₂ colloidal particles has an impact on the behavior of the crystalline phase transition and coarsening mechanisms as well. The photocatalytic activity of the selected as-prepared TiO₂ nanoparticles, which are comprised of only anatase phase, was more potent compared to that of Degussa P25 TiO₂ in toluene decomposition on a paper substrate.

Paper II: We present here the results of measurements of optical properties and photocatalytic activity that allow us to optimize the effect of polycrystalline phases of TiO₂ nanoparticles from the point of view of principal crystal structures, anatase and rutile. Six different fractions of crystal structure of TiO₂, which are in the range of 0.7 anatase: 0.3 rutile to only rutile phase, were prepared from P25 Degussa TiO₂ by means of heat treatment at 500°C-800°C. For the optical properties, opacity, brightness and CIEL*a*b* values were tested and 0.71 rutile/0.29 anatase phase composition

of TiO₂ was definitely superior to the others, even though pure rutile has the higher refractive index. The photocatalytic activity of the as-modulated TiO₂ nanoparticles was gradually decreased along with decreasing contents of anatase phase and photoactivity dropped largely from beyond 0.48 rutile ratio in toluene decomposition. Accordingly, it is obviously shown that there is an optimal range of anatase and rutile crystalline phases that possesses both better optical properties and photocatalytic activity. Consequently, it makes practically possible an optimal range of TiO₂ phase fraction in the range of 0.48 rutile:0.52 anatase and 0.71 rutile:0.29 anatase.

Paper III: Photocatalytic paper from nanosized TiO₂ was prepared using a natural zeolite microparticle retention system in papermaking and was investigated for VOC removal by prototype photocatalytic sheets. The retention of TiO₂ nanoparticles was outstandingly improved by addition of natural zeolite and, according to analysis of the factorial experimental design, natural zeolite was shown to be the primary main effect factor affecting retention in paper stock and is vigorously interactive with sequential additives of C-PAM and cationic starch. With the latent capability to adsorb contaminant due to natural zeolite, as-prepared photocatalytic papers were very effective in removing gaseous toluene, which is one of main indoor pollutants, and its ultimate removal efficiency was about 87%. Therefore, it should be pointed out that natural zeolite makes possible improving the retention of TiO₂ nanoparticles as both a microparticle retention aid and supporter, as well as enhancing the photocatalytic performance resulting from capturing the pollutant temporarily and photodecomposition under UV.

In conclusion, the TiO₂ photocatalytic paper can be effectively fabricated with natural zeolite and it possesses high photodecomposition ability for organic contaminants.

Paper IV: Nanosized TiO₂-supported natural zeolite photocatalytic papers were prepared using a microparticle retention system, with cationic starch and cationic polyacrylamide in papermaking. TiO₂ loaded on zeolite was well-matured from sol-gel derived colloids to about 10-13 nm size of anatase crystalline phase at the surface of zeolite. Fibers formed a closely-packed network, creating microvoids, and zeolite-based TiO₂ particles were attached dispersively on the web of fibers. As with the photocatalytic performance, photocatalytic paper using pre-synthesized zeolite-nano TiO₂ was definitely superior to the others in toluene removal, which were employed for a comparison including Degussa P25 TiO₂ and Ahlstrom photocatalytic paper as representative selections of currently commercially available active TiO₂ and photocatalytic paper, respectively. It was noteworthy that photocatalytic paper, based on zeolite-TiO₂ hybrid materials, achieves the desired impact of robust photocatalytic efficiency, due to the reciprocal effect with order of confinement of organic contaminant in microvoids between fiber networks, its further adsorption on zeolite and subsequent photodecomposition of adsorbate by TiO₂ nanoparticles. Notably, the results presented in this study have offered unique insights into the novel photocatalytic paper, which has sufficient photocatalytic potential to remove completely toxins, and favorably, microorganism as well.